Extensions and improvements of the electrical conductance method

Uitbreidingen en toepassingen van de elektrische conductantiemethode

DOOR

LILIAN KORNET

GEBOREN TE HELLEVOETSLUIS OP 7 JULI 1968

Promotie-Commissie

Promotor: Prof.Dr. A. Versprille

overige leden: Prof.Dr. J. Baan, RijksUniversiteit Leiden
                Prof.Dr.Ir. N. Bom, Erasmus Universiteit Rotterdam
                Prof.Dr. P.D. Verdouw, Erasmus Universiteit Rotterdam

Co-Promotor: Dr. J.R.C. Jansen

Index

Chapter 1

General Introduction

1.1 Introduction

Continuous monitoring of cardiac output is important in patients who are undergoing intensive care, thoracic surgery or a catheterization for diagnostic reasons. In these patients arterial pressure is routinely determined. In the patients, who are undergoing a catheterization for diagnostic reasons, aortic pressure is determined. During intensive care and thoracic surgery arterial pressure is determined in both the pulmonary artery and the artery femoralis or radialis. The radial or femoral catheter is a replacement of the pressure catheter in the aorta. To determine cardiac output continuously from an arterial pressure signal, the aortic pressure was reconstructed from the peripheral pressure [Wesseling et al. 1976, Gratz et al. 1992]. For this continuous cardiac output monitoring from aortic pressure, a model of the circulation is used. A parameter of this model is the compliance of the arterial system, which is the change in volume per unit of length (i.e. segmental volume) over a change in pressure. The compliance is derived from in vitro measurements using a selected group of human aorta's [Langewouters 1984]. Cardiac output can also be determined from the pulmonary arterial pressure signal, which is directly measured in this artery. Thus, a reconstruction of this pressure signal is not needed. To calculate right ventricular output, i.e. cardiac output, according to a pulse contour method, we determined the pulmonary arterial compliance. To determine arterial volume, which was needed to determine compliance we modified the conductance method. We studied the relationship between arterial volume and pressure at a large range of pulmonary arterial pressure.

To outline the context in which the research presented in this thesis has been carried out, the function of blood vessels and of large arteries in particular will be described. Next, the anatomy of arteries will be considered. Subsequently, the terms concerning mechanics of blood vessels are explained and finally the method to determine blood volume in large arteries; the conductance method, will be described.

1.2 Function of the large arteries

The ventricle supplies power to transform blood with a low pressure into blood with a high pressure. The performance of the left ventricle is strongly determined by i.e. the aortic input impedance [Burkhoff et al. 1988, Milnor 1975, Noble 1979, O'Rourke 1982] and the work of the right ventricle is strongly determined by i.e. the pulmonary input impedance [Mc Donald 1974, Milnor 1982, O'Rourke 1982 and Piene and Hauge 1976]. The input impedance can be separated into three components: vascular resistance, ₊characteristic impedance and arterial compliance. The arterial compliance enables the heart to store a fraction of the stroke volume into the arteries under a modest pressure rise. During diastole the distended arteries recoil passively to sustain blood pressure when the blood is transported downstream. Thus, the pulsatile flow out of the heart into the aorta and into the pulmonary artery is damped causing a less pulsatile flow in the capillaries.

Most studies about the mechanics of blood vessels have been done in vitro using arteries originating from the systemic circulation. Many of these studies have been performed with strips or rings, assuming isotropy and homogeneity of the vessel wall. However, experiments indicate that the arterial wall is not isotropic at in situ length [Patel et al. 1969, Cox 1975a, van Loon et al. 1977, Vorp et al. 1995]. The compliance of the arterial wall varies with the species [Berry 1974a, b], location in the arterial system [Maloney et al. 1970, Bergel 1961b, Gow and Taylor 1968, Patel et al. 1963, Learoyd and Taylor 1966, Cox 1975b, van Merode et al. 1996], transmural pressure [Bergel 1961a, Greenfield and Patel 1962, Patel et al. 1969, Langewouters et al. 1985], age [Learoyd and Taylor 1966, Band et al. 1972, Gozna et al. 1974, Harris et al. 1965, and Newman and Lallemand 1978, Langewouters et al. 1985, Reneman et al. 1986, van Merode 1988, 1993] and tone of the smooth muscle in the arterial wall [Dobrin and Rovick 1969, Goedhard et al. 1973, Gow 1972, Cox 1975b].

A decrease in arterial compliance due to an increase in blood pressure, or diseases

such as diabetes mellitus [Lo et al. 1986, Lehmann et al. 1992a], hypercholesterolaemia [Lehmann et al. 1992b, c] and growth hormone deficiency [Lehmann et al. 1993] might increase the systolic blood pressure causing additional ventricular load [Kannel 1991]. The increase in blood pressure might correspond to a lower compliance causing cardiac overload to rise even more [Kelly et al. 1992]. High blood pressure can occur more specifically in the pulmonary circulation than in the systemic circulation. This is defined as pulmonary hypertension, which is present in a variety of diseases and conditions, such as chronic obstructive lung diseases, interstitial lung diseases, chest wall abnormalities, shunts [Koerner 1988], acute hypoxia [Olivari 1991], thromboembolic diseases [Fuster et al. 1984] and heart diseases [Kanemoto 1987]. To decrease pulmonary input impedance and prevent right ventricular failure, pulmonary vessel resistance should be decreased, which often can be attained by vasodilator therapy. Vasodilator therapy might also influence vessel compliance. This influence can be caused by an effect on the vessel wall (active effect) or by an effect on pressure (passive effect). Therefore, pulmonary arterial compliance needs to be known over a large pressure range.

Arterial compliance has been used in pulse contour models to relate aortic pressure to the continuous measurement of aortic blood flow or cardiac output. This continuous measurement is especially important to monitor patients during thoracic surgery, when vascular resistance and cardiac output can change fast. In most pulse contour models, aortic compliance was used, determined during in vitro experiments [Wesseling et al. 1976, 1983, 1993, Jansen et al. 1990, Weissman et al. 1993, Tannenbaum et al. 1993]. In other models, aortic compliance has been assumed to decay exponentially in vivo [Gratz et al. 1992]. An application of these pulse contour methods to the pulmonary circulation is attractive, because pulmonary arterial pressure is often routinely monitored during thoracic surgery and in patients in the intensive care unit. Tajimi et al. [1983] used the pulmonary pressure to calculate cardiac output and assumed pulmonary arterial compliance to be constant. We studied whether the assumption of a constant compliance of the pulmonary artery is valid during in vivo conditions. The elasticity of the passive or active smooth

muscle cells will contribute to the elasticity of the total wall. Data of compliance determined in vitro can probably be extrapolated to the in vivo situation for the systemic arterial side, because the aorta has a small content of smooth muscle cells [Bader 1963, Dobrin and Rovick 1983]. However, 80 to 90% of the medial layer of the pulmonary artery, consists of smooth muscle cells [Somlyo and Somlyo 1964]. Therefore, we determined the compliance of the pulmonary artery in vivo, which will be presented in chapter 3.

1.3 Anatomy of the large arteries

The arterial wall consists of three concentric layers: the intimal, the medial and the adventitial layer. The histological architecture of the layers, especially that of the media, differs among the blood vessel types and is usually the criterion by which vessels are categorized [Rhodin 1980].

The intima consists of a mono-layer of flat endothelial cells: the endothelium. These cells form a closed layer, except in some types of capillaries and the smallest veins. The cells are in contact with the flowing blood and positioned in the direction of the blood flow. Because of its high compliance, endothelium does not contribute significantly to the stiffness of the wall [Fung et al. 1966, Wiederhielm 1965]. Outside the endothelium the basal membrane is found, which consists of collagen type IV, proteoglycans and laminin. The intima ends at the lamella elastica interna, which is a layer of concentrated elastic laminae of about 100 μm. The elastic fibres of the internal elastic lamellae are continuous and positioned in parallel in the pulmonary artery [Ingram et al. 1970]. Although the intima separates blood from the interstitium, it allows diffusion of metabolites into and out of the tissue. Furthermore, the endothelial cells produce vasoactive substances such as cyclic Adenosine MonoPhosphate (cAMP) [Fischell et al. 1989], prostacyclin [Frangos et al. 1985], Endothelium Derived Relaxing Factor [Furchgott and Zawadski 1980, Furchgott 1983, Pohl et al. 1988, Rubanyi et al. 1988], endothelin [Sumpio and Widmann 1990,

Yanagisawa et al. 1990] and the cells are sensitive to blood flow changes [Furchgott and Zawadski 1980, Furchgott 1983, Frangos et al. 1985, Pohl et al. 1988, Rubanyi et al. 1988, Melkumyants et al. 1989, Bevan et al. 1990].

The medial layer is the thickest one. The architecture of the rabbit aortic media was studied by light and electron microscopy at various distending pressures [Wolinsky and Glagov 1964]. It was shown that at physiological pressures, circumferentially aligned collagen fibres bear the tangential stressing forces while the elastin net distributes the stressing forces uniformly throughout the wall.

In the aortic media, elastin fibrils often seem to enclose smooth muscle cells on both transverse and longitudinal sections but do not form a complete sheet around individual cells [Wolinsky and Glagov 1964]. Attachments of smooth muscle cells to elastin lamellae and fibrils were observed but no attachments of muscle cells to collagen were observed [Wolinsky and Glagov 1964]. The aorta only has a small content of vascular musculature, probably without any practical importance regarding changes in vessel wall diameter [Bader 1963, Dobrin and Rovick 1969].

In the inner media of the pulmonary artery, elastin fibrils are discontinuous and interspersed with spare amounts of collagen and large numbers of smooth muscle cells [Ingram et al. 1970]. The smooth muscle cells exhibit a predominantly circumferential orientation and their contraction is mainly in the circumferential direction [Ingram et al. 1970]. They seem to be able to contract to 70-75% of their resting length [Lundholm and Mohme-Lundholm 1966]. Somlyo and Somlyo [1964] found that the medial layer of the pulmonary artery consists of 80-90% smooth muscle. Smooth muscle cells form a complete coat in the media of the pulmonary artery [Davis and Reid 1970]. Towards the end of the arterial pathway this coat is replaced by a spiral of smooth muscle cells. In the outer part of the media of the pulmonary artery there were more elastic fibres than in the inner part [Ingram et al. 1970]. At the adventitial side the media is bounded by the external elastic lamellae. The outer elastic lamellae resembled the internal elastic lamellae but smooth muscle cells were often found between the lamellae. These smooth muscle

cells were orientated obliquely and longitudinally. Smith [1976] has shown that the elastin fibres in the elastic lamellae of the pulmonary artery of rabbits are orientated in all directions. However, there is a strong tendency for circumferentially orientated fibres to predominate over longitudinally orientated ones. In the aorta, however, the angles of pitch are almost completely restricted within a narrow range of 80°, with a high predominance of circumferentially orientated fibres.

The **adventitia** is composed of proteoglycans, fibroblasts, and collagen, arranged in bundles. The adventitial collagen may prevent rupture at extremely high pressures [Remington 1955, Burton 1954]. The adventitia is removed in most in vitro studies, because of its amorphous nature.

1.4 Mechanics of blood vessels

According to the law of Laplace, the distending pressure (P) [mmHg→N/m²] acting on the longitudinal cross-section of a blood vessel is opposed by the wall tension (T) [N/m²] times twice the wall thickness times the length of the longitudinal segment. If the outer pressure is reset to zero, the equation becomes:

$$P \cdot 2 \cdot r_i \cdot l = 2 \cdot T \cdot (r_o - r_i) \cdot l \qquad (1)$$

where r_i is the inner radius [m], l the length [m], r_o the outer radius [m] and r_o - r_i the wall thickness (h) [m]. From equation 1 follows :

$$T = \frac{P \cdot r_i}{h} \qquad (2)$$

Thus when the wall is relatively thick a relatively smaller wall tension exists and the smooth muscle cells bear a smaller load. Strain (e) is defined as the amount of deformation (Δl) relative to the undeformed (unstressed) state (l_o). It is a dimensionless quantity.

Thus:

$$e = \frac{\Delta l}{l_o} \qquad (3)$$

If the stress-strain relation is linear over a small range, then the incremental Young's modulus of elasticity (E) [$N \cdot m^{-2}$] can be defined as the ratio of a small increment in stress ($\Delta\sigma$) to the corresponding increment in strain:

$$E = \frac{\Delta\sigma}{\Delta e} \qquad (4)$$

Extensibility of a vessel (κ) [$N \cdot m^{-2}$] is defined as:

$$\kappa = V \cdot \frac{\Delta P}{\Delta V} \qquad (5)$$

where V is the volume [m^3] enclosed by the vessel.

If a constant segment, and thus constant length is considered, κ can be computed from the pressure (P) versus cross-sectional area (CSA) relationship according to:

$$\kappa = CSA \cdot \frac{\Delta P}{\Delta CSA} \qquad (6)$$

The reciprocal of κ is distensibility (D) [m^2/N]:

$$D = \frac{\Delta CSA}{CSA \cdot \Delta P} \qquad (7)$$

Compliance (C) per unit length is [m^4/N]:

$$C = \frac{\Delta CSA}{\Delta P} \qquad (8)$$

In this thesis we used the term quasi-static compliance if an average change in CSA divided by an average change in pressure over several heart cycles was considered in

vivo. "Quasi" is added, because in vivo a static situation cannot occur, due to the pulsatile variation in pressure and CSA, caused by the pulsatile output of the heart. The slope of the linear regression line through the CSA versus pressure values found over a heart cycle was defined as dynamic compliance.
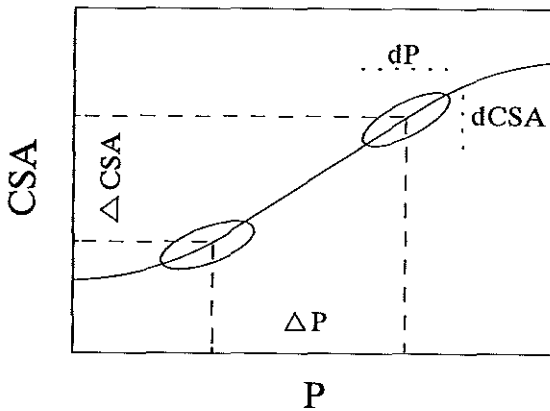
Fig. 1. Quasi-static compliance (C_{ps}) = $\Delta CSA/\Delta P$ and dynamic compliance (C_d) = $dCSA/dP$).

Viscous elements in the blood vessel wall can cause stress-relaxation [Zatzman et al. 1954], creep [Langewouters et al. 1985] and hysteresis [Patel et al. 1960, Gow 1972, Journo et al. 1992]. Stress-relaxation is the phenomenon that after sudden deformation of a material, the stress needed to maintain that deformation gradually decreases to a new steady state-level. Creep is the phenomenon that a sudden increase in stress on an elastic tissue is followed by a gradual deformation to a new characteristic shape for that stress. Pulsatile pressure will produce a CSA change, which lags behind in phase, causing a CSA versus pressure loop during a heart cycle, which is orientated counter-clockwise. This effect is called hysteresis.

Activation of the vascular smooth muscle cells increases pressure-radius hysteresis

[Dobrin and Rovick 1969]. It has been shown that viscosity is greater in activated muscular than in elastic arteries [Bulbring and Tomita 1970, Bergel 1961b]. However, some viscous behaviour was still observed in aortas with relaxed smooth muscle and in vessels in which smooth muscle cells were inactivated [Lundholm and Mohme-Lundholm 1966, Apter and Marquez 1968, Langewouters et al. 1985]. Elastin and collagen have been found to be almost purely elastic, i.e. they exhibit negligible viscous properties [Minns et al. 1973, Reuterwall 1921, Hass 1942]. Minns et al. [1973] showed that removal of the ground substance induced a decrease in stress relaxation in the aorta. We conclude that the visco-elasticity can be ascribed to activated smooth muscle cells, the ground substance and the physical interaction between the components of the vessel wall. For example, the rearrangement of elastin and collagen fibres might lead to visco-elasticity, which was made plausible by Bull [1957], who found that a nylon stocking showed visco-elasticity, although a single nylon fibre did not.

1.5 The conductance method

1.5.1 Mechanism of the conductance method

To determine compliance of a blood vessel, segmental volume should be determined besides pressure, using a method, which does not introduce a restraint on the vessel wall. The conductance method is such a method, which is also non-labour intensive and inexpensive [Baan et al. 1981, 1984, 1994, van der Velde et al. 1992, Steendijk et al. 1993]. The conductance catheter used to determine blood volume is a catheter equipped with 4-12 equidistantly placed ring electrodes. If left ventricular volume is determined (chapter 5 and 6) commonly more than 4 electrodes are used and the 1 mm wide electrodes are typically spaced 10 mm apart. Because, we wanted to determine the volume of a small blood segment in a blood vessel (chapter 2-4), we used only four electrodes. These electrodes were spaced 5 mm apart. An alternating current source of constant

amplitude drives the two outer electrodes to generate an electrical field. Current strengths are in the μ-ampere range and frequencies between 1 and 100 kHz are used. Voltage differences are measured between successive inner electrode pairs and the segmental conductances are summed to obtain total conductance. Total conductance consists of the conductance of the blood and the conductance of the fluids and tissues surrounding the blood (parallel conductance). Parallel conductance can be estimated by a saline dilution method of Baan et al. [1981, 1984] as described in the methods of chapter 2. In chapter 4 we introduce a new method to determine parallel conductance, which we regard to be more accurate. The conductance of blood depends on the blood volume, the distance between the electrodes and the conductivity of blood. The conductance method was initially only applied to estimate ventricular volumes, because shear rate during changing flow velocities as in arteries changes the conductivity of blood and, therefore, the measured conductance [Sakamoto and Kanai 1979, Visser et al. 1976]. The influence of shear rate is discussed below. Due to the large dimensions of the ventricle in comparison with the distance between the electrodes a non-homogeneous electrical field could be present in the ventricle [Baan and Mur 1984, Spinelli et al. 1986, Applegate et al. 1990]. To correct for this non-homogeneous electrical field a factor α was introduced. This factor α and its relation to the volume dependence of parallel conductance as present in the left ventricle is discussed in chapter 6.

1.5.2 Historical aspects of the conductance method

At present, the conductance method is used in cardiovascular and physiology laboratories, catheterization rooms and occasionally in operating rooms, usually for left ventricular measurements. Already in 1953, Rushmer et al. tried to determine intra-ventricular volume by placing electrodes on the ventricular wall. Geddes et al. [1966] placed the electrodes at the base and the apex. The first method was not feasible, however the second

method gave a conductance signal which correlated with volume. To avoid electrode polarization and to obtain more accuracy, electrodes were placed on a catheter using current carrying and multiple measuring electrodes in the early 70s by the group of Baan [Corten et al. 1972]. The method has been tested, both in isolated hearts against a balloon technique [Burkhoff et al. 1985] and in situ against electromagnetic flowmetery [Baan et al. 1981, Baan et al. 1984] and the fast cine-CT method [van der Velde et al. 1992] in dogs, as well as against angiography and thermal dilution in patients [Baan et al. 1984]. The results of evaluation studies showed excellent linear correlations between conductance and the volume obtained by the reference method. Other authors who compared the method with angiography [Boltwood et al. 1989] and a multiple-dimension method by ultrasonic crystals [Applegate et al. 1990] showed that the relation between conductance and the independent determined volume is non-linear if volume is varied over a large range. Also, theoretical analyses revealed that the relationship between conductance and volume is non-linear [Mur and Baan 1984, Spinelli and Valentinuzzi 1986, Kun and Peura 1994]. This non-linear relation was attributed to a non homogeneous electrical field. This would cause parallel conductance to be volume dependent. In chapter 6 we present our study on the dependence of parallel conductance on ventricular volume with use of a new method. This method was introduced in chapter 5. Another method to determine parallel conductance within the heart cycle was developed by Gawne et al. [1987]. This method is based on the use of excitation currents with dual frequencies. Blood has essentially a constant conductivity over the range of frequencies from 2 to 100 kHz [Schwan 1983]. In contrast, muscle is far more conductive above than below 12 kHz [Zheng et al. 1984]. Therefore, at the higher frequency a larger conductance is found than at the lower frequency. To relate this difference to parallel conductance, calibration is performed using the conventional saline method. Steendijk et al. [1993] improved the linearity of the conductance method by increasing the homogeneity of the electrical field using a dual-excitation technique.

1.6 Effects of shear rate on conductance measurements

1.6.1 Influence shear rate on blood

For the conductance method, blood can be described as a suspension of small electrical current insulating particles (erythrocytes) in a conductive fluid (plasma). Until now, the volume in a large blood vessel has not been determined using the electrical conductance method as was done for the ventricular volume [Baan et al. 1984], because in blood vessels a pulsatile flow and thus pulsatile change in shear rate is present. A pulsatile shear rate, might cause pulsatile orientation and deformation, de-aggregation and axial accumulation of erythrocytes [McDonald 1974, Edgerton 1974, Gollan and Namon 1968, Liebman 1974, Nakajima et al. 1990, Ninomiya et al. 1988, Sakamoto and Kanai 1979, Schmid-Schönbein and Wells 1969, Skalak and Zhu 1990, Visser et al. 1976, 1989], which in turn will cause a pulsatile change in conductivity of blood. In the ventricle a turbulent flow is present and therefore no unidirectional orientation and deformation, aggregation or axial accumulation of erythrocytes will occur.

Erythrocytes *accumulate axially* in a vessel when blood is flowing [Sakamoto and Kanai 1979, Aarts et al. 1988]. In this case a plasma layer of 3 to 7 μm appears near the wall of the vessel. The conductivity change caused by accumulation is negligible if it is measured in blood vessels larger than 1 mm, like in our experiments.

In stagnant blood, formation of *aggregates* possibly increases the conductivity [Schmid-Schönbein and Wells 1968, Snabre et al. 1987, Skalak and Zhu 1990]. These authors expect that these aggregates break up at very low shear stresses.

Orientation will not occur in a non-unidirectional blood flow, which is present within the heart and the root of the aorta at the start of systole. However, in other large vessels orientation should be considered.

Erythrocytes might also *deform* under influence of shear rate, if orientation occurs [Schmid-Schönbein and Wells 1969]. The conductivity of cell walls of erythrocytes is lower than plasma. If more erythrocytes deform and orientate in the blood flow direction,

the total path length of the electrical current through the plasma will be less. This results in a higher conductivity of blood in the direction of flow [Gollan and Namon 1968, Visser et al. 1976, Liebman 1974, Peura et al. 1978, Sakamoto and Kanai 1979, Ninomiya et al. 1988, Nakajima et al. 1990]. Because we would like to correct for the effects of blood flow on the conductance measurements in large vessels, we considered a possible effect of de-aggregation, orientation and deformation in chapter 2.

1.6.2 Formulas for shear rate

Shear rate is defined as the gradient of velocity [s^{-1}]. In case of a Poiseuille profile the distribution across the cross-sectional area of a vessel is parabolic and the shear rate is a linear function of radius [Caro et al. 1978]:

$$Shear\ Rate\ =\ \frac{\Delta v}{\Delta a}\ =\ -4<v>\frac{a}{r^2} \tag{9}$$

Here v is velocity, $<v>$ is average velocity, a is the distance and r is the radius. At the axis (a = 0) the velocity gradient is zero and it increases linearly to the wall where it has a maximum of $-4<v>/r$ for $a/r = 1$. Average shear rate across the vessel is $-2<v>/r$.

1.7 Outline of this thesis

In chapter 2, our study on the effects of shear rate on the conductivity of blood, as present in large blood vessels of piglets, will be presented. Also the influence of temperature and haematocrit on conductivity of pig blood will be considered. Correction factors for these effects were used to extend the application of the conductance catheter to the measurement of blood vessel volume. The conductance method was evaluated in the aorta of anaesthetized piglets with use of an intravascular ultrasound method as a reference.

In chapter 3 the compliance (change in volume per unit of length divided by

pressure) of the pulmonary artery is studied in vivo in piglets over a large pressure range with use of the adapted conductance method.

In chapter 4 we eliminate the effect of shear rate. We used a double indicator dilution method to estimate cross-sectional area of blood vessels, based on the injection of a "cold" hypertonic saline solution and the determination of the dilution of ions, using the conductance catheter, and the dilution of temperature using a thermistor. The method was evaluated in the aorta of anaesthetized piglets and referred to the intravascular ultrasound method.

If the conventional conductance method is applied, the influence of conductance of the tissues surrounding the blood in the vessel (parallel conductance) must be eliminated. Conventionally, this has been done by injection of saline and plotting of conductance at end-systolic ventricular volume against conductance at end-diastolic volume and extrapolation of this relationship to a point on the identity line, which was regarded as parallel conductance. In chapter 5 we introduce a new method to determine parallel conductance in blood vessels and ventricles, which is not based on the extrapolation of aregression line, but on the determination of the area under the saline (i.e. conductance) dilution curve.

In chapter 6, the new method to estimate parallel conductance is used to determine parallel conductance of the left ventricle throughout the heart cycle. In this study, we also showed that the correction factor α, as used in the literature to correct for a non-homogeneous electrical field in the left ventricle, is mathematically coupled to the slope of the linear regression line through the parallel conductance versus ventricular volume values within a heart cycle.

In chapter 7 we consider the results of our studies and give some suggestions for future studies.

Chapter 2

The Conductance Method for the Measurement of
Cross-Sectional Areas of Arteries in Vivo

L Kornet[1], JRC Jansen[1], EJ Gussenhoven[2],
MR Hardeman[3] and A Versprille[1]

1)   Pathophysiological Laboratory, Department of Pulmonary Diseases, Erasmus University, Rotterdam, The Netherlands
2)   The Interuniversity Cardiology Institute (Thorax-center Rotterdam), Erasmus University, Rotterdam, The Netherlands
3)   Department of Internal Medicine, Division of Hemorheology, Academic Medical Center, Amsterdam, The Netherlands

2.1 Introduction

To analyze the compliance of arteries, their cross-sectional areas (CSAs) and transmural
arterial pressures need to be determined at various conditions. The conductance method,
commonly used for the estimation of ventricular volumes, [Baan et al. 1981, 1984] was
modified to estimate CSAs of arteries in piglets. To calculate CSA from the blood
conductance, the conductance of surrounding tissues, which is parallel conductance, needs
to be subtracted from total measured conductance. The arterial pulsatile blood flow will
cause a pulsatile change in shear rate, which in turn might cause a pulsatile change in
blood conductivity because of the orientation and deformation of erythrocytes [Schwan
1963, Schmid-Schönbein and Wells 1969, Gollan and Namon 1970, Edgerton 1974,
Liebman 1974, Visser et al. 1976, Peura et al. 1978, Sakamoto and Kanai 1979, Smith et
al. 1979, Ninomiya et al. 1988, Visser 1989, Nakajima et al. 1990, Skalak and Zhu
1990]. This is undoubtly the main reason that the conductance method has not gained
acceptance to measure absolute CSAs of arteries in vivo. However, erythrocytes might
remain deformed and orientated throughout the heart cycle if the time for orientation and
deformation is short compared to the time of systole and the time for de-orientation and
reformation is long compared to the time of diastole. This leads to a time invariant effect
of shear rate on blood conductivity. This supposition is supported by in vitro studies,
where an increase from 0.3 to 3 Hz. in the frequency of a pulsatile flow caused a
considerable decrease in the fluctuation of the conductivity of blood [Peura et al. 1978,
Ninomiya et al. 1988]. Therefore, prior to evaluation of the conductance method, the time
courses for de-aggregation, deformation and orientation (and vice versa) of erythrocytes,
as well as their shear rate effects were determined and the influence of a pulsatile flow on
the fluctuation of shear rate within the physiological range of heart frequency was
assessed. We also determined the relation between conductivity and haematocrit and
temperature. The aim of this study was to determine the precision and accuracy of the
modified conductance method to determine average CSAs of arteries in piglets. The

conductance method was validated by comparing the CSAs found with this method to those found using an IntraVascular UltraSound method (IVUS) [Wenguang et al. 1990, 1991]. The IVUS was chosen as a reference because no restraint is put on the vessel wall, when using this method.

2.2 Methods

2.2.1 Conductance method

The cross-sectional area (CSA) of a vessel can be obtained by the measurement of the conductance of intravascular blood with a catheter, which is constructed with four electrodes equidistantly (5 mm) placed along its distal end. An alternating current of 70 μA (RMS) at 20 kHz is applied (model Sigma 5, Leycom, Cardiodynamics, Rijnsburg, The Netherlands) to the outer electrodes. The induced voltage at the inner electrodes is measured. Because the strength of the applied current is constant, the voltage induced can be converted into the sum of the conductance of the blood and the surrounding tissue segment between the inner electrodes [Baan et al. 1984]. This time varying conductance (G(t) in 1/Ohm) is related to the time varying cross-sectional area (CSA(t) in mm^2) by the relationship:

$$G(t) = \frac{CSA(t) \times \sigma_b(T, Ht, SR)}{L} + G_p(t) \tag{1}$$

where $G_p(t)$ is the effective conductance of the structures outside the blood (1/Ohm); σ_b(T ,Ht ,SR) the electrical conductivity of the blood (1/[Ohm·mm]), which depends on temperature (T), haematocrit (Ht) and shear rate (SR) and L the distance between the electrodes (mm). If the average G_p over a heart cycle and σ_b are time-invariant, CSA can be solved from G(t) according to:

$$CSA(t) = \frac{L}{\sigma_b} [G(t) - G_p] \qquad\qquad (2)$$

The parallel conductance (G_p) is determined by changing the conductivity of blood with use of hypertonic saline injections [Baan et al. 1981, 1984]. During the passage of a hypertonic salt concentration, which appears as an indicator dilution curve, paired values for conductance at systole (G_{sys}) and at diastole (G_{dias}) are determined to calculate G_p as shown in Figure 1. The value of σ_b depends on haematocrit and temperature according to Equation 3, which is given in Appendix I. Furthermore σ_b has to be corrected for a pulsatile shear rate, depending on the flow profile as is present in the descending aorta (see Appendix I, Equation 5). We found that a constant correction factor for a pulsatile shear rate could be used if measured in the descending aorta of piglets. Changes of pH, PO_2 and PCO_2, within the physiological range, do not affect the electrical conductance [Gollan and Namon 1970].

2.2.2 IntraVascular Ultrasound System

To evaluate the precision and accuracy of the conductance method for the determination of cross-sectional areas (CSAs) of arteries, the results were compared with those of the IntraVascular UltraSound method (IVUS) (DuMed, Rotterdam, The Netherlands). This method utilized a 32 MHz single-element transducer mounted on the tip of a flexible driveshaft, which was rotating and placed inside a 5F catheter. Cross-sectional images with 512·512 pixels and 256 grey levels were scanned at a speed of 25 images per second [Wenguang et al. 1990, 1991]. Axial resolution of the system was better than 0.1 mm. The maximum scan depth was 9 mm. Aortic blood pressure was displayed and recorded simultaneously with the cross-sectional images on video tape. Ultrasound images were analyzed off-line for free lumen area determination using a computer analyzing system [Wenguang et al. 1990, 1991]. The contour of the free lumen was obtained by tracking the bright echoes of the internal elastic lamina.

2.2.3 Surgical procedures and ventilatory conditions

All experiments were performed in accordance with the "Guide for Care and Use of Laboratory Animals" published by the US National Institutes of Health [NIH publication No 85-23, Revised 1985] and under the regulations of the Animal Care Committee of the Erasmus University, Rotterdam, The Netherlands.

Five piglets (five weeks old, 8.7 ± 0.6 (SD) kg body weight) were anaesthetized with an intraperitoneal injection of sodium pentobarbital (30 mg/kg body weight). Each animal was placed in supine position on a thermo-controlled operation table to maintain body temperature at about $38.5\ ^{\circ}C$. Anaesthesia was maintained by a continuous infusion of sodium pentobarbital ($8.5\ mg \cdot h^{-1}.kg^{-1}$) via an ear vein. Subsequently, ECG electrodes were connected to the right leg and the chest of the pig. Thereafter, tracheostomy was performed and the pig was connected to a volume-controlled ventilator [Jansen et al. 1989]. A ventilatory frequency of 10 breaths per minute was used. Tidal volume was adjusted to a Pa_{CO2} of 38-45 mmHg during baseline. The pigs were ventilated with ambient air and with a positive end-expiratory pressure of $2\ cmH_2O$. The time ratio of inspiration to expiration was 2:3.

A conductance catheter (diameter $= 2.4$ mm) was inserted through the carotid artery into the descending thoracic aorta. The lumen (diameter $= 0.8$ mm) of the conductance catheter was used for measuring arterial pressure and for sampling of blood. From the opposite direction, an ultrasound imaging catheter was inserted through the external iliac artery. The distal ends of both catheters were situated almost against each other under radiographic guidance. We therefore assume that the same CSA was measured by both catheters.

Through the external jugular vein a Swan Ganz catheter was inserted to measure temperature and pressure within the pulmonary artery. In addition, a four lumen catheter was inserted through this vein into the superior vena cava to measure central venous pressure and to infuse pentobarbital and pancuronium. A third catheter was inserted through the external jugular vein into the right atrium to inject hypertonic saline for the

measurement of the parallel conductance.

To avoid clotting, the pressure catheters were continuously flushed at a flow rate of 3 ml per hour with normal saline, containing 10 I.U. heparin per ml. In total, 9 ml of fluid (90 I.U. heparin) was infused per hour. A catheter was placed into the bladder to avoid retention of urine. To suppress spontaneous breathing pancuronium bromide (0.3 $mg \cdot kg^{-1} \cdot h^{-1}$) was infused, after surgery and after a loading dose of 0.2 $mg \cdot kg^{-1}$ within three minutes. Pentobarbital infusion was changed from the ear vein to the vena cava superior. At the end of the protocol an overdose of pentobarbital was given.

2.2.4 Experimental protocol

The cross-sectional area was varied by changing the aortic pressure. Various levels of arterial pressure were created by inspiratory pause procedures (IPPs) in between the normal ventilations [Versprille and Jansen 1985]. An IPP is a procedure, in which a tidal volume is inflated and held in the lungs for several seconds, followed by an expiration. If tidal volume is inflated the left ventricular output and arterial pressures decrease and remain constant from 1-2 s to 9 s after the start of the pause period. Due to a lower arterial pressure the vessel volume was smaller during the IPP. In these experiments IPPs were characterized by inflation of different volumes with an inflation time of 2.4 s, an inspiratory pause of 9 s, followed by an expiration of 3.6 s. The stepwise increase in inflation volume for the IPPs was ended when the aortic pressure reached a critical level of approximately 40 mmHg during the IPPs. To calculate the conductivity of blood (σ_b), blood was sampled to determine haematocrit before each measurement. During the IPPs, pressures, ECG and the conductance signal were stored on a disk (250Hz) for off-line analysis. The ultrasound images were recorded simultaneously on video-tape together with the aortic pressure and the time signal. Stabilization periods of 5 minutes were allowed between the IPPs. Before the series of measurements parallel conductance was determined once from three successive injections of 1 ml hypertonic saline (3 M = 17.5%) for every piglet to obtain an accurate value of G_p. To prevent loading with salt, G_p was determined

using only these three injections assuming no influence of vessel volume on G_p.

This assumption was tested in a second series of measurements in the same five animals. Again various aortic pressure levels were created by the IPPs as mentioned before. At each pressure level the conductance and pressure signals were recorded at baseline and the signals were recorded during an injection of hypertonic saline to determine parallel conductance. To prevent loading with salt only one injection was given at each volume level. Next conductivity was determined by sampling of blood. In between these measurements stabilization periods of five minutes were inserted.

To study whether injections of hypertonic saline have an effect on the cross-sectional area of the aorta we analyzed beat-to-beat changes in CSA, estimated with the IVUS, during the passage of the saline. No significant influence of the injections on the $CSA_{(IVUS)}$ of the aorta could be detected ($p > 0.95$, $n = 10$, one experiment).

2.2.5 Calculations

To calculate the conductivity of blood (σ_b), haematocrit and blood temperature were determined (see Appendix I). This conductivity was corrected for shear rate (see Appendix I). To determine the parallel conductance (G_p) in the first series performed to evaluate the conductance method, the data obtained from the three injections of hypertonic saline were pooled. These pooled data were used to calculate G_p (see Fig.1). In the second series, performed to determine the influence of vessel volume on G_p, data from only one injection were used to calculate G_p. Cross-sectional areas (CSA) were obtained from substituting σ_b, L, G_p and measured conductance (G) in Equation 2. For the first series CSAs derived from the conductance method ($CSA_{(G)}$) and the intravascular ultrasound method ($CSA_{(IVUS)}$) were analyzed and averaged over a period of three seconds. For every measurement, the mean CSA obtained by the conductance method was compared with the mean CSA obtained from the 75 images (i.e. three seconds) with the IVUS. Data are presented as mean $\pm$ standard deviation.

2.3 Results

The determination of parallel conductance (G_p) for one experiment, pooling three data sets in the first series of observations, is shown in Figure 1. In all five animals we obtained a similar fit through the G_{sys}, G_{dias} data points if three measurements were pooled ($r >$ 0.98).

For each experiment of the second series, parallel conductance was constant throughout the experiment and did not depend on vessel volume. For each experiment we determined parallel conductance for each pressure level and plotted parallel conductance versus pressure. Through these values we fitted a linear regression line. The derivatives of the five lines did not deviate significantly from zero. The variation in G_p within each experiment of the second series, was between 3 and 14%. The average G_p for each experiment was averaged for the five experiments (44.4 $\pm$ 4.2 [mOhm^{-1}], n = 5). These values did not differ significantly from the average G_p derived from the G_p's estimated from the pooled data of the first series (44.1 $\pm$ 2.5 [mOhm^{-1}], n = 5).

The continuous signal of cross-sectional area, calculated with the conductance method ($CSA_{(G)}$), in relationship to the CSA signal, determined with the intravascular ultrasound imaging method ($CSA_{(IVUS)}$), and the aortic pressure signal are shown in Figure 2. The CSA signal, obtained by the IVUS signal, shows approximately the same pattern as the CSA signal, obtained by the conductance method. However, a considerable intra-individually spread in the determination of CSAs obtained by the IVUS can be observed. The difference between minimum and maximum CSA, as obtained by the IVUS, was in general smaller than the difference between minimum and maximum CSA, as obtained by the conductance method.

The delay between the minimal value of the conductance signal with respect to that of the pressure signal as well as the delay between the maximal values was 0.007 $\pm$ 0.015 s, which is not significantly different from zero (p = 0.99). Thus, no phase-shift was detected between those points. If the CSA versus aortic pressure over a heart beat is
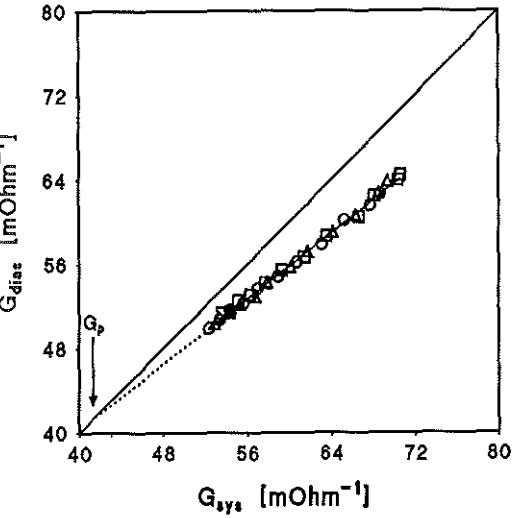
Fig. 1. A linear regression line is fitted through the conductance values determined at systole (G_{sys}) versus those at diastole (G_{dias}). The data were obtained from three hypertonic saline injections as is indicated by the three different symbols. The solid line is the line of identity. The regression line is extrapolated to the theoretical point where conductivity of blood is zero. Here $G_{sys} = G_{dias} = G_p$.
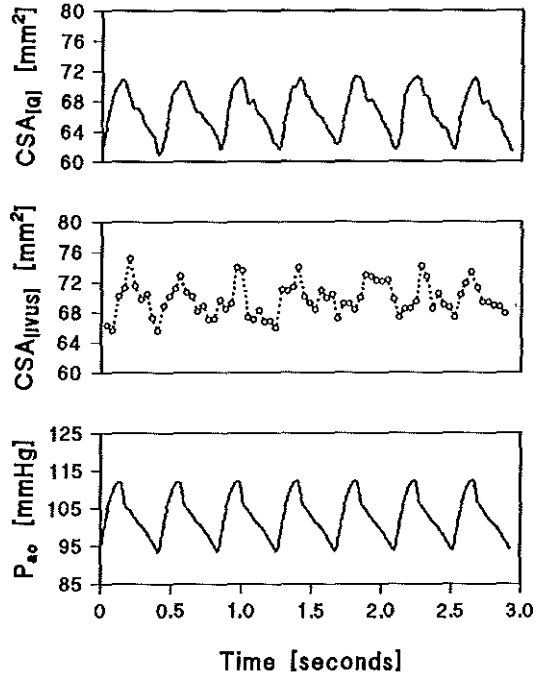
Fig. 2. The CSA calculated from the conductance signal ($CSA_{(G)}$) is given in the upper panel. The time synchronous CSA obtained from the intravascular ultrasound imaging method ($CSA_{(IVUS)}$) is shown in the panel in the middle as open circles. In the lower panel the time synchronous aortic pressure (P_{ao}) is shown.
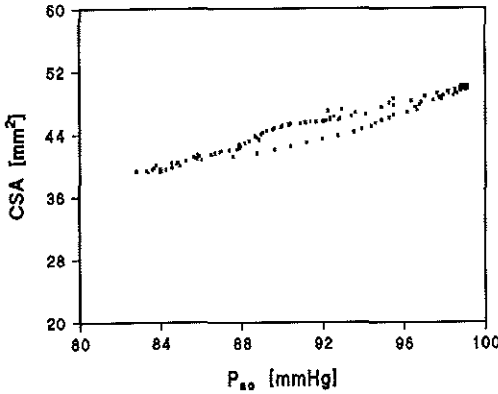
Fig. 3: Cross-sectional area versus aortic pressure throughout a heart cycle.

plotted, a loop is obtained, which is closed near the minimum and maximum values but is slightly open in the middle (Fig.3). No fluctuating influence of shear rate was detected, whereas this would be manifested by a loop, which would be open at the end of diastole due to a decreasing influence of shear rate on conductivity. The openness of the loop in the middle indicates some hysteresis of the vessel wall.

The relationship between the intravascular CSAs, averaged over three seconds, determined with the conductance method, $CSA_{(G)}$, and the intravascular ultrasound method, $CSA_{(IVUS)}$, is presented in Fig.4a for five piglets (n = 53). The regression line is close to the line of identity ($CSA_{(G)} = -0.086 + 0.999 \cdot CSA_{(IVUS)}$), and the correlation coefficient is 0.97. In a Bland-Altman scatter diagram [Altman 1990], we plotted the differences between the two types of CSAs against their means (Fig.4b). In the scatter diagram the precision and the bias of the method can be observed. It indicates the distribution of random or systematical errors and a possible dependence of the errors on the size of the blood vessel. These aspects are more difficult to deduce from the correlation diagram. The difference in CSA was independent of the diameter of the vessel and was on average -0.11 mm^2 $\pm$ 2.79 mm^2 or -0.29% $\pm$ 5.57% (2SD) of the average CSA,

as obtained with the IVUS, and the conductance method. This is not significantly different from zero.
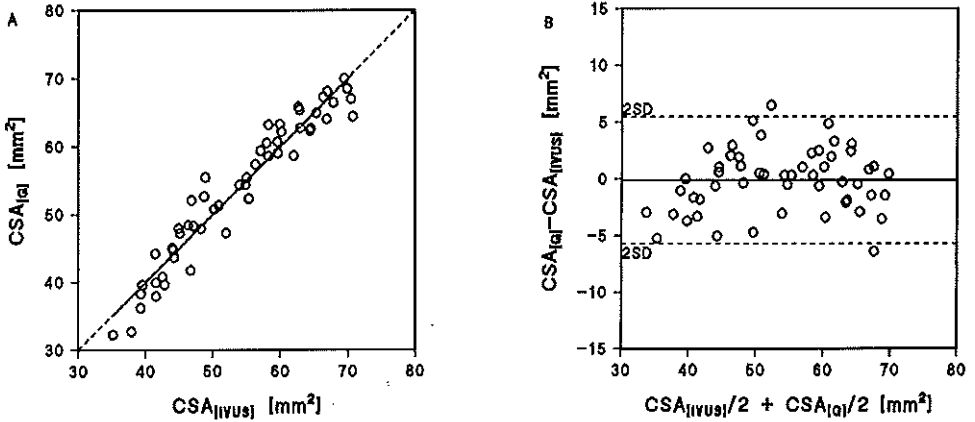
Fig. 4.A: Correlation between the average results of the conductance method ($CSA_{(G)}$) and those of the IVUS ($CSA_{(IVUS)}$). The best linear fit is given by the solid line. The line of identity is indicated as the dashed line. B: Scatter diagram of the differences between the CSAs obtained with the conductance method and the IVUS are plotted versus their means. The solid line indicates the mean difference and the dashed lines indicate the 95% confidence interval (2SD). The distribution of the differences is not significantly different from normal (kurtosis variable = -0.20, standard error = 0.64).

2.4 Discussion

2.4.1 Conductance method

To increase the precision in the determination of parallel conductance, the data of three salt dilution procedures were pooled to obtain one value of parallel conductance for each

piglet. We assumed this parallel conductance to be constant throughout the experiment independent of the condition of the animal. This assumption was tested in a second series, where only one injection was given at each aortic pressure (i.e. CSA) to prevent deterioration of the hemodynamic stability of the animal by loading with hypertonic saline injections. No influence of aortic volume on parallel conductance could be detected. This is in agreement with studies of the left ventricle, where much larger changes in volume did not change parallel conductance in spite of a volume change in the adjacent right ventricle [Lankford et al. 1990, Szwarc et al. 1994]. We conclude that parallel conductance could be determined in each experiment with three successive hypertonic saline injections and that the value could be used for all observations.

A potential source of error in the conductance measurement could be produced by a movement of the catheter perpendicular to the flow direction. This error was calculated to be maximally 7% [Axenborg and Olson 1979]. We found the conductance catheter to be in the middle of the vessel using biplane radiographic imaging. Also, the catheter was visualized in the middle of the vessel by the ultrasound imaging catheter if this catheter was moved up until its tip was positioned at the wall next to the conductance catheter. Furthermore, to avoid changes in the catheter position due to ventilatory movements we measured during an inspiratory pause.

The slope factor α is commonly used in ventricular conductance studies to correct for an inhomogeneous field. A non-homogeneous electrical field might cause parallel conductance to be volume dependent [Kun and Peura 1994]. In our experiments, parallel conductance is independent of aortic volume, including that α is 1.

Furthermore, we found in vitro linear relations between conductance and cross-sectional area as measured in glass tubes up to 257 mm^2 if a distance between the electrodes was chosen of 5 mm (Appendix, first paragraph). If the distance was smaller (3 mm) the relation between conductance and cross-sectional area was not linear anymore. We therefore assumed that a homogeneous electrical field was present in the in vitro experiments if the distance between the electrodes was 5 mm. In vivo we determined

cross-sectional areas, which were within the same range as in the in vitro experiments using also a distance between the electrodes of 5 mm, indicating that also in vivo a homogeneous electrical field was present causing the slope constant to be close 1. The homogeneity of the electrical field is probably due to the fact that the diameter of the vessel was small in comparison to the distance between the electrodes.

2.4.2 Evaluation

As shown in Figure 2 the CSA can be determined continuously with use of the conductance signal and the correction factors for temperature (Equation 3), haematocrit, shear rate (Equation 5) and parallel conductance (Fig.1). For a certain haematocrit, the influence of shear rate on conductivity of porcine blood was about three times smaller than the influence of shear rate on the conductivity of human blood as found by Visser et al. [1976, 1989] and Sakamoto et al. [1979]. This difference might be explained by the higher deformability of the human erythrocytes than that of the porcine erythrocytes as found by us (see Appendix II). We did not evaluate the continuous changes in CSA within the heart cycle by means of the IVUS because of its too low sample frequency (25 Hz) and too high intra-observer variance [Wenguang et al. 1991] (Fig.2). Furthermore, the calculated CSAs are the result of a scan with a duration of $1/25$ s $= 40$ ms. During the scan the CSA changes. Therefore, the CSAs at systole will be under-estimated and the CSAs at diastole will be over-estimated by the IVUS, resulting in a smaller difference between those values than the difference we found with the conductance method. Due to these shortcomings of the IVUS we could not determine CSA continuously with the IVUS and therefore could not evaluate the continuous value of the CSA obtained with the conductance method and study the change in influence of shear rate with use of a plot of CSA_G versus CSA_{IVUS}. To avoid the effects of the too high intra-observer variance and too low sample-frequency of the IVUS we compared the averaged CSAs obtained by both methods. The maximum distance detectable with the IVUS was 9 mm [Wenguang et al. 1990]. We excluded CSAs with a diameter larger than 9 mm because the IVUS catheter

was always positioned against the vessel wall, as observed by biplane radiographic imaging and ultrasound imaging. The CSA estimated by the conductance method is the average value between the measuring electrodes (5 mm), whereas the CSA estimated by the IVUS is the value at one single plane. Furthermore the single plane is not within the range of the measuring electrodes of the conductance method. We assumed that these differences only caused a very small bias in our results, [Caro et al. 1978, Boesiger et al. 1992] because both probes were located almost against each other in the descending aorta.

It should be noted that the difference between the cross-sectional areas found with use of the IVUS and the conductance catheter may be related to the error caused by inter-observer variance of the IVUS. The intra-observer variation of the IVUS [Wenguang et al. 1991] could be neglected, because one data point was the mean of 75 images.

Based on our results, we concluded that the conductance method is a reliable technique for estimating cross-sectional areas of the descending aorta in intact piglets.

2.5 Appendix I

2.5.1 Effect of cross-sectional area on conductance

Under no-flow conditions, the linearity of the conductance versus cross-sectional area relation was tested using a conductance catheter (diameter = 2.2 mm) with a distance between the electrodes of 5 mm. Conductance of porcine blood was determined in glass tubes, with various CSAs by positioning the catheter axially in a tube. The measurements were performed at 38.5^0C (physiological temperature in piglets) using blood with various haematocrits. Before measuring, the blood was stirred to prevent precipitation and aggregation of erythrocytes. The internal diameter of the glass tubes was measured with a micrometer. Parallel conductance was not present. We found a linear relationship between total conductance and cross-sectional area up to 250 mm^2 (diameter = 18 mm) (Fig.5). We expect that this linear relationship also holds for our in vivo experiments, where

diameters up to 9 mm are measured in the presence of parallel conductance.
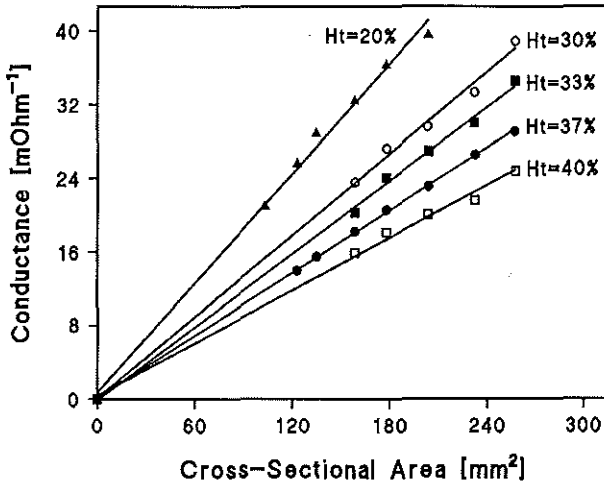
Fig.5: Relation between conductance and cross-sectional area as measured in glass tubes for various haematocrits.

2.5.2 Effect of temperature and haematocrit on conductivity

The effect of temperature on conductivity was determined with the use of a cell with four electrodes (Leycom Sigma 5DF). The cell was placed in a water bath at temperatures between 30 and 40 °C. The blood temperature was measured with a thermistor inside the cell. Immediately before each measurement, the blood was shaken to avoid precipitation and aggregation of erythrocytes. The conductivity at a given temperature was determined in a blood mixture of six pigs at four different haematocrits and plasma after step by step changes in temperature in both directions. We obtained linear regression lines (Fig.6, Table 1). Multiple linear regression was used on all data points. We found a composite equation for conductivity with temperature and haematocrit as parameters, according to:

$$\sigma_b = -1.17 \times 10^{-4} \times Ht + 2.33 \times 10^{-4} \times T - 3.82 \times 10^{-6} \times Ht \times T + 6.65 \times 10^{-3} \quad (3)$$

where σ_b is the blood conductivity in 1/[Ohm·cm], Ht the haematocrit in % and T the temperature in °C. The correlation coefficient for this multiple regression is 0.9998.
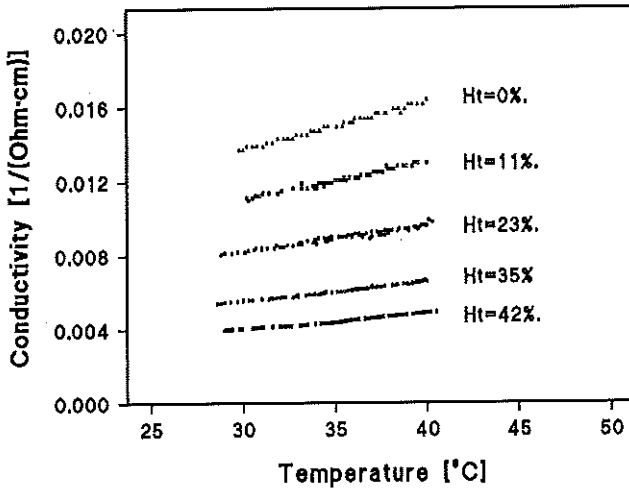
Fig. 6. Relation between conductivity (σ_b) and temperature for various haematocrits (Ht).

Table I: Dependence of the conductivity of porcine blood on temperature and haematocrit

Number of data points	Haematocrit [%]	Conductivity [1/(Ohm·cm)] $\sigma = aT + b$	Correlation Coefficient
63	42	$8.47 \cdot 10^{-5} \cdot T + 1.46 \cdot 10^{-3}$	0.996
86	35	$1.04 \cdot 10^{-4} \cdot T + 2.39 \cdot 10^{-3}$	0.996
82	23	$1.37 \cdot 10^{-4} \cdot T + 4.10 \cdot 10^{-3}$	0.996
59	11	$2.11 \cdot 10^{-4} \cdot T + 4.66 \cdot 10^{-3}$	0.997
51	0	$2.53 \cdot 10^{-4} \cdot T + 6.11 \cdot 10^{-3}$	0.997

2.5.3 Effect of shear rate on conductivity

Shear rate is defined as the gradient of velocity and is expressed in s^{-1}. The effect of shear rate was determined in a closed-loop circuit at a constant temperature at 38.5°C in a water bath. A constant blood flow was maintained by a peristaltic roller pump. Oscillations caused by the pump were damped in a compliant reservoir. The blood flowed through a glass tube having a diameter of 15 mm, in which the conductance catheter (inter-electrode distance = 5 mm, diameter = 2.4 mm) was situated along the longitudinal axis. The entrance length of the system (distance between glass tube and reservoir) was 50 cm in order to obtain a stable parabolic flow profile [Caro et al. 1978, Boesiger et al. 1992]. The conductivity of the blood was determined at various haematocrits for various flows in triplicate. The flow was constant for at least five minutes before measuring.

The percent increase in conductivity as a function of shear rate (the average of the three determinations, averaged over the CSA), for various haematocrits is shown in Figure 7a. With increasing shear rate (assuming a parabolic flow profile, mean shear rate = -$2<v>/r$, where $<v>$ = average velocity and r = radius), conductivity was increased up to a maximum. This maximum was higher at higher haematocrits. We found a maximum increase of 14% for a haematocrit of 45%. For all haematocrit values, the maximal effect of shear rate on conductivity was found above an average shear rate over CSA of about 13 s^{-1}. We averaged the plateau values for each haematocrit and plotted them as a function of haematocrit (Fig.7b). The best fit through these points was described by:

$$\Delta\sigma_b = 0.5 \times [\Delta\sigma_{max} + \Delta\sigma_{max} \times (1 - e^{-K|Ht-X50|}) \times sign(Ht-X50)] \qquad (4)$$

with the following fit parameters: X50   = 38. $\pm$ 0.42

K   = 0.16 $\pm$ 0.01

$\Delta\sigma_{max}$ = 16. $\pm$ 0.67

where $\Delta\sigma_b$ is the increase in conductivity in percent, X50 the haematocrit in percent at the steepest slope of the relationship, K the steepness of the fit in percent increase in

conductivity divided by percent haematocrit and $\Delta\sigma_{max}$ the maximum increase in conductivity in percent. Sign(Ht-X50) is +1 if the haematocrit is larger than 38%, -1 if the haematocrit is smaller than 38% and 0 if the haematocrit equals 38%.
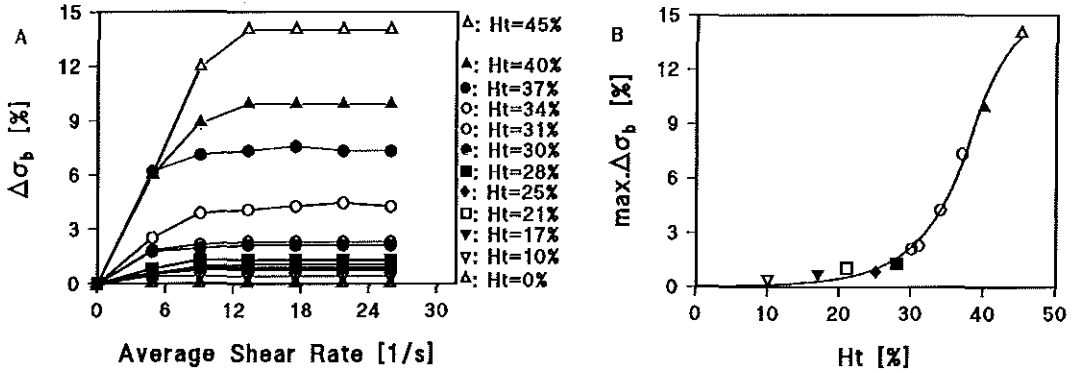
Fig. 7. A: Change in conductivity ($\Delta\sigma_b$) versus shear rate for twelve haematocrits (Ht) between 0 and 45%. It should be noted that the absolute zero level of $\Delta\sigma_b$ is different for various haematocrits. B: The maximum values of $\Delta\sigma_b$ (max.$\Delta\sigma_b$) in Figure 4a are plotted against haematocrit (Ht).

The conductivity of stagnant blood should be multiplied with the correction factor of equation 5 to obtain the conductivity of flowing blood.

$$C_{SR} = (1 + \frac{\Delta\sigma_b}{100})$$ (5)

If we extrapolate the data as shown in Fig. 9 of the paper of Boesiger et al. [1992] we expect that in vivo in the descending thoracic aorta the shear rate of 13 1/s will be exceeded during throughout almost the whole systole. The real flow pattern will be disturbed in the middle due to the central position of the catheter, causing even more shear rate than present with no catheter. We could use the correction C_{SR} in vivo because

the catheter position in vivo was the same in vivo as in vitro.

2.5.4 Time constants and influence of shear rate

The conductivity of blood depends on orientation, deformation and de-aggregation of blood caused by blood flow. The time courses of de-aggregation, deformation and orientation of erythrocytes (and vice versa) were studied by measuring the backscattering of laser light in blood (LORCA: Laser-assisted Optical Rotational Cell Analyzer, R&R Mechatronics, Hoorn, The Netherlands) [Hardeman et al. 1987, 1994]. Three phases in the diffraction of light could be detected. If a high shear rate is present erythrocytes are deformed into prolate ellipsoids with their axis aligned parallel to the flow direction. If the flow is suddenly stopped the erythrocytes get their original shape and will be oriented randomly. In the transient to random orientation a steep increase of light diffraction is shown ('upstroke'). Subsequently, the erythrocytes will aggregate resulting in a decrease of diffraction. The diffraction of aggregated blood is smaller than that of flowing blood. At acceleration, the opposite sequence will occur.

To measure the effects of deceleration and acceleration, 1-2 ml of oxygenated blood was sheared between the walls of two nested cups at a wall shear rate of 500 s^{-1}. The outer cup rotated, and the other one did not. The smaller cup had an outer radius of 17.360 mm and the larger cup had an inner radius of 17.705 mm, so the layer of blood in between was 0.345 mm thick. The rotation was abruptly stopped or started and the changes in the intensity of backscattered laser-light were determined. The acceleration as well as the deceleration measurements were performed by using six blood samples in duplicate. A sudden increase in shear rate caused a stepwise change in backscatter due to de-aggregation, orientation and deformation of erythrocytes in less than 40 ms in all blood samples. The average time for the erythrocytes to de-orientate to random positions and to return to their normal non-flow shape was 240 ms (Table 2). Aggregation had an average time constant of $t_{1/2} = 1.71$ s (Table 2).

The duration of diastole between two heart-beats of a piglet is between 125 and 200 ms

[Versprille and Jansen 1985]. Based on these times, and the time constants for (de)-orientation, (de)-formation and (de)-aggregation, we concluded that the erythrocytes are still mainly de-aggregated, orientated and deformed at the end of diastole. If the total amount of erythrocytes is plotted versus the time within a heart cycle, the percent of de-orientated and reformed erythrocytes will correspond to maximally 17% of the area under the curve assuming diastole takes as long as 200 ms. At a haematocrit of 35%, this would include a change in correction for shear rate of about 5% to (83% · 5% =) 4%. For higher heart rates this change in correction would be less than 1%. The change in correction was therefore neglected and the maximum correction of conductivity at a given haematocrit (Eq.5) has therefore been used throughout the whole heart cycle.

Table II: The time constants for the backscatter of laser-light at sudden decrease of shear rate are presented for six haematocrits. The second column shows the time from t=0 to the peak of backscatter (t). This is the time the erythrocytes retain their normal non-flow shape and de-orientate to random positions. The third column shows the time that half of the erythrocytes has been aggregated ($t_{1/2}$). The duplicate blood samples of each pig gave the same values.

Haematocrit pig [%]	t (reform, de-orientate) [s]	t (1/2 aggregation) [s]
28	0.23	2.27
35	0.22	2.71
35	0.31	1.64
36	0.24	1.31
38	0.25	1.25
40	0.20	1.10
Average Standard Deviation	0.24 0.04	1.71 0.64

2.6 Appendix II

2.6.1 Deformability Index

The higher maximun influence of shear rate on conductivity of human blood than for porcine blood might be explained by the smaller deformability index of the porcine erythrocytes than that of the human erythrocytes (Fig. 8). The deformability index is (A-B)/(A+B), where A is the axis of the erythrocyte in the direction of the blood flow and B is the axis perpendicularly positioned at radius A. The deformability index of human and porcine erythrocytes was measured at various shear stresses at $21^{\circ}C$ using the LORCA (Laser associated Optical Rotational Cell Analyzer) developed by the department of Rheology at the university of Amsterdam [Hardeman 1987]. Shear stress is shear rate multiplied by the viscosity of the suspending medium. Blood was diluted with Rheomacrodex (100 g/l) and glucose.H_2O (55 g/l), obtained from Pharmacia AB.Sweden, and centrifuged in a cup with an inner radius of 17.360 mm and an outer radius of 17.705 mm. Mohandas et al. [1980] found that dextran only minimally influences deformability. At various shear stresses the transmission of a laser beam was determined (number of repeats per measurement = 15). The transmission was converted into a deformability index. The deformability index first increased with applied shear stress and next reached a plateau. The average maximum deformability index for human erythrocytes (n = 6) was 0.62 $\pm$ 0.01 (SD) whereas the maximum deformability index for piglets (n = 6) was 0.46 $\pm$ 0.03 (SD) (Fig.8).
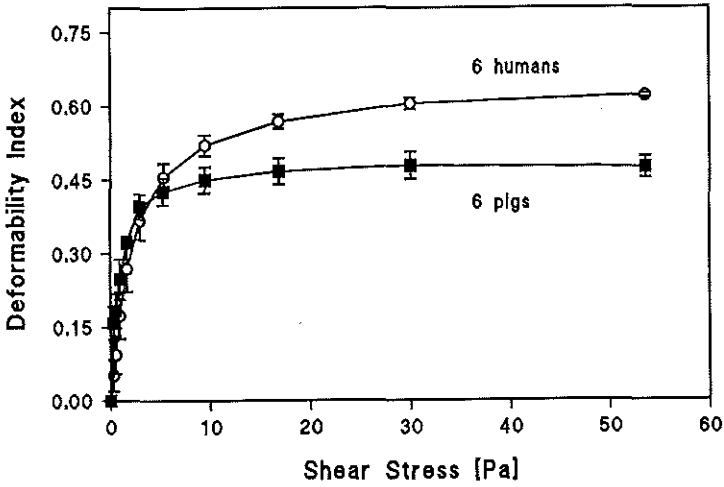
Fig. 8: The deformability index of erythrocytes of pigs and humans is plotted versus shear stress.

Chapter 3

The Compliance of the Porcine Pulmonary Artery
Depends on Pressure and Heart Rate

L Kornet[1], JRC Jansen[1], FCAM te Nijenhuis[1],
GJ Langewouters[2] and A Versprille[1]

1)   Pathophysiological Laboratory, Department of Pulmonary Diseases, Erasmus
     University, Rotterdam, The Netherlands
2)   TNO Biomedical Instrumentation, Academic Medical Centre, Amsterdam, The
     Netherlands

3.1 Introduction

To compute pulmonary blood flow beat-to-beat from the arterial pressure curve by using a windkessel model, the dynamic compliance of the pulmonary artery must first be known. Dynamic compliance is the change in cross-sectional area (CSA) related to the change in pulmonary arterial pressure (P_{pa}) during a heartbeat (see Chapter 1, Fig. 1). Static compliance is the change in mean CSA related to the change in mean P_{pa} (see Chapter 1, Fig.1). We define static compliance measured in vivo as pseudo-static compliance, because the pressure and CSA fluctuates cyclically during one heartbeat.

In most literature on vessel compliance no distinction is made between static, pseudo-static and dynamic compliance, e.g. instead of dynamic compliance, static compliance, as obtained from in vitro experiments [Langewouters 1984], was used for the aorta to compute aortic blood flow [Jansen et al. 1990, Weissman et al. 1993, Wesseling et al. 1993]. This is possible only if creep is negligible and no influence of pressure and heart rate is present. Various authors, indeed, found that creep of the pulmonary artery is negligible [Gozna et al. 1974, Greenfield and Griggs 1963, Ingram et al. 1970, Johnson and Henry 1985, Patel et al. 1960, Shelton and Olson 1972]. They also found a constant dynamic compliance over a limited range of pulmonary arterial pressure. However, other authors predicted an effect of pressure on dynamic compliance if windkessel models were used to describe the pulmonary arterial circulation [Grant et al. 1991, Lieber et al. 1994]. Furthermore, it has been suggested that heart rate is a major determinant of aortic compliance [Marcus et al. 1994]. Accordingly, aortic compliance has been adjusted for pressure and heart rate to compute aortic blood-flow beat-to-beat from the aortic pressure, using windkessel models [Jansen et al. 1990, Weissman et al. 1993, Wesseling et al. 1993]. In anaesthetized pigs, we compared the relation between mean CSA and mean pulmonary arterial pressure obtained over a large pressure range under conditions of a spontaneously changing heart rate to that obtained at a constant heart rate. Furthermore, we studied whether dynamic compliance of the pulmonary artery is constant during a

cardiac cycle, and we compared the relationship between dynamic compliance and mean pulmonary arterial pressure in both series. CSA was determined using a conductance method [Baan et al. 1984].

3.2 Methods

3.2.1 Surgical procedures and ventilatory conditions

All experiments were performed in accordance with the "Guide for Care and Use of Laboratory Animals" published by the US National Institute of Health [NIH publication No. 85-23, Revised 1985] and in accordance with the regulations of the Animal Care Committee of the Erasmus University, Rotterdam, The Netherlands.

Nine piglets (5-7 weeks old, 12.0 $\pm$ 1.3 kg body weight) were anaesthetized with an intraperitoneal injection of pentobarbital sodium (30 mg·kg^{-1} body weight). The animals were placed in supine position on a thermo-controlled operating table to maintain body temperature at about 38.5 °C. Anaesthesia was maintained by a continuous infusion of pentobarbital sodium (8.5 mg·kg^{-1}·h^{-1}) via an ear vein. ECG electrodes were placed subcutaneously in the right leg and on the chest near the xyphoid cartilage. After tracheostomy, the pigs were connected to a volume-controlled ventilator [Jansen et al. 1989] ventilated with ambient air. The ventilatory rate was set at 10 breaths per minute. Tidal volume was adjusted to a P_{aCO2} of 38-42 mmHg during baseline. The ratio of inspiration to expiration was 2 : 3. A positive end-expiratory pressure of 2 cmH$_2$O was applied.

A catheter was inserted through the right common carotid artery into the aortic arch for measuring arterial pressure and sampling of blood. A four-lumen catheter was inserted via the right external jugular vein into the superior vena cava to measure central venous pressure, to inject a hypertonic salt solution and to infuse pentobarbital and pancuronium. After thoracotomy at the left site of the sternum, a four electrode catheter

surrounded by a fluid-filled sheath for measuring pressure, was inserted through the right ventricular wall into the pulmonary artery to measure its CSA by the electrical conductance method and temperature of the pulmonary arterial blood. The pressure-transducer was located merely 10 cm from the site of measurement, to avoid damping of the pressure signal by the fluid sheath [Baan et al. 1971]. All electrodes of the conductance catheter were positioned in the pulmonary trunk with the proximal electrode downstream from the pulmonary valve and outside the pressure sheath. The thorax remained open during the experiment; thus pulmonary arterial pressure was equal to transmural wall pressure. A pacemaker electrode was fixed at the right auricle.

To avoid clotting in the catheters, the three pressure catheters were continuously flushed at a flow rate of 3 ml·h^{-1} with saline (0.9% NaCl) containing 10 I.U. heparin per ml. A catheter was placed in the bladder to prevent retention of urine. After the surgical procedures, pancuronium bromide (0.3 mg·kg^{-1}·h^{-1}, after a loading dose of 0.2 mg·kg^{-1}) was given intravenously to suppress spontaneous breathing. The pentobarbital infusion was switched from the ear vein to the vena cava superior. The surgical procedures were followed by a stabilization period of about half an hour.

3.2.2 Conductance method

To determine the cross-sectional area (CSA) of the pulmonary artery, the vascular conductance method was modified from the intra-ventricular conductance method [Baan et al. 1984]. Here, only the essentials will be presented. The catheter has four electrodes equidistantly (5 mm) placed at its distal end. An alternating current of 70 μA (RMS) and 20 kHz is applied to the two outer electrodes and the induced voltage is measured at the two inner electrodes using a model Sigma 5 signal conditioner-processor (Leycom, Cardiodynamics, Rijnsburg, The Netherlands). An offset is caused by the conductance of the surrounding tissues, which is called parallel conductance. The time varying cross-sectional area (CSA(t) [mm^2]) is related to the time varying measured conductance (G(t) [1/Ohm]) by the relationship:

$$CSA(t) = \frac{L}{\sigma_b(t)} (G(t) - G_p) \tag{1}$$

where G_p is parallel conductance [1/Ohm], L the distance between the electrodes [mm] and $\sigma_b(t)$ the electrical conductivity of the flowing blood [1/(Ohm·mm)].

G_p is determined by changing the conductivity of blood with the use of salt injections [Baan et al. 1984] During passage of a hypertonic salt concentration, which gradually decreases as a dilution curve, a series of paired G_{sys} (conductance at systole) and G_{dias} (conductance at diastole) values can be obtained. If the linear regression line through these values is extrapolated to the point where conductivity of blood is zero, G_{sys} = G_{dias} = G_p.

In vitro experiments [Chapter 2] revealed that conductivity of stagnant blood (σ_b(static) [1/{Ohm·cm}]) depends on temperature (T [^{0}C]) and haematocrit (Ht [%]) according to:

$$\sigma_b(static) = -1.17 \times 10^{-4} \times Ht + 2.33 \times 10^{-4} \times T - 3.82 \times 10^{-6} \times Ht \times T + 6.65 \times 10^{-3} \tag{2}$$

The Pearson correlation coefficient of this multiple regression is 0.9998. This conductivity needs to be corrected for shear rate caused by blood flow, which leads to orientation and deformation of erythrocytes [Sakamoto and Kanai 1979]. The maximum effect of shear rate on conductivity was found above a shear rate of 13/s, averaged across the CSA of the glass tube [Chapter 2]. The maximum effect of shear rate on the percentage increase in conductivity ($\Delta \sigma_b$) is related to haematocrit (Ht) in percentage according to:

$$\Delta \sigma_b = 0.5 \times [\Delta \sigma_{max} + \Delta \sigma_{max} \times (1 - e^{-K|Ht-X50|}) \times sign(Ht-X50)] \tag{3}$$

with the following fit variables: X50 $= 38.20 \pm 0.42$

K $= 0.16 \pm 0.01$

$\Delta\sigma_{max} = 16.48 \pm 0.67$

where X50 is the haematocrit in percentage at the steepest slope of the relationship, K the steepness of the fit in percentage increase in conductivity divided by percentage haematocrit and $\Delta\sigma_{max}$ the maximum increase in conductivity in percentage. Sign(Ht-X50) is +1 if the haematocrit is larger than 38%, it is -1 if the haematocrit is smaller than 38% and it is 0 if the haematocrit equals 38%. Maximum shear rate is exceeded almost throughout systole [Sømod et al. 1993], particularly if a catheter is positioned in the vessel. We found that erythrocytes orientate and deform almost instantaneously and de-orientate and reform in 240 ± 40 ms [Chapter 2] which is longer than the diastolic period for the animals described in this paper. Therefore, to obtain conductivity of flowing blood (σ_b), conductivity of stagnant blood (σ_b(static)) was multiplied with a constant correction factor for the influence of shear rate (F_{SR}) throughout the heart cycle according to:

$$F_{SR} = 1 + \frac{\Delta\sigma_b}{100} \qquad (4)$$

3.2.3 Experimental protocol

Using nine animals, we performed a series of observations at a spontaneously changing heart rate, followed by a second series in six of these animals performed at a constant heart rate, which was about equal to the highest value of the first series. Before each series, parallel conductance (G_p) was determined from the data obtained after three injections of a hypertonic salt solution (5ml, 3M), each injected during an expiratory pause of 12 seconds. During both series, mean pulmonary arterial pressure was changed by decreasing blood volume in steps of 10 to 20 ml every three minutes. This bleeding procedure was stopped at an aortic pressure of approximately 40 mmHg. Shortly before

each bleeding, 0.5 ml blood was sampled to determine haematocrit. Next, the signals of the pulmonary arterial pressure, blood temperature and electrical conductance were sampled during an expiratory pause of 12 seconds at a frequency of 250 Hz. The signals were stored on a hard disk for off-line analysis. After each series, all blood of the bleeding steps was slowly reinfused.

3.2.4 Calculations

Haemodynamic variables, such as pulmonary arterial pressure, venous pressure, aortic pressure, heart rate and CSA, were determined at normovolaemic baseline conditions and after maximal bleeding. Each of the variables was averaged over all heart cycles for 5 seconds of an expiratory pause period. To calculate mean CSA, the average total conductance was used according to the equations 1 - 4.

Pseudo-static compliance (i.e. $C_{ps} = \Delta mCSA/\Delta mP_{pa}$) is the derivative of the mean CSA versus mean P_{pa} relationship. Dynamic compliance (i.e. $C_d = \Delta CSA/\Delta P_{pa}$) is the slope of the linear regression line through the CSA versus pulmonary arterial pressure values during the heart cycles. Dynamic compliance can be determined without determination of parallel conductance, because this term only introduces an offset in the CSA signal. Because some de-orientation and shape recovery of erythrocytes might occur at the end of diastole, we validated whether such an effect of de-orientation and reformation at diastole caused a significant error in the determination of compliance obtained from the whole heart cycle. For this reason, compliances, determined from systolic periods, were compared with compliances determined from diastolic periods obtained during 5 seconds in an expiratory pause procedure. A systolic period was defined as the period from end-diastolic pressure to the incisura of the dicrotic notch of the peak systolic pressure. A diastolic period was defined as the period from the incisura of the dicrotic notch to the end-diastolic pressure. No significant difference existed between dynamic compliances determined during the systolic periods and those determined during the diastolic periods (mean difference $C_{d,systole} - C_{d,diastole} = 0.007 \pm 0.081$ (SD) [$mm^2/mmHg$], p = 0.003,

paired t-test, n = 227). These findings supported our previous conclusion that the effect of shear rate on conductivity can be considered constant during the whole heart cycle. The reason for this is the high heart rate in piglets. We used dynamic compliance obtained from the whole heart cycle, using one correction factor for shear rate.

Data are presented as mean ± standard deviation.

3.3 Results

3.3.1 Haemodynamic variables

The haemodynamic data at normovolaemic baseline conditions and those after maximal bleeding are given for both series in Table 1.

Variable	series 1, at changing heart rate		series 2, at constant heart rate	
	baseline	maximal bleeding	baseline	maximal bleeding
mP_{ao} [mmHg]	84.41 ± 9.36	38.96 ± 11.88	90.12 ± 9.44	42.11 ± 9.07
mP_{pa} [mmHg]	20.26 ± 5.60	11.00 ± 2.93	26.78* ± 3.99	12.75 ± 2.99
mP_{cv} [mmHg]	4.25 ± 2.44	1.75 ± 1.57	6.04 ± 1.67	2.01 ± 1.63
HR [Hz]	2.17 ± 0.36	3.75 ± 0.43	3.85 ± 0.31	3.85 ± 0.31
mCSA [mm^2]	160.3 ± 34.4	104.1 ± 43.8	154.8* ± 36.7	121.7 ± 38.1

Table 1: For six experiments the haemodynamic variables are given for both series at baseline and after maximal bleeding: mean pulmonary arterial pressure (mP_{pa}), mean aortic pressure (mP_{ao}), mean central venous pressure (mP_{cv}), heart rate (HR) and mean cross-sectional area (mCSA). * ; change is significant compared to the same volemic condition in series 1.

Mean pulmonary arterial pressure (mP_{pa}) was significantly higher (paired t-test, n = 6, p < 0.05, Fig.1) and mean CSA significantly lower (paired t-test, n = 6, p < 0.05, Fig.1) at the start of the second series at a high heart rate than the corresponding values at the start of the first series where heart rate was low. Mean aortic pressure (mP_{ao}) and mean central venous pressure (mP_{cv}) were not significantly different (paired t-test, n = 6, p > 0.05). After maximal bleeding at the end of series 1 and at the end of series 2, no significant differences were found between mP_{ao}, mP_{pa}, mP_{cv}, HR and mean CSA (paired t-test, n = 6, p > 0.05).

3.3.2 Pseudo-static compliance

The mean pulmonary arterial CSA versus mean P_{pa} relationships measured at spontaneously changing and at constant heart rates is presented in Figure 1. In all series each bleeding step caused a lower P_{pa} and a lower CSA. The shape of the CSA versus P_{pa} curve was sigmoid for both series. During series 1, heart rate (HR) increased with successive steps of bleeding. In all experiments the CSA versus pressure relationship was steeper for series 1 at increasing heart rate than for the series 2 at constant heart rate. The largest change in CSA coincided with the largest change in HR. After reinfusion of blood the CSA and heart rate returned to their normovolaemic baseline values.

To find the best mathematical description of the relationship between CSA and pressure, we fitted linear, exponential, hyperbolic and inverse tangent functions through the CSA versus pressure points using the least squares Marquardt method. In each experiment where heart rate changed during bleeding, the exponential fit procedure gave the smallest sum squared error (Fig.1A-I). In series 2, where heart rate was constant, an exponential function was also used (Fig.1D-I).

The equation of the exponential function to fit the CSA versus pulmonary arterial pressure data is expressed:

$$CSA = CSA_{ps,0} + \frac{CSA_{ps,1} - CSA_{ps,0}}{\left[1 + \exp\dfrac{(P_{ps,0} - P_{pa})}{P_{ps,1}}\right]} \tag{5}$$

where $CSA_{ps,0}$ is the minimum asymptotic value for the CSA [mm^2]; $CSA_{ps,1}$ the maximum asymptotic CSA value [mm^2]; $P_{ps,0}$ the pressure [mmHg] where the CSA versus pressure curve is steepest and thus pseudo-static compliance is maximal and $P_{ps,1}$ the difference between the pressure $P_{ps,0}$ and the pressure where the compliance is 79% of the maximum value. The results of the fit are given in figure 1. The derivative of the fit through the mean CSA versus mean pressure points ($\delta CSA/\delta P$) is defined as the pseudo-static compliance (C_{ps}). The derivative of the exponential fit (Eq.5) is given by equation 6.

$$C_{ps} = \frac{\dfrac{(CSA_{ps,1} - CSA_{ps,0})}{P_{ps,1}} \times \exp\dfrac{(P_{ps,0} - P_{pa})}{P_{ps,1}}}{\left[1 + \exp\dfrac{(P_{ps,0} - P_{pa})}{P_{ps,1}}\right]^2} \tag{6}$$

For $P_{pa} = P_{ps,0}$ the equation becomes:

$$C_{ps,max} = \frac{(CSA_{ps,1} - CSA_{ps,0})}{4P_{ps,1}} \tag{7}$$

where $C_{ps,max}$ is the maximum pseudo-static compliance [mm^2/mmHg].

Without intending to suggest a physiological relationship between heart rate and mean P_{pa}, we found an exponential relationship between heart rate and P_{pa} (series 1). This function is a mirror image of the function fitted through the CSA versus pressure data (Fig. 1). The least squares Marquardt method was also used. The formula of the exponential function is expressed:

$$HR = HR_0 - \frac{(HR_1 - HR_0)}{\left[1 + \exp\dfrac{(P_{HR,0} - P_{pa})}{P_{HR,1}}\right]} \qquad (8)$$

where HR_0 and HR_1 are the maximum and minimum asymptotic heart rate values [Hz] respectively; $P_{HR,0}$ the pulmonary arterial pressure [mmHg] where the HR versus pressure curve is steepest; $P_{HR,1}$ the pressure difference between the pressure $P_{HR,0}$ and the pressure where the change in heart rate is 79% of the maximum change in heart rate. The maximal steepness of the heart rate versus pressure fit is given by:

$$S_{HR,max} = \frac{HR_0 - HR_1}{4 P_{HR,1}} \qquad (9)$$

where $S_{HR,max}$ is expressed in [Hz/mmHg]. In figure 1 the results of the fit are given.

The maximum pseudo-static compliance, $C_{ps,max}$ correlated positively with the maximum decrease in heart rate, $-S_{HR,max}$ according to: $C_{ps,max}$ = -3.48 mm^2/Hz·$S_{HR,max}$ + 7.24 mm^2/mmHg (r = +0.97, p < 0.05). Furthermore, a correlation was found between the pressure where pseudo-static compliance was maximal and the pressure where the change in heart rate was maximal: $P_{ps,0}$ = 0.91·$P_{HR,0}$ + 1.71 mmHg (r = 0.94, p < 0.05).

3.3.3 Dynamic compliance

All loops of CSA versus pulmonary arterial pressure within a heart cycle were almost closed and a linear regression line appeared to be the best fit through each individual loop. The loops coincided with the pseudo-static relationship of mean CSA versus mean P_{pa} at constant heart rate (Fig.2B), whereas they did not with the pseudo-static relationship at increasing heart rate (Fig.2A).

Individual plots of dynamic compliance versus mean pulmonary arterial pressure are given for both series (Fig.3A-I). A bell-shaped curve was fitted through the data

according to equation 6. Using six animals, we compared the data from series 1 with those of series 2. In two of these animals we started our measurements at the second series below the pressure where dynamic compliance was maximum. To fit the dynamic compliance versus pressure data of these series, we used the maximum compliance of the first series of the same experiment.

Maximum dynamic compliance values ($C_{d,max}$) in the series of the high constant heart rate was found at higher pulmonary arterial pressures ($P_{d,0}$) than in the series with the increasing heart rate (mean difference = 8.00 $\pm$ 3.28 mmHg, p = 0.002, paired t-test, n = 6,) (Fig.3D-I). In the series at the constant heart rate, the bell-shaped curves were wider than in the series with the increasing heart rate, which was indicated by the larger width parameters (P_1) (mean difference = 2.11 $\pm$ 0.95 mmHg, p = 0.003, paired t-test, n = 6) (Fig.3D-I). Figure 3D, F, H and I show that maximum dynamic compliance ($C_{d,max}$) is about the same for the two series of measurements. The mean difference between $C_{d,max}$ of the first and second series is -0.13 $\pm$ 0.56 (paired t-test, n = 4, p = 0.689).
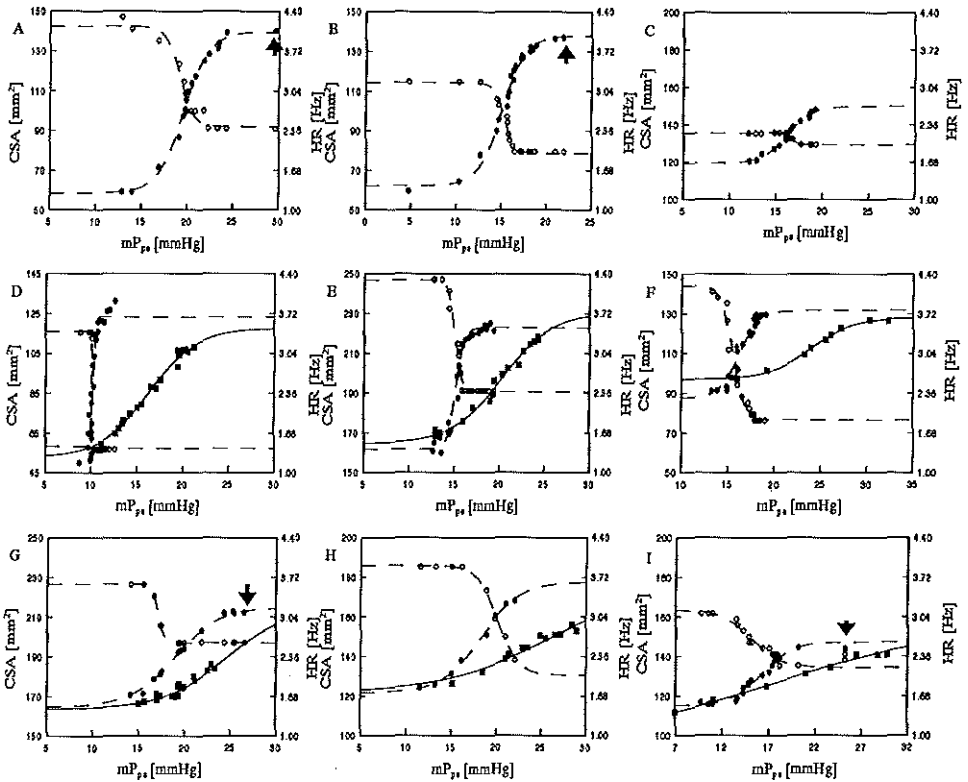
Fig. 1. Mean CSA versus mean pressure

Mean pulmonary cross-sectional area (CSA) and heart rate (HR) are plotted on the left and right Y-axis respectively against mean pulmonary arterial pressure (mP$_{pa}$) on the X-axis. Two series were done in six (D-I) of the nine (A-I) animals. Closed symbols are the data points of CSA vs. mP$_{pa}$ for series 1 (●) and series 2 (■). Open symbols are the data points of HR vs. mP$_{pa}$ for series 1 (○). The arrows indicate data points obtained after reinfusion of blood. Fits are drawn through the CSA versus pressure points and through the heart rate versus pressure points.
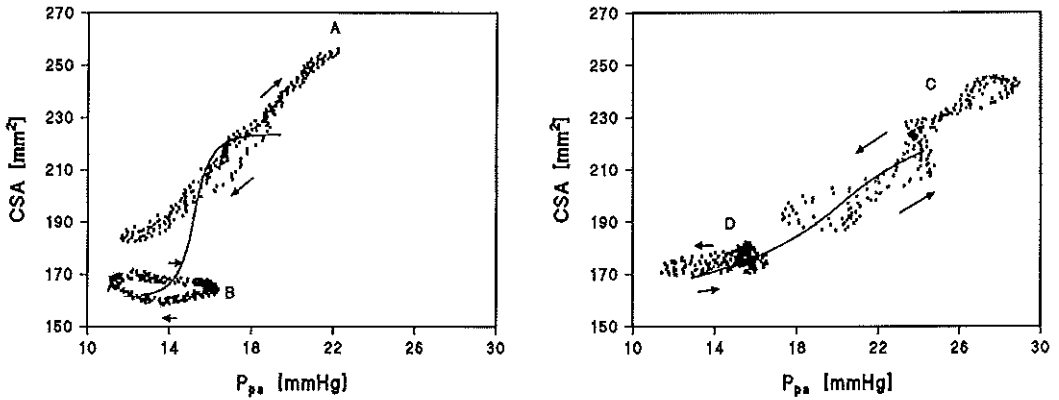
Fig. 2. CSA versus mean pressure over several heart cycles

CSA, cross-sectional area of the pulmonary artery. P_{pa}, pulmonary arterial pressure.

The slopes of loops A and B in the left panel represent dynamic compliance versus mean pulmonary arterial pressure value for experiment H (one piglet), in the series where heart rate increased. For the loops A, mean P_{pa} is 19 mmHg, mean CSA 226 mm^2, dynamic compliance 7.2 mm^2/mmHg and heart rate 2.4 Hz. For the loops B, mean P_{pa} is 14 mmHg, mean CSA 165 mm^2, dynamic compliance -0.6 mm^2/mmHg and heart rate 4.3 Hz. The fit through the mean CSA versus mean P_{pa} of the first series of experiment H is drawn as a solid line.

The slopes of loops C and D in the right panel represent dynamic compliance versus mean pulmonary arterial pressure value for experiment H, in the series where heart rate was constant. For the loops C, mean P_{pa} is 24 mmHg, mean CSA 220 mm^2, dynamic compliance 5.69 mm^2/mmHg and heart rate 4.3 Hz. For the loops D, mean P_{pa} is 15 mmHg, mean CSA 171 mm^2, dynamic compliance 1.11 mm^2/mmHg and heart rate 4.3 Hz. The fit through the mean CSA versus mean P_{pa} of the second series of experiment H is drawn as a solid line.
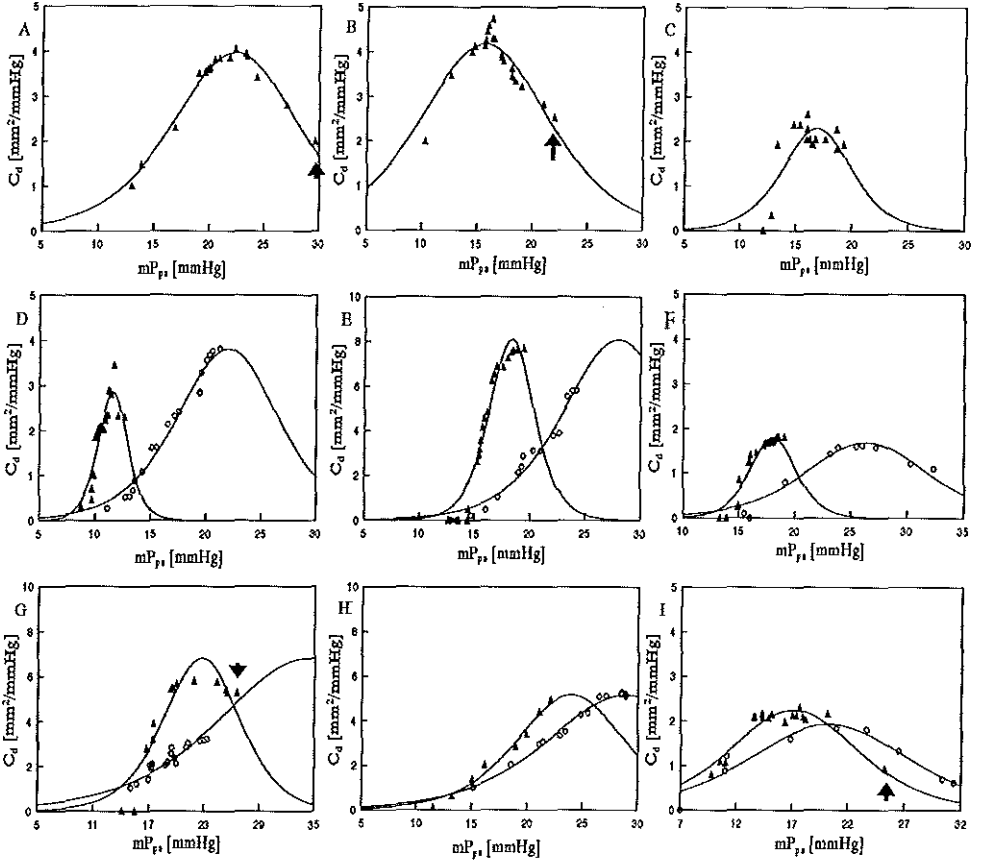
Figure 3. Dynamic compliance versus pressure

Dynamic compliance (C_d) versus mean pulmonary arterial pressure (mP_{pa}) for a series with changing heart rate (closed triangles) and for a series with constant heart rate (open circles). Two series were done in six (D-I) of the nine animals (A-I). The arrows indicate the measurement taken after blood is returned to the animal but, before pacing, the heart is started as indicated by arrows.

3.4 Discussion

3.4.1 Experimental conditions

In our experiments, the slightly curved conductance catheter was positioned in the centre of the pulmonary artery using radiographic imaging. The catheter did not affect the pulmonary arterial wall mechanically, thus avoiding local spasm of the vascular smooth muscle cells [Arndt et al. 1971]. Perpendicular movement of the catheter out of the vessel centre would cause a maximum error of 7% in the conductance signal [Axenborg and Olson 1979]. To avoid such positional changes caused by ventilatory movements we measured during prolonged expiratory pauses.

3.4.2 The effect of pressure

According to our data, pseudo-static compliance depends on pulmonary arterial pressure. We found the same for dynamic compliance. We found a sigmoid CSA versus pressure for the pulmonary artery like was found for the aorta [Langewouters 1984].

The compliance of the pulmonary artery is larger than the compliance of the aorta, which we attributed to different ratios and quantities of collagen and elastin in both vessels [Apter et al. 1966, Wolinsky and Glagov 1964].

3.4.3 The effect of heart rate

The CSA was smaller at the same mean pulmonary arterial pressure if heart rate was higher (Fig.1D-I). This is probably due to an increase in smooth muscle tone. An increase in heart rate due to bleeding might reflect an increase in sympathetic activity induced by a lower arterial pressure. An increase in sympathetic activity will lead to an increase in vessel tone [Ingram et al. 1968]. In all experiments during normovolaemia, pulmonary arterial pressure was higher and CSA was lower at a higher heart rate (Fig. 1). Therefore, the vasoconstriction could also be caused by the higher heart rate itself. We attributed the increase in pulmonary arterial pressure, when the heart rate was

increased, to an increase in flow and/or an increase in downstream flow resistance. It is unlikely that the decrease in CSA could be explained by an increase in shear rate due to an increase in flow, because shear rate would have caused vasodilation [Melkumyants et al. 1994]. In addition to the amount of stretch [Harder et al. 1987, Khalil et al. 1987, Kirber et al. 1988, Kulik et al. 1988, Naruse and Sokabe 1993], probably the rate of cyclic stretch of the pulmonary artery also increases vessel tone [Sumpio and Widmann 1990, Sparks 1964, Winston et al. 1993].

The mean CSA versus mean P_{pa} curve was steeper for the series where heart rate increased, than for the series where heart rate remained constant (Fig.1D-H). The maximum pseudo-static compliance correlated with the maximum increase in heart rate. The corresponding pressures were also correlated. We assume that these results can be explained by the model in figure 4, where, at various smooth muscle tones, the collagen is the limiting factor for vessel distension at high pulmonary arterial pressures. At physiological pressures the mean CSA will decrease if smooth muscle tone increases during an increase in heart rate (A ⇒ B). Furthermore, as mentioned above, an increase in pulmonary arterial pressure occurred if heart rate increased, which caused the CSA to shift along the mean CSA versus mean pressure curve (B ⇒ C). Thus, we assume that the mean CSA versus pressure relationship at an increasing heart rate can be deduced from a population of relationships at various constant heart rates, implying that pseudo-static compliance will be overestimated if heart rate increases. Our idea of shift corresponds with the shift of the static diameter versus pressure curve found in the iliac and carotid artery during norepinephrine administration, which also caused smooth muscle contraction [Cox 1975]. Our idea of shift also corresponds with our observations that the pressure, where dynamic compliance was maximum, was highest for the series determined at the high constant heart rate and that maximum dynamic compliance did not depend on heart rate.

$$P_{pa} \, [mmHg]$$
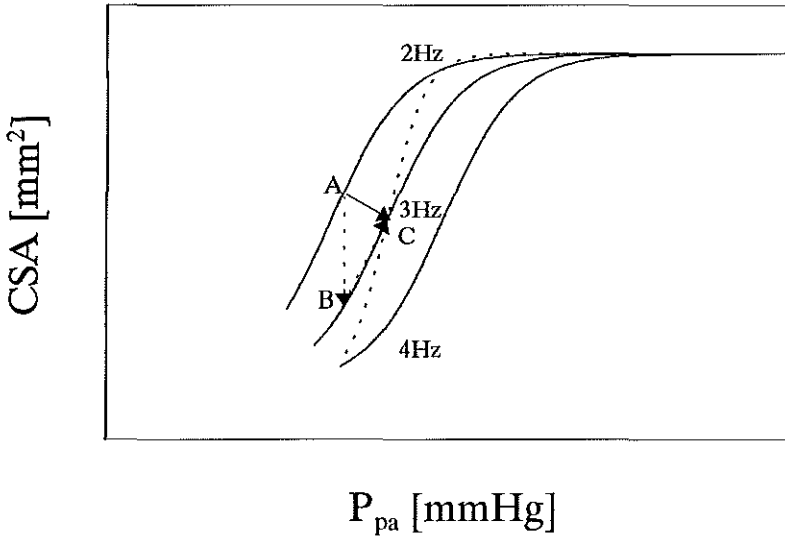
Fig. 4. Schematic explanation of heart rate effects on mean CSA versus mean pressure relationship in the pulmonary artery

The solid lines are cross-sectional area (CSA) versus pressure curves at a constant heart rate and the dashed line is a CSA versus pressure curve at an increasing heart rate. If, at A, heart rate is increased from 2 to 3Hz the CSA will decrease and reach point B. Due to pacing, pulmonary arterial pressure will increase and the CSA will shift via the CSA versus pressure curve for 3Hz and will reach point C. This procedure is repeated if heart rate is increased from 3 to 4Hz. If heart rate is increased in small steps the resultant curve will be the dashed line, which is steeper than the solid line.

3.4.4 Dynamic compliance

The almost closed CSA versus pressure loops over a heartbeat indicate a negligible viscous resistance in the vessel wall, including hardly any energy being dissipated [Patel et al. 1960, Shelton and Olson 1972]. Furthermore, because of the closed loops, it is unlikely that the erythrocytes were reformed and de-orientated at the end of diastole.

The maximum dynamic compliance we found (4.33 ± 2.19 mm^2/mmHg) was similar to the constant dynamic compliance found by Patel et al. [1960] for the pulmonary artery of dogs (4.94 ± 1.85). Ingram et al. [1970] (2.82 ± 1.15) and Johnson and Henry [1985] (2.25) found a much lower compliance for the pulmonary artery in dogs. In humans, Greenfield and Griggs [1963] found a value of 10.04 ± 2.45. Differences might be dependent on differences in pressure, heart rate, vessel volume, age and species.

3.4.5 Conclusions

In summary, we conclude that the pulmonary artery constricts if heart rate becomes higher. Therefore, literature on pseudo-static compliance during conditions of changing heart rate should be reconsidered. Furthermore, we conclude that a constant dynamic compliance within a heart cycle can be used in a windkessel model because the relation between CSA and pressure is essentially linear within a heart cycle. If a windkessel model is used to estimate flow from pulmonary arterial pressure, dynamic compliance should be determined separately for each individual and adapted following changes in heart rate or pulmonary arterial pressure.

Chapter 4

Determination of the Mean Cross-Sectional Area of the Thoracic Aorta using a Double Indicator Dilution Technique

L Kornet[1], JRC Jansen[1], EJ Gussenhoven[2] and A Versprille[1]

1) Pathophysiological Laboratory, Department of Pulmonary Diseases, Erasmus University, Rotterdam, The Netherlands
2) The Interuniversity Cardiology Institute, Erasmus University, Rotterdam, The Netherlands

.

4.1 Introduction

Several methods are available to determine the cross-sectional (CSA) area of blood vessels. Mechanical devices include a strain-gauge caliper [Mallos 1962], a device which moves a metal core in a coil to change the inductance of the coil [Pagani et al. 1975], and ultrasonic distance crystals [Pagani et al. 1975, 1978, Vatner et al. 1980, 1982, Gross et al. 1981, Tomoike et al. 1981, Johnson and Henry 1985, Gentile et al. 1988, Latson et al. 1988]. They have the disadvantage of introducing a restraint on the vessel wall. Devices which do not affect the vessel wall are a photo-electrical apparatus, used only in vitro [Schabert et al. 1980], X-ray angiography [Leitz and Arndt 1968, Arndt et al. 1971, Gonza et al. 1974, Merillon et al. 1978, Stefanadis et al. 1987], IntraVascular UltraSound (IVUS) [Wenguang et al. 1990, 1991] and ultrasound wall-tracking techniques [Hoeks et al. 1990]. Angiography, IVUS and ultrasound wall-tracking techniques are expensive and the first two techniques require labour-intensive analyses. If ultrasound wall-tracking techniques are used then only a diameter of a blood vessel is determined, instead of the whole cross-section. Furthermore, the angle of the ultrasound beam should be 90° to determine the diameter of a blood vessel.

We developed a new method to determine the mean cross-sectional area of a blood vessel without affecting the vessel wall using an intravascular conductance technique. The method presents CSA on-line, thus doesn't require off-line labour-intensive analyses, and is relatively inexpensive. The CSA, obtained with the double indicator dilution method ("cold" and ions), was compared with the CSA obtained with an IVUS.

4.2 Methods

4.2.1 Ion mass balance for calculation of mean CSA

If a hypertonic saline solution is injected upstream, a change in conductance is detected

downstream in the blood circulation (dilution of ions). The conductivity balance is based on the assumption that the amount of ions which conduct electrical current is the same at the injection and detection site. The injectate (at room temperature) is heated by the blood after injection, increasing the conductivity of the injectate. Therefore, the conductivity of the injectate is corrected for blood temperature. Assuming complete mixing of indicator and blood, the following conductivity balance can be written:

$$\int_{t_1}^{t_2} \dot{Q}_i(t) \, [\sigma_i - \sigma_b] \, dt = \int_{t_1}^{t_2} \Delta \sigma_b(t) \, \dot{Q}_b(t) \, dt \qquad (1)$$

Where, t is time; t_1 the time of injection; t_2 the end of integration when all injected ions have passed the detector site; $\dot{Q}_i$ the input flow of the injectate; σ_i the electrical conductivity of the injectate at blood temperature; σ_b the conductivity of the blood before injection; $\Delta\sigma_b$ the change in conductivity of the blood, due to the injection of the hypertonic saline; $\dot{Q}_b$ the mean blood flow at the position where CSA is determined. If the injection is fast and $\dot{Q}_b(t)$ is constant, the equation can be rewritten as:

$$Q_i(\sigma_i - \sigma_b) = \dot{Q}_b \int_{t_1}^{t_2} \Delta \sigma_b(t) \, dt \qquad (2)$$

where Q_i is the volume of the injectate. The change in conductivity of blood ($\Delta\sigma_b$) could not be determined directly in these experiments, instead conductance (G) was determined at the site where CSA is determined using a conductance catheter [Baan et al. 1984]. The conductance catheter is constructed with four electrodes equidistantly (5 mm) placed at its distal end. An alternating current of 70 μA (RMS) and 20 kHz is applied to the two outer electrodes (model Sigma 5, Leycom, Cardiodynamics, Rijnsburg, The Netherlands). The induced voltage between the two inner electrodes is measured. An offset is caused by the conductance of the surrounding tissues, which is called parallel conductance ($G_p^{'}$) [Baan et al. 1984]. The time varying conductance (G(t)) measured by the conductance catheter is related to the time varying cross-sectional area ($CSA_{GD}(t)$) by the relationship:

$$G(t) = \frac{CSA_{GD}(t) \times \sigma_b(t)}{L} + G_p(t) \tag{3}$$

where L is the distance between the electrodes. If mean G_p over each heart cycle is constant during the injection of the hypertonic saline, the change in conductivity can be written as:

$$\Delta \sigma_b(t) = \frac{L \times \Delta G(t)}{\overline{CSA}_{GD}(n)} \tag{4}$$

where $\overline{CSA}_{GD}$ is the intra-ventricular cross-sectional area averaged over a heart cycle occurring in the dilution curve and n the number of the heart cycle.

Substituting $\Delta\sigma_b(t)$ in equation 2 gives:

$$Q_i(\sigma_i - \sigma_b) = \frac{\dot{Q}_b \times L}{\overline{CSA}_{GD}(n)} \int_{t_1}^{t_2} \Delta G(t)\, dt \tag{5}$$

If measured at steady-state conditions as during an Inspiratory Pause Procedure (IPP), $\overline{CSA}$ averaged over a heart cycle will not change. An IPP is a procedure, in which a tidal volume is inflated and held in the lungs for several seconds, followed by an expiration [Versprille and Jansen 1985]. During the IPP, arterial pressure and left ventricular output remain constant from 1-2 s after the start of the pause period. Furthermore, in chapter 2 we found no influence of injectate on vessel volume. Therefore, mean CSA during a heart cycle, will remain constant after an injection of indicator given during the IPP, and equation 5 can be rewritten as:

$$\overline{CSA}_{GD} = \frac{\dot{Q}_b \times L}{Q_i(\sigma_i - \sigma_b)} \int_{t_1}^{t_2} \Delta G(t)\, dt \tag{6}$$

In our experiments σ_b is a factor 25 lower than σ_i (NaCl injectate = 3M) and can be neglected, giving:

$$\overline{CSA}_{GD} = \frac{\dot{Q}_b \times L}{Q_i \times \sigma_i} \int_{t_1}^{t_2} \Delta G(t) \, dt \tag{7}$$

We injected "cold" hypertonic saline in the right atrium and determined the CSA in the thoracic aorta. The assumption that the amount of injected ions equals the amount of detected ions is incorrect, because a part of the injected ions entered "open" side-branches such as the truncus branchiocephalicus, arteria subclavia sinistra and arteria carotis. With "open" we mean that the flow of the side-branch does not re-enter the main-branch before the site where the CSA is determined. If complete mixing of indicator with blood occurs, the amount of injected ions ($Q_i \cdot \sigma_i$) will be distributed in each branch in proportion to flow [Zierler 1962]. Thus, the amount of ions passing the detection site should be multiplied by the flow at the detection site ($\dot{Q}_b$) divided by the total cardiac output before branching ($\dot{Q}_T$), giving:

$$\overline{CSA}_{GD} = \frac{\dot{Q}_b \times L}{\dfrac{\dot{Q}_b}{\dot{Q}_T} Q_i \times \sigma_i} \int_{t_1}^{t_2} \Delta G(t) \, dt \tag{8}$$

Equation 8 can be rewritten as:

$$\overline{CSA}_{GD} = \frac{\dot{Q}_T \times L}{Q_i \times \sigma_i} \int_{t_1}^{t_2} \Delta G(t) \, dt \tag{9}$$

These equations imply that the fraction of cardiac output and the fraction of injected ions passing the detection site are equal. Conductance, determined after injection of the injection of the ("cold") hypertonic saline, was averaged for each heart cycle and plotted versus time. A baseline was drawn from the start (t_1) to the end of the dilution curve (t_2). The area under the baseline was subtracted from the area under the total dilution curve to obtain the area under the dilution curve ($\int \Delta G(t)$), which is corrected for accumulation of salt in the vessel wall and recirculation. L, Q_i and σ_i are known. $\dot{Q}_T$ is determined using

the thermodilution method, which is based on the law of conservation of thermal energy [Jansen 1995, Stewart 1921, Zierler 1962]. Herefore, the change in temperature is processed after injection of a known amount of "cold" (hypertonic) saline, which is the same injection as used to induce a change in conductance. For practical reasons we determined cardiac output in the pulmonary artery. It would also be possible to determine the temperature signal in the thoracic aorta, because the change in temperature of the blood, due to the injection of the "cold" injectate, will be equal before and after branching.

4.2.2 IntraVascular UltraSound

To evaluate the determination of CSAs with the use of the dilution signals of conductance and temperature, the results were compared with those of IntraVascular UltraSound (IVUS) (DuMed, Rotterdam, The Netherlands). This method is based on a 32 MHz single-element transducer mounted on the tip of a flexible driveshaft, which was rotating and placed inside a 5F catheter. Cross-sectional images with 512·512 pixels and 256 grey levels were scanned at a speed of 25 images per second. Axial resolution of the system was better than 0.1 mm. The maximum scan depth was 9 mm. CSAs with a diameter larger than 9 mm were excluded, because the IVUS catheter was positioned against the vessel-wall, as visualised by the method itself and radiographic imaging. Blood pressure and time was displayed simultaneously on a video screen. Ultrasound images were analyzed off-line for free lumen area determination using a computer analyzing system [Wenguang et al. 1990, 1991].

4.2.3 Surgical procedures and ventilatory conditions

All experiments were performed in accordance with the "Guide for Care and Use of Laboratory Animals" published by the US National Institute of Health [NIH publication No. 85-23, Revised 1985] and in accordance with the regulations of the Animal Care Committee of the Erasmus University Rotterdam, The Netherlands.

Six piglets (5-7 weeks old, 9.3 $\pm$ 0.9 kg body weight) were anaesthetized with an intraperitoneal injection of pentobarbital sodium (30 mg·kg^{-1} bodyweight). The animals were placed in supine position on a thermo-controlled operating table to maintain body temperature at about 38.5 °C. Anaesthesia was maintained by a continuous infusion of pentobarbital sodium (8.5 mg·h^{-1}·kg^{-1}) via an ear vein. ECG electrodes were placed in the right leg and on the chest of the pig near the xyphoid cartilage. After tracheostomy, the pigs were connected to a volume-controlled ventilator [Jansen et al. 1989] and ventilated with ambient air against a positive end-expiratory pressure of 2 cmH$_2$O. The ventilatory frequency was 10 breaths per minute. Tidal volume was adjusted to a P$_{aCO2}$ of 38-45 mmHg during baseline.

A conductance catheter was inserted through the carotid artery into the descending thoracic aorta to detect the saline conductance dilution curve. The lumen of the conductance catheter was used for measuring arterial pressure and sampling of blood. From the opposite direction, an ultrasound imaging catheter was inserted through the femoral artery. The distal ends of both catheters were situated close to each other under radiographic guidance. Therefore, we regarded the CSAs, measured by both catheters, to be equal. Through the external jugular vein a Swan Ganz catheter (5F) was inserted to detect the temperature dilution curve and pressure within the pulmonary artery. In addition, a four lumen catheter was inserted through the jugular vein into the superior vena cava to measure central venous pressure and to infuse pentobarbital and pancuronium. A third catheter was inserted through the jugular vein into the atrium to inject the "cold" hypertonic saline to be able to process a temperature change in the pulmonary artery and a conductance change in the thoracic aorta.

To avoid clotting, the three pressure catheters were continuously flushed at a flow rate of 3 ml·h^{-1} with saline (0.9% NaCl), containing 10 I.U. heparin per ml. A catheter was placed into the bladder to prevent retention of urine. After surgery, pancuronium bromide (0.3 mg·h^{-1}·kg^{-1}, after a loading dose of 0.2 mg·kg^{-1}) was infused to suppress spontaneous breathing. Pentobarbital infusion was switched from the ear vein to the vena

cava superior. The surgical procedures were followed by a stabilization period of about half an hour.

4.2.4 Experimental protocol

Cross-sectional area (CSA) was changed by changing aortic pressure. Various levels of arterial pressure were created by Inspiratory Pause Procedures (IPPs) in between normal ventilations [Versprille and Jansen 1985]. Between each IPP there was a stabilisation period of 15 minutes. The IPPs were characterized by an inflation time of 2.4 s, an inspiratory pause of 15 s, followed by an expiration of 3.6 s. A series of IPPs consisted of a stepwise increase in inflation volume with 5 ml per kg body weight. The series was ended if the aortic pressure reached a critical level of approximately 40 mmHg during the IPP. At 6.3 seconds after the beginning of an IPP, a hypertonic "cold" solution (2.5 ml, 3 M NaCl at room temperature) was injected. During the IPPs, pressures, ECG, tempera-ture and the conductance signal were stored on disk for analyses at a sample frequency of 250 Hz. The intravascular ultrasound images were recorded simultaneously on videotape with the pressure and time signal.

4.2.5 Calculations

For every measurement, the mean CSA, obtained with the double indicator dilution method during the passage of the temperature and conductance dilution curves, was compared with the CSA, which was the mean of all IVUS images (more than 100), obtained within the same period. Mean values are given $\pm$ standard deviation.

4.3 Results

The relationship between the intravascular CSA, determined with the double indicator dilution method, CSA_{GD}, and the IntraVascular UltraSound, CSA_{IVUS}, are presented for

six piglets (n = 44) in figure 1A. The regression line is close to the line of identity (CSA_{GD} = -1.83 + 1.06·CSA_{IVUS}), and the correlation coefficient is 0.96. In a Bland-Altman scatter diagram [Altman 1990], the differences between the two CSAs were plotted against the mean CSAs obtained using both methods (Fig.1B). The difference was independent of the diameter of the vessel. The difference was on average -0.99 mm^2 ± 2.64 mm^2, (mean CSA_{GD} = 46.84 ± 8.21 mm^2, mean CSA_{IVUS} = 47.82 ± 9.08 mm^2) and not significant.
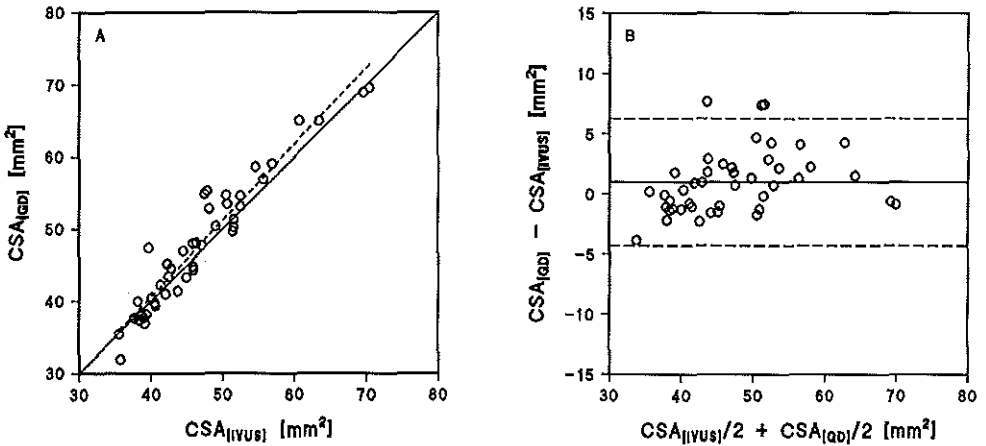
Fig.1A: Correlation between the average results of the double indicator dilution method (CSA_{GD}) and those of the IVUS (CSA_{IVUS}). The best linear fit is given by the dashed line. The line of identity is indicated as the solid line.

B: Scatter diagram of the differences between the CSA_{GD}-values obtained with the double indicator dilution method and those with IVUS plotted versus the mean CSA of both methods. The solid line indicates the mean difference and the dashed lines indicate the 95% confidence interval (2SD).

4.4 Discussion

A new, cheap, simple and non-labour intensive method was evaluated to determine the mean CSA of the thoracic aorta on-line. We assume that this double indicator dilution method can also be used to determine CSAs of other arteries in vivo.

In patients who are undergoing intensive care, cardio-thoracic surgery or a catheterization for diagnostic reasons, arterial pressure is routinely determined. In patients who are undergoing a catheterization for diagnostic reasons, normally a pressure catheter is present in the aorta. During intensive care and cardio-thoracic surgery, arterial pressure is determined in both the pulmonary artery and the artery femoralis or radialis using respectively a pulmonary arterial catheter (PAC) and a radial or femoral arterial catheter. These catheters and the aortic catheter can easily be extended with four electrodes to determine the dilution of ions. The dilution of temperature can be determined with use of the thermistor, which also can be mounted at the tip of an aortic, radial or femoral catheter and is routinely mounted at the tip of the PAC. The "cold" hypertonic saline can be injected into the right atrium, using the injection lumen of the PAC. According to our experience in man with such catheter the pulmonary artery can be catheterized.

Determination of an arterial cross-sectional area in patients can be used to monitor the effect of drug therapy on the cross-sectional area and compliance in the operating room, without the need for expensive and labour-intensive ultrasound methods. Furthermore, obstructions and aneurysms can possibly be detected by moving the catheter in the longitudinal direction through the vessel.

4.4.1 Parameters influencing conductance

Before this study, the volume in a large blood vessel has not been determined using the electrical conductance as was done for the ventricular volume [Baan et al. 1984], because in blood vessels a pulsatile flow and thus pulsatile change in shear rate is present. A

pulsatile shear rate, will cause a pulsatile orientation and deformation of erythrocytes, which in turn will cause a pulsatile change in conductivity of blood [Nakajima et al. 1990]. In the ventricle a turbulent flow is present, which causes no unidirectional orientation and deformation of erythrocytes. To determine the CSA (i.e. segmental volume) of a blood vessel using the conductance signal, the conductivity should be corrected continuously, depending on shear rate, heart rate and the time constant of (de)-orientation, (de)-formation and (de)-aggregation of the erythrocytes. The problem of the pulsatile change in conductivity of blood was eliminated with use of the double indicator dilution method. With use of this method baseline conductivity of blood was eliminated. We used the change in blood conductivity, and thus the change in conductance, after the injection of "cold" hypertonic saline, to determine cross-sectional area. During passage of the salt ions as a dilution curve, the amount of erythrocytes and their behaviour probably do not change. Thus, the change in conductance was not affected by shear rate.

The effect of the "cold" injectate on conductivity of blood by changing blood temperature could be neglected. A blood temperature of 38.0 °C instead of 38.5 °C at a haematocrit of 30% due to the injection of a "cold" solution, will decrease blood conductivity by merely 0.3% .

The quantity of total injected salt in our piglets was about 400 mg/kg, which was below that used therapeutically in case of a hypovolaemic shock [Kien and Kramer 1989, Velasco et al. 1980] and must therefore be considered harmless. We did not observe any negative effects on haemodynamic conditions. In medical practice we expect that the amount of injected salt ions related to body weight will be lower than in these experiments, because cardiac output per body weight is lower and series of IPPs will not be necessary.

4.4.2 Evaluation of the double indicator dilution method

With the IntraVascular UltraSound the CSA is determined at one position in a vessel, whereas a mean CSA between the measuring electrodes is determined with the double

indicator dilution method. We assume that this difference caused a very small bias in the results [Caro et al. 1978], because both probes were located close to each other in the descending aorta.

It should be noted that the difference between the IVUS and the double indicator dilution method may be related to the error caused by inter-observer variation of the IVUS. The intra-observer variation of the IVUS [Wenguang et al. 1991] could be neglected, because one data point was the mean of more than 100 images, measured during passage of the dilution curve. The difference between the CSAs obtained with the double indicator dilution method and the IVUS was not significant. Based on our results we conclude that the double indicator dilution method is a reliable technique to estimate cross-sectional areas of blood vessels.

Chapter 5

A New Approach to Determine Parallel Conductance

L Kornet[1], JRC Jansen[1], JJ Schreuder[2], ET van der Velde[3]
and A Versprille[1]

1) Pathophysiological Laboratory, Department of Pulmonary Diseases, Erasmus
    University Rotterdam, The Netherlands.
2) Department of Anaesthesiology, University Hospital Maastricht,
    The Netherlands.
3) Department of Cardiology, University Hospital Leiden,
    The Netherlands.

5.1 Introduction

The electrical conductance method has been used to measure volumes or volume changes of the large blood vessels and ventricles in vivo by positioning a catheter in a blood vessel or ventricle and measuring the electrical conductance [Baan et al. 1984, 1988, McKay et al. 1984 Burkhoff et al. 1985, Spinelli et al. 1986, Gawne et al. 1987, Boltwood et al. 1988, Ferguson et al. 1988, 1989, Lankford et al. 1990, Odake et al. 1992, Szwarc et al. 1994, Chapter 2]. This method has several advantages over other methods, which determine intra-vascular or intra-ventricular volumes. The vessel or ventricular wall is not affected, precise geometric assumptions of the ventricle or vessel, or labour-intensive analyses are not required and the method is inexpensive. The conductive tissues and fluids surrounding the vessel or ventricle contribute to the measured electrical conductance of the blood inside the vessel or ventricle, causing an offset in the relation between intra-vascular or intra-ventricular volume and conductance. This offset is called parallel conductance. Several investigators did not quantify parallel conductance and presented instead the changes in conductance as a measure for changes in volume [Spinelli et al. 1986, Ferguson et al. 1988, 1989]. To improve the conductance method to the measurement of absolute volumes, a method to determine tissue conductance has been introduced by Baan et al. [1984, 1988]. They determined conductance of the tissues, surrounding the blood in the left ventricle, by changing the specific conductivity (σ_b) of blood by injecting hyper-tonic saline into the pulmonary artery. The conductance signal was recorded and the successive conductance values at end-diastole (G_{dias}) were plotted versus the corresponding values at end-systole (G_{sys}). A linear regression line was fitted through these data and extrapolated to the identity line of G_{dias} and G_{sys} where the conductivity of blood (σ_b) was regarded to be zero. This value on the identity line was defined as parallel-conductance (G_p^l). A disadvantage of this extrapolation method is that a small error in the determined G_{dias} and G_{sys} values will result in a large error in the extrapolated value of parallel conductance.

We evaluated a new observer-independent method to estimate parallel conductance ($G_p{}^a$), which is based on the integration of an area under an ion (conductance) dilution curve and compared the precision and reproducibility of our new method to the conventional method. Firstly, parallel conductances, obtained with use of both methods ($G_p{}^a$ and $G_p{}^l$) were obtained in the aorta of anaesthetized piglets and compared pairwise. The standard deviations of the observations in the aorta of each piglet were calculated for both methods, assuming a constant parallel conductance in each piglet. Secondly, the inter-observer variation of the conventional method to estimate parallel conductance of the left and right ventricle of goats was obtained. The averaged value of those obtained by three observers was compared to the single value of parallel conductance obtained with use of the new method. To compare the reproducibility of both methods in each condition of the goats, the values of parallel conductance in the left as well as the right ventricle were determined with both methods. The differences between two duplicate values of our new method were compared to those of the conventional method.

5.2 Methods

5.2.1 The conductance method

The general principles of the conductance method have been described extensively elsewhere [Baan et al. 1984, 1989]. Therefore, only the configuration needed for our study will be mentioned. Two types of conductance catheters were used. Type 1 was the conductance catheter used for the intra-aortic volume measurements. This catheter was constructed with four circular electrodes, equidistantly (5 mm) placed along its tip, and an alternating current of 70 μA (RMS) and 20 kHz was applied to the two outer electrodes. Type 2 was the conductance catheter (7F, Sentron, Roden, The Netherlands) for the intra-ventricular volume measurements. This catheter was constructed with ten circular electrodes mounted at equal distances near the tip. The catheter was positioned in the left or

right ventricle along the longitudinal axis and a 20 kHz., 30 μA RMS current was applied between the outermost electrodes (1 and 10) and between the two adjacent electrodes (2 and 9). Both types of catheters were connected to a signal-processor system (Model Leycom Sigma 5DF; Cardiodynamics, Leiden, The Netherlands). For the aortic and the left as well as right ventricular measurements, the volume of a segment ($Q_{segment}$) between two measuring electrodes at any time t can be calculated as:

$$Q_{(segment)}(t) = \frac{L^2}{\sigma_b} [G_{segment}(t) - G_{p,segment}] \tag{1}$$

where t is time, L the distance between two adjacent electrodes, σ_b the conductivity of blood, $G_{segment}(t)$ the time-varying conductance between two electrodes and $G_{p,segment}$ part of the parallel conductance. Equation 1 can be rewritten as:

$$G_{p,segment} = G_{segment}(t) + \frac{Q_{segment}(t) \cdot \sigma_b}{L^2} \tag{2}$$

In the aorta only one segmental conductance between two electrodes was determined. In the ventricles five segmental conductances were determined from six adjacent electrodes (3-4, 4-5, 5-6, 6-7, 7-8); total left or right ventricular parallel conductance (G_p) was calculated from the sum of the five segmental parallel conductances.

$$G_p = \Sigma G_{p,segment1-5} \tag{3}$$

Likewise, the total conductance can be calculated from the sum of the conductances of the segments according to:

$$G(t) = \Sigma G(t)_{segment1-5} \tag{4}$$

In this study we determined parallel conductance using two methods.

5.2.2 Parallel conductance obtained by extrapolation of the G_{dias} versus G_{sys} relationship
If the conventional method to estimate parallel conductance (G_p^l) is used [Baan et al.

1984, 1989], the assumptions are made that 1) the injection of a hypertonic saline solution increases the blood conductivity but does not affect the volume of the ventricle or aorta, 2) the conductivity of the surrounding structures is constant, 3) the specific conductivity of the blood in the left and right ventricle and 4) the conductivity of the blood in the aorta does not change from the beginning of the ejection- to the end of the ejection-phase of the ventricle, because the σ_b changes only in the filling phase of the aorta or ventricle. To obtain G_p^l, the two best identifiable points of the conductance signal in the cardiac cycle were used, i.e. the values at end-diastole (G_{dias}) and at end-systole (G_{sys}). Because actual stroke volume ($Q_{LV,sys}$ - $Q_{LV,dias}$) is constant, changes in conductance are due to altered blood conductivity, not volume. From the G_{sys} versus G_{dias} plot, with σ_b increasing in the ascending limb of the dilution curve after the injection of hypertonic saline, parallel conductance was solved by extrapolation to that theoretical point where conductivity of blood is theoretically zero. Than the following holds:

$$If\ \sigma_b\ \rightarrow\ 0,\ then\ G_{dias}\ =\ G_{sys}\ =\ G_p^l \qquad (5)$$

Thus G_p^l is the intersection point between the regression line of the relationship between G_{dias} and G_{sys} and the identity line (G_{dias} = G_{sys}). The use of this method relies on the constancy of G_p during the intervention and a small random distribution without bias of G_{dias} versus G_{sys} with respect to the regression line. Since salt might accumulate in the wall or enter the coronary circulation, only those G_{sys} and G_{dias} values were considered, which where positioned in the first part of the curve where conductance increased [Baan et al. 1984, 1989]. To determine parallel conductance in the aorta and ventricle 1) the linear regression line with the highest correlation coefficient for the relation between conductances at systole versus those at diastole was used. In the ventricle also, those heart beats were chosen of which 2) the summed value of parallel conductances approximated the parallel conductance determined with use of the total conductance signal as much as possible and 3) parallel conductance obtained for each segment was positive. Because of these three criteria, the determination of parallel conductance in the ventricle was

observer-dependent. To calculate G_p^1 the software package CONDUCT-PC (Cardiodynamics) was used.

5.2.3 Parallel conductance obtained from the conductance dilution curve

The indicator dilution method for hypertonic saline can be described by a mass balance, in which the concentration of ions which conduct electrical current is the same at the injection and the detection site. With the assumption of complete mixing of indicator and blood, the following conductivity balance can be formulated:

$$\int_{t_1}^{t_2} \dot{Q}_i(t) \, (\sigma_i - \sigma_b) \, dt = \int_{t_1}^{t_2} \Delta \sigma_b(t) \, \dot{Q}_b(t) \, dt \tag{6}$$

where, t is time, t_1 the time of injection, t_2 the end of integration when all indicator has passed the detector site, $\dot{Q}_i(t)$ the input flow of the injectate, σ_i the electrical conductivity of the injectate at blood temperature, σ_b the conductivity of the blood before injection, $\Delta\sigma_b$ the change in conductivity of the blood after the injection of the hypertonic saline and $\dot{Q}_b(t)$ the blood flow. If the injection is given as a bolus and $\dot{Q}_b(t)$ is constant, the equation can be rewritten as:

$$Q_i(\sigma_i - \sigma_b) = \dot{Q}_b \int_{t_1}^{t_2} \Delta \sigma_b(t) \, dt \tag{7}$$

where Q_i is the volume of the injectate. If parallel conductance as well as stroke volume is the same during successive cardiac cycles, at which hypertonic saline passes the ventricle, then a change in conductance is due to a change in blood conductivity. Thus:

$$\Delta \sigma_b(t) = \frac{L^2}{\overline{Q}_v(n)} \Delta G(t) \tag{8}$$

where $\overline{Q}_v$ is the intra-ventricular or -vascular volume averaged over a heart cycle occurring in the dilution curve and n the number of the heart cycle.

Substitution of $\Delta\sigma_b(t)$ in equation 7 and rearrangement of the equation gives:

$$\frac{\overline{Q}_V(n)}{L^2} = \frac{\dot{Q}_b \int_{t_1}^{t_2} \Delta G(t)\, dt}{Q_i(\sigma_i - \sigma_b)} \qquad (9)$$

Substitution of $\overline{Q}_V(n)/L^2$ in equation 1-4 gives:

$$\overline{G}_p^a(n) = \overline{G}(n) - \frac{\sigma_b \dot{Q}_b \int_{t_1}^{t_2} \Delta G(t)\, dt}{Q_i(\sigma_i - \sigma_b)} \qquad (10)$$

$\overline{G}_p^a(n)$ is the parallel conductance averaged over the nth heart cycle. We assume that $\overline{G}_p^a$ does not change between successive heart cycles and that $\overline{G}_p^a(n)$ can be written as $\overline{G}_p^a$. $\overline{G}(n)$ was the averaged conductance per n^{th} heart cycle before hypertonic saline passed the conductance catheter. We determined $\dot{Q}_b$ with use of the thermodilution method [Jansen et al. 1981, 1990] and the conductivity of blood (σ_b) and the hypertonic injectate (σ_i) with use of a cell (Leycom Sigma 5DF) at body temperature [Chapter 2]. In the ventricles a non-unidirectional flow is present [Baan et al. 1984, 1988], leading to no overall orientation or deformation of erythrocytes. Arterial pulsatile blood flow, however, will cause a pulsatile change in shear rate, which in turn might cause a pulsatile change in blood conductivity due to the orientation and deformation of erythrocytes. We assume that the behaviour of erythrocytes and thus the influence of shear rate on conductivity of blood is equal for successive cardiac cycles within the dilution curve. Therefore, a constant factor was used to correct the conductivity for the influence of shear rate in blood vessels of piglets [Chapter 2]. L and Q_i are known. Conductance was averaged for each heart beat and plotted versus time. $\int \Delta G(t)$ is the area under the conductance dilution curve. If the conductance dilution curve was measured in the aorta, no shift in baseline was present (Fig. 1). However, a small shift in baseline was present if the conductance dilution curve was measured in the right and left ventricle (Fig. 2). After subtracting the baseline conductance, a fit was drawn through the dilution curve using a "Log Normal" model

[Jansen et al. 1987] by minimizing the least square errors between the fit and the data to remove noise on the conductance signal and to estimate the area under the dilution curve.
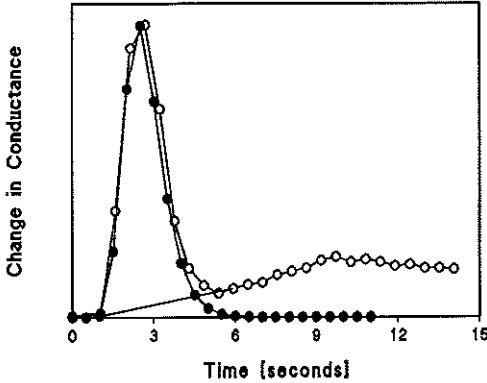
Fig. 1: Conductance dilution curve determined in the left ventricle. A baseline was subtracted.
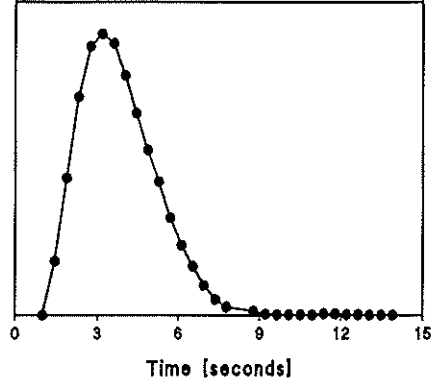
Fig. 2: Conductance dilution curve determined in the descending thoracic aorta.

5.2.4 Surgical procedures

All experiments were performed in accordance with the "Guide for Care and Use of Laboratory Animals" published by the US National Institute of Health [NIH publication No. 85-23, Revised 1985] and in accordance with the regulations of the Animal Care Committee. We compared parallel conductances obtained with use of the two methods in the aorta of piglets and in the right and left ventricle of goats.

Piglets In the Patho-Physiological Laboratory of the Erasmus University of Rotterdam we anaesthetized six piglets (5-7 weeks old, 9.3 ± 0.9 (SD) kg body weight) with an intraperitoneal injection of pentobarbital sodium (30 mg·kg⁻¹ bodyweight). The animals were placed in supine position on a thermo-controlled operating table to maintain

body temperature at about 38.5 °C. Anaesthesia was maintained by a continuous infusion of pentobarbital sodium (8.5 mg·h^{-1}·kg^{-1}). After tracheotomy, the pigs were connected to a volume-controlled ventilator [Jansen et al. 1989]. The ventilatory frequency was 10 breaths per minute and a positive end-expiratory pressure of 2 cmH$_2$O was applied. A conductance catheter was inserted into the descending thoracic aorta through the carotid artery. The lumen of the conductance catheter was used for measuring arterial pressure and for sampling of blood. Through the external jugular vein a Swan Ganz catheter (5F) was inserted into the pulmonary artery to measure temperature and pressure. In addition, a four lumen catheter was inserted into the superior vena cava through the jugular vein to measure central venous pressure and to infuse pentobarbital and pancuronium. A third catheter was placed near the entrance of the right atrium to inject cold hypertonic saline. After surgery, pancuronium bromide (0.3 mg·h^{-1}·kg^{-1}, after a loading dose of 0.2 mg·kg^{-1}) was infused to suppress spontaneous breathing.

Goats We used data of experiments, which had another main goal, i.e the study of the effect of cardiomyoplasty on the circulation, in which the dorsal latissimus was wrapped around the heart. The studies were performed in the Physiological Laboratory of the University of Limburg, Maastricht. Seven goats (51 - 80 kg body weight) were anaesthetized with an intraperitoneal injection of thiopental sodium (15 mg·kg^{-1} bodyweight). The animals were placed in supine position on a thermo-controlled operating table to maintain body temperature at about 38.5 °C. Anaesthesia was maintained by ventilation with oxygen/nitro-oxide (1:2) and 1.5% Fluorothane. After tracheotomy, the goats were connected to a volume-controlled ventilator (Siemens Servo Ventilator). The ventilatory frequency was 15 breaths per minute and a positive end-expiratory pressure of 2-5 cmH$_2$O was applied. Via the left femoral artery a conductance catheter was forwarded into the left ventricular cavity under fluoroscopic guidance. Also a conductance catheter was forwarded into the right ventricular cavity under fluoroscopic guidance. Through the external jugular vein a Swan Ganz catheter (5F) was inserted into the pulmonary artery to measure temperature and pressure and to inject hypertonic saline for the determination of parallel

conductance in the left ventricle. In the vena cava an injection catheter was placed near the entrance of the right atrium to inject hypertonic saline for the determination of parallel conductance in the right ventricle. In addition, a pressure catheter was placed in the aorta via the right femoral artery.

5.2.5 Experimental protocol aortic measurements

Cross-sectional area of the aorta was changed by changing its pressure. Various levels of aortic pressure were created by inspiratory pause procedures (IPPs) in between the normal ventilations [Versprille and Jansen 1993]. An IPP is a procedure, in which a tidal volume is inflated (2.4 s) and held in the lungs during an inspiratory pause of 15 seconds, followed by an expiration (3.6 s). If tidal volume is inflated, left ventricular output and arterial pressure decrease and remain constant from about 1.5 s to 9 s after the start of the pause period. Each pressure level was imposed twice; once to determine the baseline level of conductance and once to determine parallel conductance and cardiac output, using one injection of hypertonic saline. The injection of 2.5 ml (17.5%) saline (room temperature) was given at one second after the beginning of the IPP. In a previous study we found that such injections of 2.5 ml solution did not affect the volume of the descending thoracic aorta [Chapter 2]. The inflation volumes of the successive IPP procedures were increased stepwise. This series was ended if the aortic pressure reached a critical level of approximately 40 mmHg. During the IPPs, pressures, ECG, temperature and the conductance signal were acquired at a sample frequency of 250 Hz and stored on disk for analysis. After each saline injection the conductivity of blood at blood temperature was measured off-line using a conductivity cell. Between each cold hypertonic saline injection a stabilisation period of 15 minutes was allowed.

5.2.6 Experimental protocol ventricular measurements

Two times at two conditions (before and after the wrapping procedure), an injection of NaCl solution (5 to 7.5 ml, 6 - 17.5%) was given at the beginning of a prolonged end-

expiratory pause of about 12 seconds. During the end-expiratory pauses the signals of conductances and pressures were acquired at a sample-frequency of 200 Hz and stored on disk for analysis. Before the measurements cardiac output (CO) was determined by thermodilution (COM-2, Baxter). The injection of 10 ml ice-cold glucose was done at the beginning of the prolonged end-expiratory pause. The results of five (CO) measurements were averaged. In between the CO measurements, periods of 1 to 3 minutes were allowed for stabilization.

5.2.7 Data analyses

We used only those measurements, where the total conductance dilution curve was obtained during a pause procedure.

Each single estimate of parallel conductance obtained with use of the conventional method in the descending thoracic aorta was compared to the value obtained with the new method. In each animal the standard deviations of both methods were calculated, assuming a constant parallel conductance within each animal.

Parallel conductance obtained with the conventional dilution method in the left and right ventricle was determined off-line by three observers. These results were averaged per observation. This averaged value was compared to the corresponding single value of parallel conductance obtained with use of the new method. In each condition of the goats, the differences in parallel conductance between the first and second measurement were obtained to compare the reproducibility with each of both methods. It was assumed that parallel conductance was constant for a constant condition of an animal.

Significance was assumed if $p \leq 0.05$.

5.3 Results

5.3.1 Measurements in the aorta of piglets

Parallel conductance was obtained in the descending thoracic aorta at various volemic conditions in five piglets with the conventional (G_p^l) and the new method (G_p^a). Using a paired t-test, the mean difference between G_p^a and G_p^l for all measurements was 0.278 $\pm$ 0.417 [1/Ohm] (SD) (n = 39), which was not significantly different from zero. Therefore the average outcome of both methods was the same.

Using a paired t-test, the mean difference between the standard deviation (SD) of the G_p^l- and G_p^a-values of all individual experiments was SD,G_p^l - SD,G_p^a = 0.30 [1/Ohm] with 95%CI = 0.127 → 0.463, p = 0.006. Thus the reproducibility of the G_p^a-method was significantly better than that of the G_p^l-method.

5.3.2 Measurements in the right and left ventricle

Parallel conductance obtained with the conventional (G_p^l) and the new method (G_p^a) were obtained in the left and right ventricle, two times at two conditions for seven goats. For each observation G_p^l was analyzed by three observers and the average value and standard deviation were calculated. The standard deviation averaged for all observations (n = 36) was 6.82 [1/Ohm] (mean G_p^l = 104.60 [1/Ohm]).

Using a paired t-test for all observations, the mean difference of G_p^l, averaged for three observers, and the corresponding value of G_p^a was -5.75 $\pm$ 16.49 [1/Ohm], which is not significantly different from zero. Therefore the average outcome of both methods is not different.

The differences in parallel conductances between the first and second observation in each condition of an animal in the left and the right ventricle were calculated. These differences were averaged for all duplicate values (n = 15). Firstly, these averaged differences in parallel conductances were determined with use of the conventional method by each of the three observers and were -8.81 $\pm$ 15.34, -7.46 $\pm$ 16.41 and 0.74 $\pm$ 19.74 [1/Ohm]. Secondly, the averaged difference between the duplicate values for all observers was -5.56 $\pm$ 11.59. Thirdly, the averaged difference between the duplicate values calculated with use of the new method was 1.00 $\pm$ 11.86. Thus, the reproducibility of the G_p^a-

method was similar to that of the G_p^l-method.

Seven measurements (7/43 = 8%) were excluded from the data set for analysis with the conventional method, based on expert knowledge of either one of the observers. However, these measurements could be analyzed with the new method and were in the range of values determined at the same condition.

5.4 Discussion

The estimates of parallel conductance obtained with use of both parallel conductance estimation methods were the same in the aorta and the ventricles respectively. In the aorta, the variation in parallel conductance obtained with the new method (G_p^a) was significantly lower than that of the conventional method (G_p^l). In the left and right ventricle the variation in G_p^a was equal to that in G_p^l, in spite of the fact that the G_p^l method is observer dependent, whereas the G_p^a-method is not observer-dependent. When parallel conductance in the left or right ventricle was determined with use of the G_p^l-method, seven measurements were rejected by either one of the three observers. Because of the chance that some measurements are rejected if the G_p^l-method is used, more measurements will be needed than with use of the new method to obtain the same accuracy. Thus, using the new method the number of injections with hypertonic saline can be kept as low as possible, preventing a possible deterioration of the condition of the patient [Kien and Kramer 1989].

To obtain a reliable G_p^a-value, the hypertonic saline injection should be given as a bolus and the cardiac output should be measured at the same condition. In the experiments where the parallel conductances in the left and right ventricle were determined with use of the G_p^a-method, the cardiac output was determined 3-15 minutes before or after the determination of the conductance dilution method, whereas in the aorta this was determined at the same time, which might explain the better reproducibility in the aorta with

use of the new method than obtained with the conventional method. We conclude that the new approach has advantages above the conventional method because of 1) a better reproducibility if it is used for the aorta, 2) the necessity of a smaller number of injections to obtain the same accuracy, 3) the simultaneous determination of parallel conductance and cardiac output and, 4) the possibility to automate the procedure.

Chapter 6

The volume-dependency of parallel conductance and its consequence for volume estimation of the left ventricle in patients.

L Kornet[1], JRC Jansen[1], ET van der Velde[2], JJ Schreuder[3] and A Versprille[1]

1) Pathophysiological Laboratory, Department of Pulmonary Diseases, Erasmus University, Rotterdam, The Netherlands
2) Department of Cardiology, Academic Hospital Leiden, The Netherlands
3) Department of Anaesthesiology, Academic Hospital Maastricht, The Netherlands

6.1 Introduction

The electrical conductance method can be used to determine left ventricular volumes continuously by relating the electrical conductance of blood in the left ventricle to its volume [Baan et al. 1981, 1984]. Besides blood, the tissues surrounding the ventricle contribute to the measured conductance and cause an offset in the conductance signal. This is called parallel conductance (G_p).

To determine G_p the conductance values at end-systole were plotted versus those at the preceding end-diastole during a heart beat-to-beat increase in conductivity of blood after the injection of hypertonic saline. The linear regression line through these values was extrapolated to the identity line. This value was regarded as parallel conductance (G_p^l) [Baan et al. 1981, 1984, 1988]. Stroke volume determined with use of the conventional conductance method was smaller than stroke volume obtained by an independent method as thermodilution [Jansen et al. 1981, 1987, 1990]. Conductance derived stroke volume was related to a reference stroke volume with use of a correction factor α, which is the ratio between both stroke volumes. The reason for this factor α was attributed to a non-homogeneous electrical field within the ventricle [Baan 1981, Applegate et al. 1990]. Kun and Peura [1994] hypothesized that such a non-homogeneous electrical field might cause parallel conductance to be volume dependent. Also, other authors found or suggested parallel conductance to depend on ventricular volume [Spinellli et al. 1986, Boltwood et al. 1989, Applegate et al. 1990, Lankford et al. 1990, Cassidy and Teitel 1992, Kun and Peura 1994, Szwarc et al. 1995], although a significant dependence could not always be shown [Boltwood et al. 1989, Applegate et al. 1990, Szwarc et al. 1994].

We hypothesized that the assumption of a constant parallel conductance throughout the heart cycle is incorrect and that parallel conductance is dependent on left ventricular volume. This hypothesis might imply that a correction with α is not needed if parallel conductance is determined throughout the heart cycle. We tested the hypothesis with use of a conductance dilution technique, with which we could estimate parallel conductance

(G_p^a) throughout the heart cycle as present in the left ventricle of patients. First the varying G_p^a-values, averaged per heart cycle during the time period of the dilution curve, obtained by this method were compared with the constant G_p^l-values obtained by the conventional method. Second, G_p^a was determined throughout the heart cycle. Third, the factor α was calculated as the ratio between the stroke volume, obtained by the conductance method using the conventional method to estimate parallel conductance, and that obtained by a thermodilution method. Because, the non-homogeneous field was indicated to be the reason for the need of α [Baan et al. 1981, Applegate et al. 1990] and the dependence of parallel conductance on left ventricular volume [Kun and Peura 1994], we studied whether a mathematical coupling between α and the slope of the relation between ventricular volume and parallel conductance (G_p^a) existed.

6.2 Methods

6.2.1 The conductance method

The general principles of the conductance method have been described extensively elsewhere [Baan et al. 1981, 1984, 1988, 1989]. Therefore, only the configuration needed for our study will be mentioned. Ten circular electrodes are mounted at equal distances near the tip of a catheter (7F, Sentron, Roden, The Netherlands) positioned in the left ventricle along the longitudinal axis. This catheter is connected to a signal-processor system (Model Leycom Sigma 5; Cardiodynamics, Oegstgeest, The Netherlands), which applies a 20 kHz., 30 μA RMS current between both the most outer electrodes (1 and 10) and between the two adjacent electrodes (2 and 9). This dual excitation was used to produce a more homogeneous electrical field, compared to single excitation [Steendijk 1992]. Left ventricular volume for a segment ($Q_{LV,segment}$) between two measuring electrodes at any time t is calculated as:

where L is the distance between two adjacent electrodes, σ_b the conductivity of blood,

$$Q_{(LV, segment)}(t) = \frac{L^2}{\sigma_b}[G(t) - G_p(t)] \tag{1}$$

$G(t)$ the time-varying conductance between the electrodes and $G_p(t)$ the time-varying conductance of the tissues surrounding the ventricle. Five segmental conductances are measured from six adjacent electrodes (3-4, 4-5, 5-6, 6-7, 7-8) and total left ventricular volume (Q_{LV}) is calculated from the sum of the five segmental volumes.

$$Q_{(LV)} = \frac{1}{\alpha}\Sigma Q_{(LV, segment 1 \rightarrow 5)} \tag{2}$$

α is the ratio between conductance derived stroke volume and stroke volume, determined by a reference method (e.g. thermodilution). In this study we have corrected for parallel conductance with use of two methods.

6.2.2 Parallel conductance obtained by extrapolation of a G_{dias}, G_{sys} curve

For the conventional method to estimate parallel conductance ($G_p^{\,l}$) [Baan et al. 1981, 1984], the assumption is made that the conductivity of the surrounding structures is not influenced by the injection of hypertonic saline and that $G_p^{\,l}$ is also constant during a heart cycle. Furthermore, it is assumed that the specific conductivity of the blood does not change from end-diastole to end-systole (injection phase), because σ_b will change only in the filling phase of the left ventricle, due to mixing of the hypertonic saline and blood. To eliminate the influence of mechanical ventilation on blood flow, the influence of the hypertonic saline injection on conductance was measured during a prolonged end-expiratory pause procedure. To obtain $G_p^{\,l}$, the two best identifiable points of the conductance signal in the cardiac cycle are used, i.e. the values at end-diastole (G_{dias}) and at end-systole (G_{sys}). From the G_{sys} versus G_{dias} plot, with σ_b increasing heart beat-to-beat in the ascending limb of the dilution curve after the injection of hypertonic saline, parallel conductance can be solved by extrapolation to that theoretical point where blood conductivity is zero. The following holds:

$$If\ \sigma_b\ \rightarrow\ 0,\ then\ G_{dias}\ =\ G_{sys}\ =\ G_p^l \qquad (3)$$

Thus G_p^l is the intersection point between the regression line of the relationship between G_{dias} and G_{sys} and the identity line ($G_{dias} = G_{sys}$).

To calculate G_p^l the software package CONDUCT-PC (Cardiodynamics) was used.

6.2.3 Parallel conductance obtained from the conductance dilution curve

Also this method to estimate parallel conductance is based on the dilution of hypertonic saline. Each injection of hypertonic saline was given near the entrance of the right atrium, and conductance was detected in the left ventricle. To eliminate the influence of mechanical ventilation on blood flow, the influence of the hypertonic saline injection on conductance was measured during a prolonged end-expiratory pause procedure. The indicator dilution method for hypertonic saline can be described by a mass balance, in which the concentration of ions which conduct electrical current is the same at the injection and detection side. With the assumption of complete mixing of indicator and blood, the following conductivity balance can be formulated:

$$\int_{t_1}^{t_2} \dot{Q}_i(t)\,(\sigma_i - \sigma_b)\,dt\ =\ \int_{t_1}^{t_2} \Delta \sigma_b(t)\,\dot{Q}_b(t)\,dt \qquad (4)$$

Here, t is time, t_1 the time of injection, t_2 the end of integration when all injected ions have passed the detector side, $\dot{Q}_i(t)$ the input flow of the injectate, σ_i the electrical conductivity of the injectate at blood temperature, σ_b the conductivity of the blood before injection, $\Delta\sigma_b$ the change in conductivity of the blood due to the injection of the hypertonic saline and $\dot{Q}_b(t)$ the blood flow. Average blood flow ($\dot{Q}_b$) was determined by thermodilution during the same condition of the patient as the conductance dilution curve was determined. If the injection is given as a bolus and $\dot{Q}_b(t)$ is constant, the equation can be rewritten as:

$$Q_i(\sigma_i - \sigma_b) = \dot{Q}_b \int_{t_1}^{t_2} \Delta\sigma_b(t)\,dt \qquad (5)$$

where Q_i is the volume of the injectate.

We assumed that a correction of left ventricular volume with α is not necessary ($\alpha = 1$). If parallel conductance is the same at corresponding moments in the successive cardiac cycles, during which hypertonic saline passes the ventricle, and stroke volume remains constant then the change in conductance is caused only by the change in conductivity and the following holds:

$$\Delta\sigma_b(t) = \frac{L^2}{\overline{Q_{LV}}(n)\,\Delta G(t)} \qquad (6)$$

where $\overline{Q_{LV}}$ is the intra-ventricular volume averaged over a heart cycle occurring in the dilution curve and n the number of the corresponding heart beat.

Substituting $\Delta\sigma_b(t)$ in equation 5 and rearrangement of the equation gives:

$$\frac{\overline{Q_{LV}}(n)}{L^2} = \frac{\dot{Q}_b \int_{t_1}^{t_2} \Delta G(t)\,dt}{Q_i(\sigma_i - \sigma_b)} \qquad (7)$$

Substituting $\overline{Q_{LV}}(n)/L^2$ in equation 1 and 2 gives:

$$\overline{G}_p^a(n) = \overline{G}(n) - \frac{\sigma_b \dot{Q}_b \int_{t_1}^{t_2} \Delta G(t)\,dt}{Q_i(\sigma_i - \sigma_b)} \qquad (8)$$

$\overline{G}_p^a(n)$ is the parallel conductance averaged over the nth heart cycle. We assume that $\overline{G}_p^a$ does not change between successive heart cycles and that $\overline{G}_p^a(n)$ can be written as $\overline{G}_p^a$. $\overline{G}(n)$ was the averaged conductance per n^{th} heart cycle before hypertonic saline passed the conductance catheter. In contrast to the conventional method to determine parallel conductance, Q_i, $\dot{Q}_b$ and σ_i should be known. $\dot{Q}_b$ was determined with use of the thermodilution method [Jansen 1981, 1987, 1990] and conductivity of blood (σ_b) and the

hypertonic injectate (σ_i) were determined at body temperature with use of a cell (Leycom Sigma 5DF). To obtain $\int \Delta G(t)dt$ the whole dilution curve of ions (conductance) was monitored during an end-expiratory pause procedure (Fig 1). As shown in Figure 1, $G_p{}^a$ was averaged per heart cycle over all heart cycles during the passage of the conductance dilution curve. A dilution curve was plotted through the average conductance versus time values. A baseline (G(t)) was drawn from the start to the end of the dilution curve. The area under the curve ($\int \Delta G(t)dt$) was obtained by subtracting the area under the baseline from the area under the total dilution curve. The baseline was subtracted to correct for accumulation of salt in the ventricle wall, passage of saline in the adjacent ventricle and recirculation.

To study the varying parallel conductance ($G_p{}^a$) during a heart cycle, the conductance signal was divided in 10 equal time intervals for each heart cycle during the dilution curve. The first interval started at the beginning of systole and the last interval ended at the end of diastole. For every i^{th} interval, the conductance signal was averaged and plotted versus time. In Figure 1B conductance is averaged for the firsth interval of the heart cycles during the dilution curve. Again a dilution curve was plotted through the average conductance versus time values and the area under the dilution curve was obtained by subtracting the baseline. In figure 1C the area under a dilution curve, constructed for the sixth interval within each heart cycle, is shown. It should be noted that the baseline of a dilution curve is different for the various intervals.

6.2.4 Patient studies

We used data from six patients who had undergone cardiomyoplasty because of dilated cardiomyopathy. The study has been approved by the medical ethics committees of the various hospitals, where the patients were accommodated. Informed patient consent was obtained for insertion of catheters. The patients were sedated and heparinized before catheterization. A pulmonary arterial thermodilution catheter was positioned in the pulmonary artery and a lumen of this catheter, positioned near the entrance of the right
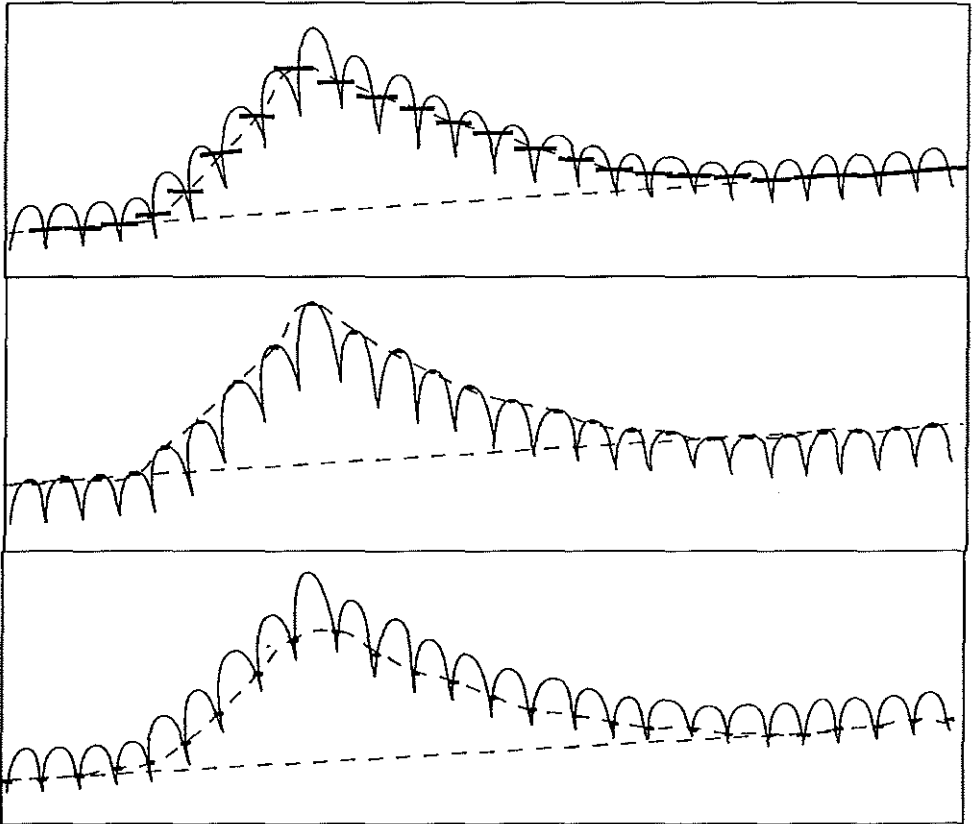
Fig. 1: The effect of the injection of hypertonic saline is determined as conductance. Besides the conductivity of blood conductance depends on ventricular volume and therefore varies pulsatile within a heart cycle. Average conductance over a heart cycle (Fig. A) or average conductance over a time interval (1th interval, Fig. B; 6th interval Fig. C) within a heart cycle is determined and a dilution curve is plotted through the average conductance versus time values. A baseline is subtracted to obtain the area under the curve.

atrium, was used for the injection of saline. A catheter equipped with two micro-manometers was positioned in the left ventricle via the left femoral artery for the measurement of aortic and left ventricular pressures. The 10-electrode conductance catheter was inserted via the right femoral artery into the left ventricle. An injection of NaCl solution (5 to 7.5 ml, 6 - 17.5%) was given twice at the beginning of a prolonged end-expiratory pause of about 12 seconds. During the end-expiratory pauses the signals of conductances and pressures were acquired at a sample-frequency of 200 Hz and stored on disk for analysis. Shortly, before the measurements cardiac output (CO) was determined by thermodilution (COM-2, Baxter). The injection of 10 ml ice-cold glucose was done at the beginning of the prolonged end-expiratory pause. The results of five (CO) measurements were averaged. In between the CO measurements, periods of 1 to 3 minutes were allowed for stabilization. Stroke volume (Q_{SV}^{TD}) was calculated by dividing CO, obtained by thermodilution, by heart rate.

6.2.5 Data analyses

Firstly, the parallel conductances G_p^I and G_p^a, averaged over the heart cycles within the dilution curve, were compared. Secondly, G_p^a was determined for each of the ten intervals within a heart cycle and plotted versus the corresponding ventricular volume ($Q_{LV}^{G(a)}$). To obtain stroke volume, end-diastolic minus end-systolic ventricular volume was calculated with the conductance method, using the constant parallel conductance G_p^I, and the time-varying parallel conductance G_p^a. Because left ventricular volume ($Q_{LV}^{G(a)}$) is an average value of a certain interval, the maximum and minimum $Q_{LV}^{G(a)}$ will be slightly under- and over-estimated respectively. Therefore, we used the maximum and minimum conductance found in each heart cycle during the dilution curve to calculate stroke volume ($Q_{SV}^{G(a)}$). This stroke volume was compared to stroke volume obtained by thermodilution (Q_{SV}^{TD}). To obtain α, stroke volume obtained by the conventional conductance method ($Q_{SV}^{G(l)}$) was divided by stroke volume calculated with use of the thermodilution method (Q_{SV}^{TD}).

6.3 Results

6.3.1 Comparison of the two methods to estimate parallel conductance

The values obtained by both methods to estimate parallel conductance were not significantly different, whereas the mean difference = -7.18 ± 15.47 [1/Ohm], (mean G_p^i = 141.64 [1/Ohm] and mean G_p^a = 134.46 [1/Ohm]).

6.3.2 Parallel conductance depends on left ventricular volume

For a typical measurement, the values of parallel conductance (G_p^a) and left ventricular volume ($Q_{LV}^{G(a)}$) were plotted as a function of the ten intervals occurring within the heart cycle (Fig. 2). The first interval started at the beginning of systole and the last interval ended at the end of diastole. At the interval where left ventricular volume was minimum, parallel conductance was maximum for each measurement. For all measurements (n = 12), the change in G_p^a in percentages of the average G_p^a for the corresponding measurement was averaged for each interval and plotted versus the intervals (Fig. 3). At end-diastole (interval 10) G_p^a was 92% and at end-systole (interval 5) G_p^a was 110% of the G_p-value averaged over the whole heart cycle, for the corresponding measurement.

In the example of figure 2, parallel conductance (G_p^a) was plotted versus left ventricular volume ($Q_{LV}^{G(a)}$) and a linear regression line was the best fit through the values (Fig. 4). Again, it is obvious that parallel conductance (G_p^a) decreased with increasing left ventricular volume ($Q_{LV}^{G(a)}$). The duplicate measurements in each patient resulted in the same linear regression lines of parallel conductance versus left ventricular volume. We compared slopes and intercepts of the first and second measurement and found no significant difference (paired-t-test, p ≥ 0.05). Therefore, we plotted one linear regression line through all data of each patient (Table 1). The slopes as well as the intercepts of these linear regression lines were significantly different between the patients.
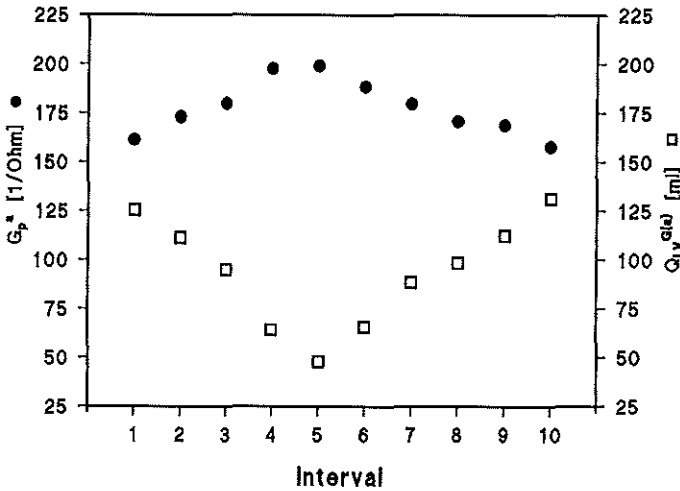
Fig. 2: For one typical measurement $G_p{}^a$ and $Q_{LV}{}^{G(a)}$ are plotted versus the corresponding ten equally divided time-intervals within the heart cycle.
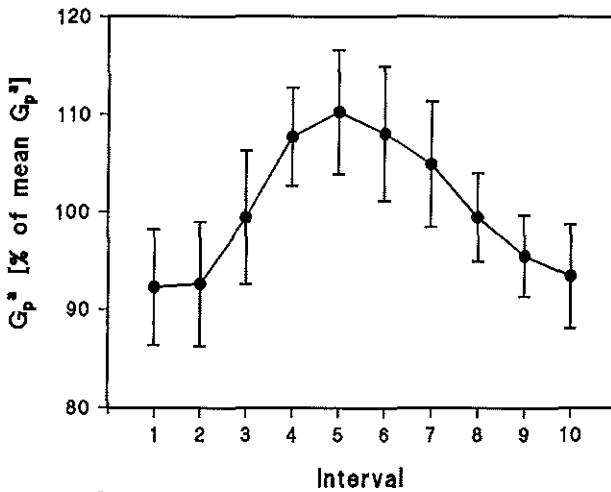
Fig.3: $G_p{}^a$, averaged for all measurements, is plotted, as a percentage of the mean $G_p{}^a$ in the heart cycle for the corresponding measurement, versus the corresponding ten equally divided time-intervals within the heart cycle. The error bars present $\pm\ 2 \cdot SD$.
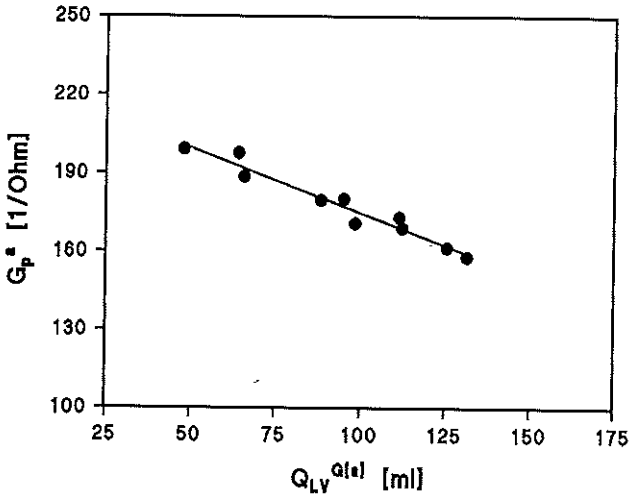
Fig. 4: For a typical measurement G_p^a is plotted versus $Q_{LV}^{G(a)}$. A linear regression line is drawn through these values.

6.3.3 Stroke volume and 1/α

Stroke volume obtained from the new conductance method $(Q_{SV}^{G(a)})$ did not differ significantly from stroke volume obtained by thermodilution (Q_{SV}^{TD}) (paired t-test, $Q_{SV}^{TD} - Q_{SV}^{G(a)} = 3.27$ (p $\geq$ 0.05) [ml]). Thus, ventricular volume did not need a correction with 1/α (Equation 2) if the new method to estimate parallel conductance was used.

Stroke volume obtained by the conventional conductance method $(Q_{SV}^{G(l)})$ was significantly smaller than Q_{SV}^{TD} (paired t-test, $Q_{SV}^{TD} - Q_{SV}^{G(l)} = 41.83$ [ml], p $\leq$ 0.05). Therefore, 1/α $(Q_{SV}^{TD}/Q_{SV}^{G(l)})$ did significantly differ from one (paired t-test, 1/α = 2.09 (p $\leq$ 0.05).

Table 1: The linear regression lines through the parallel conductance (G_p^a) versus left ventricular volume ($Q_{LV}^{G(a)}$) values from all measurements of each experiment are shown.

patient	slope (d) ± SD 1/[Ohm·ml]	intercept ± SD [1/Ohm]	R^2
1	-0.559 ± 0.025	228.40 ± 3.19	-0.98
2	-0.359 ± 0.032	192.95 ± 4.14	-0.93
3	-0.396 ± 0.021	219.50 ± 2.12	-0.99
4	-0.569 ± 0.021	229.14 ± 2.11	-0.99
5	-0.242 ± 0.073	198.64 ± 3.07	-0.76
6	-0.540 ± 0.034	141.78 ± 1.51	-0.97

6.4 Discussion

In this study we have shown that parallel conductance decreased during a heart cycle if ventricular volume increased. In each patient this relationship between parallel conductance and ventricular volume appeared to be reproducible, but between patients a large variation in this relationship was found. We conclude that the conductivity of the tissues and fluids surrounding the blood in the ventricle is different between patients, but constant in one patient. Probably the tissues of one patient are more hydrated than those of another.

Lankford et al. [1990] introduced a method to calculate parallel conductance throughout the heart cycle. This method depended on the G_p^l-method as described by Baan et al. [1981, 1984] and had the same large inaccuracy as reported for this method [Boltwood et al. 1989, Applegate et al. 1990, Szwarc et al. 1994]. We assume that

parallel conductance will be estimated more accurately throughout the heart cycle with use of our new method, because it is based on the estimation of an area under the conductance versus time curve (dilution curve of ions) instead of the extrapolation of a line through conductance values at systole versus those at diastole.

Lankford et al. [1990] indicated that the values of parallel conductance as found during a heart cycle varied about 10% of their mean, however, the values did not differ significantly from the mean over the heart cycle.

Szwarc et al. [1995] also indicated that the values of parallel conductance as found within a heart cycle varied about 10% of their mean and in contrary to the previous author he found that the values were significantly different between each other. The change in ventricular volume over a heart cycle found by Szwarc et al. followed the same pattern as we found (Fig. 3A).

Our observation that parallel conductance decreased linearly with increasing left ventricular volume is in contradiction with studies where average left ventricular volume was varied [Boltwood 1989, Applegate et al. 1990]. In these studies, it was reported that parallel conductance remained constant, if measured under steady-state conditions or measured during aortic or pulmonary arterial occlusion, but decreased with decreasing left ventricular volume during vena caval occlusion. Probably an unknown factor influenced parallel conductance, which might have been the filling of the right ventricle.

Szwarc et al. [1995] showed that parallel conductance at a low end-diastolic volume is 6 ± 16% higher than that at a high end-diastolic volume, but this difference was not significant. They also showed that α was 0.62 ± 0.24 at high end-diastolic volumes and was 0.81 ± 0.15 at low end-diastolic volumes, but again significance was not obtained. Possibly, the parallel conductance was over-estimated at high end-diastolic volumes and under-estimated at low end-diastolic volumes due to the reported increase in α, which accompanied left ventricular volume reduction [Szwarc et al. 1995].

Cassidy and Teitel [1992] used one constant value for parallel conductance and assumed parallel conductance to be independent of ventricular volume. They found a better

correlation between total volume (volume of the blood in the left ventricle and tissues surrounding the blood), obtained by the conductance method, and volume obtained by cineangiography, than between ventricular blood volume, obtained by the conductance method, and that obtained by cineangiography. They suggested that an error was introduced in the calculation of blood volume, if parallel conductance is assumed to be volume-independent. Theoretical studies predict a dependence of parallel conductance on volume [Spinelli et al. 1986, Kun and Peura 1994], because the larger the ventricle, the smaller the density of the electric current at the myocardial boundary and the smaller the leakage current (parallel conductance).

In conclusion, we used a new conductance dilution method to determine parallel conductance throughout the heart cycle and found a linear relation between parallel conductance and left ventricular volume. The correction factor α is assumed to be a correction for an inhomogeneity of the electrical field [Baan et al. 1981, Applegate et al. 1990]. Furthermore, a non-homogeneous electrical field was suggested to cause parallel conductance to be volume dependent [Kun and Peura 1994]. The slope of the relation between parallel conductance and left ventricular volume and the factor α, as obtained with use of the conventional conductance method, appeared to be mathematically coupled, which is described in the Appendix. We conclude that a correction with α is not needed if parallel conductance is determined throughout the heart cycle. However, if a constant parallel conductance is assumed throughout the heart cycle, a correction with α must be made.

6.5 Appendix

We supposed that α is needed because of an incorrect use of a constant parallel conductance throughout the heart cycle. Therefore, we supposed a mathematically

coupling between α and the slope of the time-varying parallel conductance (G_p^a) versus left ventricular volume ($Q_{LV}^{G(a)}$) relationship. In figure 5 our reasoning is schematically given. The measured total conductance (G_{tot}) increases linearly if ventricular volume (Q_{LV}) increases. From G_{tot}, parallel conductance (G_p^l or G_p^a) is subtracted to obtain conductance of the blood segment (G_B^l or G_B^a respectively), which can be used to calculate ventricular volume. The superscript "l" means obtained after subtracting the constant G_p^l from the total conductance. The superscript "a" means obtained after subtracting the volume dependent G_p^a from the total conductance. The value determined at end-systole is indicated as a subscript "sys", the value and end-diastole is indicated as a subscript "dias" and the mean value is indicated as a subscript "mean". The G_p^a, averaged over a heart cycle equals G_p^l at mean left ventricular volume ($Q_{LV,mean}$). We found that G_p^a decreases linearly if ventricular volume increases. If G_p^l is subtracted from the total conductance signal at diastole, the conductance of blood (G_B^l) is under-estimated with a value $G_{dif,dias}$. G_{dif} is the difference between G_p^l and G_p^a. Likewise, if G_p^l is subtracted from the total onductance signal at systole ($G_{tot(sys)}$), the conductance of the blood (G_B) is over-estimated with a value $G_{dif,sys}$. Thus:

$$G_{B,dias}^{a} = G_{B,dias}^{l} + G_{dif,dias} \qquad (9)$$

and:

$$G_{B,sys}^{a} = G_{B,sys}^{l} - G_{dif,sys} \qquad (10)$$

Furthermore it was mentioned before that:

$$\frac{1}{\alpha} = \frac{Q_{SV}^{TD}}{Q_{SV}^{G(l)}} \qquad (11)$$

Our results show that stroke volume obtained by thermodilution: Q_{SV}^{TD}, is not significantly different from stroke volume obtained by the conductance method with use of the new parallel conductance estimation method; $Q_{SV}^{G(a)}$. Thus from equation 11 follows:

$$\frac{1}{\alpha} = \frac{Q_{SV}^{G(a)}}{Q_{SV}^{G(l)}} \tag{12}$$

If a correction with α is not needed, from equation 1 and 2 follows:

$$Q_{SV}^{G(a)} = (G_{B,dias}^{a} - G_{B,sys}^{a}) \cdot \frac{L^2}{\sigma_b} \tag{13}$$

and:

$$Q_{SV}^{G(l)} = (G_{B,dias}^{l} - G_{B,sys}^{l}) \cdot \frac{L^2}{\sigma_b} \tag{14}$$

Combining equation 12, 13 and 14 gives:.

$$\frac{Q_{SV}^{G(a)}}{Q_{SV}^{G(l)}} = \frac{G_{B,dias}^{a} - G_{B,sys}^{a}}{G_{B,dias}^{l} - G_{B,sys}^{l}} \tag{15}$$

Here $Q_{SV}^{G(l)}$ is ventricular stroke volume obtained by the conductance method with use of the G_p^l-method and $Q_{SV}^{G(a)}$ is ventricular stroke volume obtained by the conductance method with use of the G_p^a-method. Substituting equation 9, 10 and 12 in equation 15 gives:

$$[G_{B,dias}^{l}+G_{dif,dias}] - [G_{B,sys}^{l}-G_{dif,sys}] = \frac{1}{\alpha} \cdot [G_{B,dias}^{l}-G_{B,sys}^{l}] \tag{16}$$

Furthermore:

$$G_{B,dias}^{l} = \frac{Q_{LV,dias}^{G(l)} \cdot \sigma_b}{L^2} \tag{17}$$

and :

$$G_{B,sys}^{1} = \frac{Q_{LV,sys}^{G(1)} \cdot \sigma_b}{L^2} \tag{18}$$

If in equation 16 all factors are multiplied with L^2/σ_b the following equation is obtained:

$$[Q_{LV,dias}^{G(1)} + G_{dif,dias} \cdot \frac{L^2}{\sigma_b}] - [Q_{LV,sys}^{G(1)} - G_{dif,sys} \cdot \frac{L^2}{\sigma_b}] = \frac{1}{\alpha} [Q_{LV,dias}^{G(1)} - Q_{LV,sys}^{G(1)}] \tag{19}$$

The sum of $G_{dif,sys}$ and $G_{dif,dias}$ can be used to calculate the negative slope of the linear regression line; d, through the G_p^a versus $Q_{LV}^{G(a)}$ values (Fig. 5) according to:

$$G_{dif,sys} + G_{dif,dias} = d \cdot (Q_{LV,sys}^{G(a)} - Q_{LV,dias}^{G(a)}) \tag{20}$$

From substituting equation 20 ($G_{dif,sys}$ and $G_{dif,dias}$) into 16 follows:

$$\frac{1}{\alpha} = 1 + \frac{Q_{SV}^{G(a)}}{Q_{SV}^{G(1)}} \cdot \frac{L^2}{\sigma_b} \cdot d \tag{21}$$

The $1/\alpha$ calculated with equation 21, averaged for each experiment, was compared to the $1/\alpha$ ($Q_{SV}^{TD}/Q_{SV}^{G(l)}$), averaged for each experiment. No significant difference was found using a paired t-test, with $1/\alpha$(calculated) − $1/\alpha(Q_{SV}^{TD}/Q_{SV}^{G(l)})$ = 0.25 (p $\geq$ 0.05). Thus the factor α is most probably mathematically coupled to the slope (d) of the linear regression line through the G_p^a versus $Q_{LV}^{G(a)}$ values.
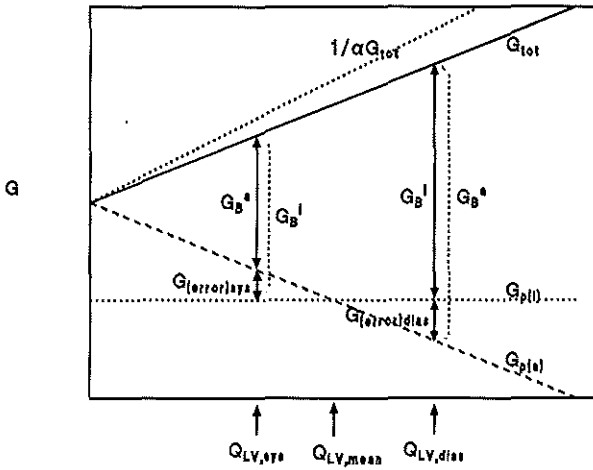
Fig. 5: The correction for a non-constant parallel conductance is schematically drawn. The solid line presents total conductance (G_{tot}) plotted versus ventricular volume. Above this line $1/\alpha \cdot G_{tot}$ is drawn as a dashed line. The dotted horizontal line is the constant G_p^l and the striped line is the linearly decreasing G_p^a. G_{dif} is the difference between G_p^l and G_p^a. G_B is the conductance of blood obtained with (l) the G_p^l method or (a) the G_p^a method.

Chapter 7

Final Considerations and Suggestions for Future Research

7.1 Introduction

To determine blood flow per heart beat in the pulmonary artery from the pulmonary arterial pressure wave, a three-element model of pulmonary input impedance is needed. This model includes pulmonary arterial characteristic impedance, pulmonary arterial compliance and vascular resistance. In this thesis, the pulmonary arterial compliance was determined from the changes in cross-sectional area of the pulmonary artery with use of a conductance method. This chapter comprises (i) an evaluation of the applications of the conductance method to determine cross-sectional areas (i.e. segmental blood volumes) of vessels and ventricles, (ii) explanations of the influence of pulmonary arterial pressure and heart rate on the compliance of the pulmonary artery, and (iii) a discussion of the clinical relevance of our findings.

7.2 Measurement of blood vessel volumes

As mentioned extensively, the measured electrical conductance determined in a blood vessel or ventricle consists of the conductance of blood and the conductance of the tissues and fluids surrounding the blood (parallel conductance). Because parallel conductance is about 60% of the total conductance, errors in the estimation of parallel conductance will have a large influence on the calculated blood conductance and thus on the calculated blood vessel volume. Therefore, an accurate determination of parallel conductance is needed. We presented a new approach to determine parallel conductance (chapter 5), which has advantages above the conventional method, namely: 1) a better reproducibility if it is measured in a blood vessel, 2) a smaller number of injections is required to obtain the same accuracy, 3) the possibility to determine parallel conductance and cardiac output simultaneously, and 4) the procedure can be fully automated.

   To extent the application of the conductance method to the determination of segmental

volume of a blood vessel, the blood conductivity determined with use of a cell, needed to be corrected for the influence of pulsatile flow and thus pulsatile shear rate. Shear rate causes orientation and deformation of erythrocytes, leading to an increase in conductivity of blood. In chapter 2 we concluded that the erythrocytes in pig blood will still be mainly de-aggregated, orientated and deformed at the end of a diastole. This conclusion was based on the time of a diastole within a heart cycle in piglets, and the time constants for (de-)orientation, (de-)formation and (de-)aggregation of pig erythrocytes. Because the influence of shear rate on conductivity hardly varied within a heart cycle, one correction factor was used throughout the heart cycle. In humans, the time of a diastole is about 2 to 5 times larger than in piglets. Then, it is doubtful whether it is allowed to use a single correction factor for shear rate, even if the time constants for (de-)orientation, (de-)formation and (de-)aggregation are the same for human erythrocytes and for pig erythrocytes. Visser [1989] used human blood for his experiments and showed in one individual example that conductivity increased instantaneously after a stepwise increase in shear rate from zero to a certain value. From his observation, we concluded that conductivity of human blood can be corrected during systole using a single correction factor for shear rate. However, this conclusion is valid only during systole when shear rate exceeds the value at which erythrocytes are maximally orientated and deformed. Thus, compliance of large blood vessels in humans can possibly be determined with use of the conductance method if the systolic phase of the heart cycle is only taken into account.

In a later study, we discovered an alternative method to determine the cross-sectional area of large arteries, where the influences of shear rate and parallel conductance on the estimated blood conductance were eliminated. This method was based on a double indicator dilution method (chapter 4). Shear rate and parallel conductance did not influence the data obtained with the double indicator dilution method, because only the change in measured conductance was used to determine the cross-sectional area of a blood vessel. Therefore, the double indicator dilution method can probably also be used to determine segmental volumes of large human arteries, where the influence of shear rate on conductivity is higher [Visser

1989] and more pulsatile than in the arteries of pigs. However, this method needs to be tested in large arteries of patients with use of a reference method.

We showed that it is possible to determine the dynamical change of cross-sectional area within a heart cycle. For that reason, the conductance signal corresponding to a full heart cycle was subdivided in ten equal time intervals per heart cycle (chapter 6). To our opinion, this technique is applicable in the heart catheterization laboratory, the intensive care unit and during thoracic surgery, where patients are routinely catheterized with aortic or pulmonary arterial pressure catheters. Such catheters should be equipped with four electrodes to determine also cross-sectional area throughout the heart cycle. The cross-sectional area determined throughout the heart cycle during a dilution curve with use of the double indicator dilution method can be used to calibrate the measured conductance signal to derive a measure of cross-sectional area continuously. The continuous cross-sectional area measurement together with the continuous pressure measurement will give a continuous compliance measurement. The measurements of cross-sectional area and compliance might be useful to monitor the effect of drug therapy in the operating room continuously, without the need for expensive labour intensive ultrasound methods. Furthermore, by moving the catheter through the vessel obstructions and aneurysms can possibly be detected. Such applications of the conductance catheter need further study in patients.

7.2 Compliance of the pulmonary artery

To determine pulmonary arterial flow from pulmonary arterial pressure, compliance of the pulmonary artery needs to be known. In literature, it is assumed that pulmonary arterial compliance is constant [Patel et al. 1960, Ingram et al. 1970, Johnson et al. 1985 and Greenfield and Griggs [1963]. However, we found a large dependence of pulmonary arterial pressure on compliance. This dependence was affected by heart rate and was different for the various pigs, which we will try to explain.

Effect of pressure

In this section we will explain the influence of pulmonary arterial pressure on the compliance of the pulmonary artery (chapter 3). Various physical models of the mechanical properties of the arterial walls have been presented. Langewouters [1984] modeled the elasticity of the aorta by a parallel arrangement of two non-linear springs with highly different moduli of elasticity (Fig. 1). The modulus of elastin (E_e) decreases slightly until it is fully straightened and is constant thereafter. At a low extension, the modulus of collagen (E_c) is low but it increases strongly with extension. Armentano et al. [1991] modeled the elastic modulus of the whole aortic wall by defining 1) the elastic modulus of elastin fibres (E_e), 2) the elastic modulus of collagen fibres (E_c) and 3) the recruitment of collagen fibres (f_c) supporting wall stress at a given transmural pressure. This model was based on the morphological observations of Wolinsky and Glagov [1964]. Later, they [Barra et al. 1993, Armentano et al. 1995] also assessed the elastic contribution of vascular smooth muscle cells with use of an extended Maxwell model (Fig. 2),
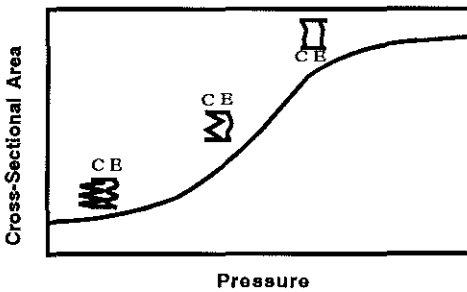

Fig. 1: Schematical presentation of cross-sectional area versus pressure in a blood vessel. E is elastin and C is collagen.

This model consists of a contractile element (CE), an elastic spring (SEC) coupled in series with the CE, and a parallel elastic component (PEC). The SEC (Series Elastic Compound) is composed of elastin arranged in series with smooth muscle cells (CE = contractile

element). The PEC is composed of elastin in parallel with collagen. The collagen is presented by a number of springs that contribute to tension at different degrees of extension. Thus, the incremental elastic modulus of the whole arterial wall (E_{inc}) might be written as:

$$E_{inc} = E_e + E_c \cdot f_c + E_{sm} \cdot F_a \tag{1}$$

where E_e is the elastic modulus of elastin, E_c the elastic modulus of collagen, f_c the fraction of recruited collagen fibres, E_{sm} the elastic modulus of the elastic fibres in series with the activated smooth muscle cells and F_a the activation function of activated smooth muscle cells. This model described by Armentano et al. [1995] has the following limitations: 1) the tension developed by the SEC will depend on the degree of vascular smooth muscle contraction behaviour, which they did not consider; 2) besides elastin and collagen, the resting tension of vascular smooth muscle cells might contribute to the tension of the PEC; 3) the elastin is presented by a single elastic modulus. However, at lower pressures the elastin is folded and has a higher elastic modulus than when aligned as at higher pressure.
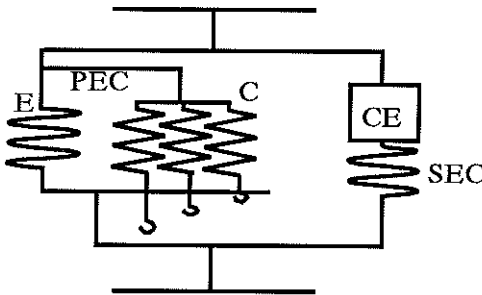
Fig. 2: Schematical presentation of modified Maxwell model [Barra et al. 1993]. C indicates collagen; E, elastin; SEC, series elastic component; PEC, parallel elastic component; and CE, contractile element. To indicate the recruitment of collagen fibers the collagen is represented by a number of springs that contribute to tension at different degrees of extension and thus simulate the elastic behaviour of the collagen fibres represented by the product $E_c \cdot f_c$, where E_c is the elastic modulus of collagen fibres and f_c the fraction collagen fibres recruited to support wall stress.

Effects of heart rate

We found an effect of heart rate on the cross-sectional area of the pulmonary artery. We assume that smooth muscle tone of the vessel is affected by heart rate. Two mechanisms can be taken into account to explain this, firstly the frequency of pulsatile shear stress and secondly the frequency of stretch.

Shear stress induced the release of endothelium derived relaxing factor [Furchgott and Zawadski 1980, Furchgott 1983, Pohl et al. 1986, Rubanyi et al. 1986] and prostacyclin [Frangos et al. 1985]. The release of endothelium derived relaxing factor was greater when flow (and thus shear stress) was oscillatory than when it was steady [Furchgott and Zawadski 1980, Furchgott 1983, Pohl et al. 1986, Rubanyi et al. 1986, Hutcheson and Griffith 1991]. Also the release of prostacyclin increased 16-fold more if human endothelial cells in culture were subjected to pulsatile shear stress than when the cells were in a stationary culture [Frangos et al. 1985]. Thus, the vasoconstriction, which we found after an increase in heart rate, cannot be explained by an increase in cyclic shear stress, because this would lead to vasodilation.

Due to the high stretch frequency of smooth muscle cells, calcium accumulates in the cell causing contraction directly [Bialecki et al. 1992, Coburn 1987, Fischell et al. 1989, Kirber et al. 1988, 1992, Kulik et al. 1988, Monos et al. 1986, Walsh and Singer 1980, Winston et al. 1993] or causing the release of vasocontrictors which causes contraction [Kulik et al. 1991]. For example, Sumpio and Widmann [1990] demonstrated that bovine aortic endothelial cells produce a basic level of endothelin under stationary conditions and that this level increases a factor five to sixfold with cyclic stretch. Endothelin is a peptide, which induces extensive and prolonged vasoconstriction [Yanagisawa et al. 1988]. So, probably the influence of an increase in heart rate on the cross-sectional area of the pulmonary artery can be explained from the effect of an increase in cyclic stretch.

To study this effect more clearly, cross-sectional area versus pressure curves of the pulmonary artery should be determined at various constant heart rates. However, at very low blood pressures the heart rate increases. To determine the mechanical properties at a constant

heart rate, the heart rate should be lowered. This could be attained by the administration of drugs followed by pacing of the heart. However, such drug should have no effect drug on the vessel wall.

7.4 Application of findings

Pulse contour methods are based on a windkessel model, which usually consists of a characteristic impedance, vascular resistance and arterial compliance. Conventionally, flow is determined from the aortic pressure wave with use of a model of the systemic arterial circulation [Wesseling et al. 1976, 1983, 1993, Jansen et al. 1990, Weissman et al. 1993, Tannenbaum et al. 1993]. A parameter of this model is the aortic compliance, which can be derived from the measured cross-sectional areas obtained at various pressures in in vitro experiments [Langewouters 1984]. Probably such application is reliable, because the aorta contains only a small amount of smooth muscle cells [Bader 1963, Dobrin and Rovick 1983] so that heart rate probably does not affect the compliance. The medial layer of the pulmonary artery, however, consists for 80-90% of smooth muscle cells [Somlyo and Somlyo 1964]. We found that heart rate influenced the cross-sectional area of this vessel and we therefore concluded that cross-sectional area and compliance measurements of the pulmonary artery in vitro cannot be extrapolated to the in vivo situation. In our study we also found a large variation between the compliance values of individual piglets. In general, it would be best to determine cross-sectional area and compliance in each individual patient, because the vessel of a particular patient does not have to resemble the data obtained from a group of human beings.

Our extensions and improvements of the electrical conductance method to measure cross-sectional area's of blood vessels may result in an extension of the application of the pulse contour method to patients, healthy human beings and animals.

Summary

Chapter 1

Continuous monitoring of cardiac output is important in patients who are undergoing intensive care, thoracic surgery or a catheterization for diagnostic reasons. In these patients aortic or pulmonary arterial pressures are routinely determined. From one of these pressures cardiac output can be determined continuously with use of a windkessel model of the circulation. A parameter of this model is the compliance of the arterial system, which is the change in volume per unit length (i.e. segmental volume) over a change in arterial pressure. To measure the change in segmental volume we used the electrical conductance method. In chapter one we have explained: 1) the context in which the research has been carried out, 2) the function of blood vessels, the large arteries in particular, 3) the anatomy of arteries, 4) the terms concerning the mechanics of blood vessels, and 5) the electrical conductance method used, to determine segmental blood volume in large arteries.

Chapter 2

In this chapter a modified conductance method to determine cross-sectional areas (CSAs) of arteries in piglets in vivo was evaluated. The method utilized a conductance catheter having four electrodes. Between the outer electrodes an alternating current was induced and between the inner electrodes the voltage difference or conductance was measured. CSA was determined from measured conductance minus parallel conductance, which is the conductance of the tissues surrounding the vessel, times the length between the measuring electrodes of the conductance catheter divided by the conductivity of blood. The parallel conductance was determined by injecting hypertonic saline to change blood conductivity. The conductivity of blood was calculated from temperature and haematocrit and it was corrected for shear rate. The equations to calculate the conductivity of blood and the

correction for shear rate were obtained from in vitro experiments. In vivo average aortic CSAs, determined with the conductance method ($CSA_{(G)}$), were compared to those determined with the intravascular ultrasound method ($CSA_{(IVUS)}$). The regression equation between both values was $CSA_{(G)} = -0.09 + 1.00 \cdot CSA_{(IVUS)}$, r = 0.97, n = 53. The mean difference between the values was -0.29% $\pm$ 5.57% (2SD). We conclude that the modified conductance method is a reliable technique to estimate the average cross-sectional area of arteries in piglets.

Chapter 3

The modified conductance was used to determine the cross-sectional area of the pulmonary artery, which was used to calculate the compliance of the pulmonary artery. The influence of mean pulmonary arterial pressure (mP_{pa}) on dynamic (C_d) and pseudo-static compliance (C_{ps}) of the pulmonary artery was studied at a constant and a changing heart rate. C_d is the change in cross-sectional area (CSA) related to the change in P_{pa} throughout a heart cycle. C_{ps} is the change in mean CSA related to the change in mean P_{pa}. If C_d is known pulmonary blood flow can be computed from the P_{pa}, using a windkessel model. We studied whether C_{ps} can be used interchangeably with C_d. In nine anaesthetized pigs, we determined mean CSA and C_d of the pulmonary artery at various P_{pa} levels ranging from approximately 30 to 10 mmHg, established by bleeding. Two series of measurements were carried out, one at a spontaneously changing (n = 9) and one at a constant heart rate (n = 6). C_{ps} depended on pressure. The mean CSA versus mean P_{pa} curves were sigmoid and steepest in the series with the increasing heart rate (by bleeding). The CSA versus P_{pa} loop during a heart cycle, giving C_d, was approximately linear and almost closed. The C_d versus mean P_{pa} relationship was bell-shaped. Its width was smaller if the heart rate increased during the series of measurements. The pressure, where C_d was maximum, was higher at higher heart rates. Furthermore, maximum C_d was not affected by heart rate.

Because the pulmonary artery constricts with increasing heart rate, C_{ps} will be overestimated during procedures where heart rate increases. C_d should be determined to calculate flow because it changes with mean pulmonary arterial pressure and heart rate.

Chapter 4

In Chapter 2 and 3 a conductance method was used, in which the obtained cross-sectional area needed a correction for the influence of shear rate on conductivity and the influence of parallel conductance. We do not know if we can use a constant correction factor throughout the heart cycle to correct the conductivity of human blood for the influence of a pulsatile shear rate. To eliminate the problem of a pulsatile shear rate and parallel conductance we present a double indicator dilution technique, to determine the mean cross-sectional area (CSA) of a blood vessel in vivo. Analogous to the thermodilution method, dilution of hypertonic saline was measured by a conductance technique. Because, the change in conductance instead of absolute conductance was used to calculate CSA, pulsatile changes in shear rate of blood and conductance of surrounding tissues had no effect on our data. To calculate CSA from an ion mass balance, cardiac output was needed and estimated from the thermodilution curve using the same "cold" (hypertonic) saline injection. The mean CSA, obtained from this double indicator dilution method (CSA_{GD}), was compared to the CSA obtained from the IntraVascular UltraSound method (IVUS) in 44 paired observations in six piglets. The regression line is close to the line of identity ($CSA_{GD} = -1.83 + 1.06 \cdot CSA_{IVUS}$), and the correlation coefficient is 0.96. The difference between both CSAs is independent of the diameter of the vessel, on average -0.99 mm^2 ± 2.64 mm^2 (mean $CSA_{GD} = 46.84$ ± 8.21 mm^2, mean $CSA_{IVUS} = 47.82$ ± 9.08 mm^2) and not significant. The results show that the double indicator dilution method is a reliable technique to estimate cross-sectional areas of blood vessels in vivo.

Chapter 5

To determine segmental aortic or ventricular volume continuously, the conductance of the tissues and fluids surrounding a blood vessel or ventricle (parallel conductance) should be determined. To estimate parallel conductance the conductance values at end-systole are plotted versus those at end-diastole during a heart beat-to-beat increase in conductivity of blood after the injection of hypertonic saline. The linear regression line plotted through these values is extrapolated to the identity line and this extrapolated value is regarded as parallel conductance. We present a new observer-independent method to estimate parallel conductance ($G_p{}^a$), which is based on the analyses of the dilution curve after the injection of a small bolus of hypertonic saline and the determination of flow, and compared this method to the conventional method ($G_p{}^l$), which is observer-dependent.

$G_p{}^a$ and $G_p{}^l$ were determined in the descending thoracic aorta of piglets and were not significantly different. The reproducibility of the $G_p{}^a$-method was significantly better than that of the $G_p{}^l$-method. In the left as well as right ventricle of goats, $G_p{}^l$ and $G_p{}^a$ were obtained two times at two conditions. Each observation was analyzed by three observers and the average $G_p{}^l$-value and standard deviation were calculated. The standard deviation averaged for all measurements (n = 36) was 6.82 [1/Ohm] (mean $G_p{}^l$ = 104.60 [1/Ohm]). $G_p{}^a$ was not significantly different from $G_p{}^l$, averaged for the three observers. The reproducibility of the $G_p{}^a$-method was similar to that of the $G_p{}^l$-method. Seven measurements (7/43 = 8%) were excluded from the data set for analysis with the conventional method, by either one of the observers. However, these measurements could be analyzed with the new method and were in the range of values determined at the same condition. We conclude that the new approach has advantages above the conventional method because of 1) a better reproducibility if is measured in the aorta, 2) the necessity of a smaller number of injections to obtain the same accuracy, 3) the simultaneous determination of parallel conductance and cardiac output and, 4) the possibility to automate the procedure.

Chapter 6

A factor α is used to calibrate stroke volume derived with the conductance to that obtained by a reference method. It is assumed that α is needed to correct for a non-homogeneous electrical field. If the conventional method to determine parallel conductance is used, it is assumed that parallel remains constant within a heart cycle. Theoretical studies, however, show that parallel conductance would be volume dependent if the electrical field is non-homogeneous. In this chapter we hypothesized that parallel conductance depends on left ventricular volume and that the calibration with α is used to correct for the fact that parallel conductance does not remain constant within a heart cycle as assumed. We tested the hypothesis with use of a conductance dilution technique. Parallel conductance decreased with increasing left ventricular volume and a linear regression line was the best fit through the parallel conductance versus ventricular volume values. The twice determined estimates of slope and intercept of this linear regression line, were equal within the same patient but were significantly different between patients. The slope appeared to be mathematically coupled to the factor α. In conclusion either parallel conductance should be determined throughout the heart cycle using the new method so that the correction factor α is not needed or a correction factor α should be used if parallel conductance is assumed to be constant.

Chapter 7

This chapter comprises an evaluation of the methodology and findings. It appeared that the compliance of the pulmonary artery depends on pressure and heart-frequency. Furthermore a large variation was found between animals. To estimate flow from an arterial pressure signal, the arterial compliance should be determined in each patient or experimental animal. In the heart catheterization laboratory, the intensive care unit and during

thoracic surgery, patients are routinely catheterized with pulmonary arterial or aortic pressure catheters. If these catheter would be provided with four electrodes to determine segmental volume throughout the heart cycle, then flow can be determined from the arterial pressure wave. The segmental volume determined within the heart cycle during the passage of the diluted indicator can be related to the conductance measurement to derive segmental volume. This continuously obtained segmental volume can be used to continuously calculate compliance. Compliance, segmental volume and pressure can be used not only to determine blood flow, and to evaluate the effects of drugs on the circulation but probably also to detect vessel obstructions and aneurysms.

Samenvatting

Hoofdstuk 1

De continue berekening van bloedstroomsterkte is van belang bij patiënten die 1) zich op de "intensive care" bevinden, 2) die een thoraxoperatie ondergaan en 3) die een katheterisatie ondergaan voor diagnostische redenen. Bij deze patiënten bevindt zich routinematig een arteriële drukkatheter in de arteria pulmonalis of aorta. Uit één van deze bloeddrukken kan de bloedstroomsterkte bepaald worden met behulp van een windketelmodel van de circulatie. Een parameter van dit model is compliantie. Compliantie is een verandering van het volume van het bloedvat per lengte eenheid gedeeld door de verandering in bloeddruk. Om de verandering van het volume van het bloedvat per lengte eenheid te bepalen hebben we gebruik gemaakt van de elektrische conductantiemethode. In hoofdstuk één hebben we 1) de context waarin dit onderzoek is uitgevoerd, 2) de functie van de bloedvaten en de arteriën in het bijzonder, 3) de anatomie van de arteriën, 4) de termen die betrekking hebben op de mechanische eigenschappen van bloedvaten en 5) de elektrische conductantiemethode die we gebruikt hebben om het volume van de grote arteriën per lengte eenheid te bepalen, besproken.

Hoofdstuk 2

In dit hoofdstuk wordt de modificatie en evaluatie van een elektrische geleidbaarheidsmethode, de zogenaamde conductantiemethode ter bepaling van het volume van een bloedvat, beschreven. Een katheter met vier ringvormige elektroden, die op gelijke afstanden geplaatst zijn, werd in een bloedvat gepositioneerd. Tussen de buitenste elektroden werd een elektrisch veld opgewekt en tussen de binnenste werd de elektrische spanning gemeten. Deze spanning wordt bepaald door de geleiding van het bloed in het vat met de weefsels die om het bloed in het vat liggen. De geleiding van het bloed is afhankelijk van de afstand tussen de elektroden op de conductantiekatheter, de dwarsdoorsnede van het bloedvat en de geleidbaarheid van het bloed. Omdat bloed beschouwd kan worden als een suspensie

van kleine isolerende deeltjes (bloedcellen) in een geleidende vloeistof (plasma) wordt de geleidbaarheid van het bloed naast de temperatuur bepaald door het aantal bloedcellen (hematocriet). Het bloed in het midden van het bloedvat stroomt sneller dan aan de rand van het bloedvat waardoor er tijdens de pompfase van het hart verschillende krachten (afschuifsnelheid) op de bloedcellen komen te staan. Hierdoor zullen de bloedcellen zich richten en vervormen waardoor de effectieve weglengte van een elektronenstroom kleiner wordt en de geleidbaarheid van het bloed toeneemt. Wij vonden dat, indien het bloed plotseling gaat stromen, het richten en vervormen van varkensbloedcellen vrijwel onmiddellijk plaatsvindt en dat, indien het bloed plotseling tot stilstand komt, het ontrichten en het terugkeren van de bloedcellen tot hun oorspronkelijke vorm langer duurt dan de vulfase van het hart. Doordat de terugkeer van de bloedcellen tot hun oorspronkelijke vorm meer tijd vergt dan de duur van de vulfase van het hart concludeerden wij dat een constante factor gebruikt mag worden om voor de effecten van het richten en vervormen van bloedcellen te corrigeren. Uit de geleiding van het bloed in de aorta van 5 varkens bepaalden we de dwarsdoorsnede van de aorta. Daartoe dienden we vooraf de geleiding van de omliggende weefsels, de afstand tussen de elektroden en de geleidbaarheid van bloed, die berekend kan worden uit de hematocriet, de afschuifsnelheid en de temperatuur, te bepalen. De zo verkregen dwarsdoorsnede ($CSA_{(G)}$) werd uitgezet tegen de gelijktijdig met de intravasculaire-ultrageluid-methode verkregen dwarsdoorsnede ($CSA_{(IVUM)}$) voor verschillende volumes van het vat, die verkregen werden door adempauzes. De lineaire regressielijn door deze waarden had de volgende vergelijking: $CSA_{(G)}$ = -0.09 + 1.00· $CSA_{(IVUM)}$, r = 0.97, n = 53. Het gemiddelde verschil tussen beide waarden was -0.29% ± 5.57% (2SD). Wij concludeerden dat de gemodificeerde conductantiemethode een betrouwbare techniek is om dwarsdoorsneden van arteriën te schatten in biggen.

Hoofdstuk 3

Met behulp van de in hoofdstuk 2 beschreven conductantiemethode hebben wij de

dwarsdoorsnede van de arteria pulmonalis bepaald. Met deze dwarsdoorsnede en de gelijktijdig in de arteria pulmonalis bepaalde bloeddruk werd de compliantie van de arteria pulmonalis berekend. De invloed van de gemiddelde pulmonaire arteriële bloeddruk op de dynamische en pseudostatische compliantie werd bepaald bij een constante en een veranderende hartfrequentie onder verschillende condities verkregen door verbloeding. Dynamische compliantie is de verandering in dwarsdoorsnede gedeeld door de verandering in bloeddruk over een hartslag. De pseudostatische compliantie is de verandering in gemiddelde dwarsdoorsnede gedeeld door de verandering in gemiddelde bloeddruk. De dynamische compliantie kan gebruikt worden om uit de arteriële bloeddruk, de bloedstroomsterkte te berekenen. Wij hebben nagegaan of dynamische compliantie vervangen kan worden door pseudostatische compliantie. In negen genarcotiseerde biggen hebben we de gemiddelde dwarsdoorsnede en dynamische compliantie van de arteria pulmonalis bepaald bij drukniveaus tussen de 30 en 10 mmHg. Twee series metingen werden gedaan; één bij een spontane hartfrequentie (n = 9), waarbij de hartfrequentie van normaal bij een normale bloeddruk veranderde in een hoge hartfrequentie bij een lage bloeddruk, en één bij een hoge constante hartfrequentie (n = 6) waarbij het hart geprikkeld werd. De Pseudostatische compliantie bleek afhankelijk van de bloeddruk te zijn. De curven van de gemiddelde dwarsdoorsnede tegen de bloeddruk waren sigmoide van vorm en het steilst in de serie waar de hartfrequentie toenam. De lusvormige curve van de dwarsdoorsnede tegen de bloeddruk over een hartslag was vrijwel lineair en bijna gesloten. De relatie tussen de dynamische compliantie tegen de bloeddruk was klokvormig. Deze klokvorm was smaller indien de hartfrequentie tijdens de serie metingen toenam. De bloeddruk, waar de dynamische compliantie maximaal was, was hoger voor de serie met de hogere hartfrequentie. Verder bleek de maximale compliantie binnen een serie metingen niet beïnvloed te worden door de hartfrequentie. Doordat de longslagader contraheert indien de hartfrequentie toeneemt, zal de pseudostatische compliantie worden overschat bij procedures waarbij de hartfrequentie toeneemt en de bloeddruk daalt. Om bloedstroomsterkte uit de pulmonaire arteriële bloeddruk te bepalen, dient de dynamische compliantie van de arteria pulmonalis bepaald te worden voor iedere conditie voor ieder individu afzonderlijk.

Hoofdstuk 4

In het vorige hoofdstuk hebben we gebruik gemaakt van een conductantiemethode waarbij er gecorrigeerd moest worden voor de geleiding van de om het bloed heen liggende weefsels (parallelgeleiding) en de effecten van afschuifsnelheid op de geleidbaarheid van biggenbloed. Het is overigens nog onduidelijk of er ook voor andere diersoorten een constante correctiefactor voor afschuifsnelheid gebruikt kan worden. Om het probleem van een pulserende afschuifsnelheid en de bepaling van de parallelgeleiding te omzeilen werd een dubbele indicatorverdunningstechniek gebruikt om gemiddelde dwarsdoorsneden van arteriën te bepalen. Analoog aan de thermodilutiemethode wordt met behulp van de conductantiemethode de verdunning van ionen gemeten na het inspuiten van een hypertone zoutoplossing. Hierbij wordt alleen de verandering in geleiding bepaald en hebben pulsatiele veranderingen in afschuifsnelheid en de geleiding van weefsels die zich om het bloed heen bevinden geen effect. Om dwarsdoorsneden te berekenen uit een ionmassabalans moet de gemiddelde bloedstroomsterkte bekend zijn. Deze werd bepaald met behulp van de thermodilutiemethode na injectie van dezelfde "koude" hypertone zoutoplossing. De uitkomsten van gemiddelde dwarsdoorsnede, verkregen met behulp van de dubbele indicatorverdunningstechniek (CSA_{GD}), werden vergeleken met de uitkomsten verkregen met behulp van de IntraVasculaire-Ultrageluid-Methode (IVUM) in 44 gepaarde observaties in zes biggen. De lineaire regressielijn door deze waarden lag dicht bij de identiteitslijn (CSA_{GD} = -1.83 + 1.06·CSA_{IVUM}, r = 0.96). Het verschil tussen beide dwarsdoorsneden was niet significant en gemiddeld: -0.99 mm^2 ± 2.64 mm^2 (gemiddelde CSA_{GD} = 46.84 ± 8.21 mm^2, gemiddelde CSA_{IVUM} = 47.82 ± 9.08 mm^2). Op grond van de resultaten concludeerden wij dat de dubbele indicatorverdunningstechniek een betrouwbare techniek is om de gemiddelde dwarsdoorsnede van arteriën in vivo te bepalen.

Hoofdstuk 5

Naast de bepaling van een gemiddeld bloedvolume kan het bloedvolume van een bloedvat of

ventrikel ook continu in de tijd bepaald worden met de conductantiemethode. Hiervoor moet
. de parallelgeleiding bepaald worden. Deze bepaalt men door de waarden van de geleiding
van een minimaal ventrikelvolume, aan het begin van de vullingsfase, uit te zetten tegen de
waarden van een maximaal ventrikel volume, aan het begin van de ejectiefase. Deze waarden
worden slag op slag op slag bepaald tijdens de toenemende geleidbaarheid van het bloed na
de injectie van een hypertone zoutoplossing. De lineaire regressielijn door deze waarden
wordt geëxtrapoleerd naar de identiteitslijn, die gelijke waarden van de minimale en
maximale ventrikelvolumes aangeeft. Deze geëxtrapoleerde waarde wordt beschouwd als
parallelgeleiding. In dit hoofdstuk evalueerden wij een nieuwe methode om parallelgeleiding
te bepalen die niet gebaseerd is op de extrapolatie van een lijn maar op de bepaling van het
oppervlak onder een geleidingverdunningscurve verkregen na de injectie van een hypertone
zoutoplossing. De parallelgeleiding werd bepaald met zowel de conventionele als deze nieuwe
methode in de aorta van vijf biggen bij verschillende volumes en in de linker zowel als de
rechter ventrikel van zeven geiten bij twee condities. De waarden van parallelgeleiding
verkregen met de twee methoden bleken niet significant te verschillen. Indien de
parallelgeleiding in de aorta bepaald werd, bleek de nieuwe methode significant minder
spreiding te geven dan de conventionele methode. Indien de parallelgeleiding werd bepaald
in de linker of rechter ventrikel was de mate van spreiding voor beide methoden gelijk. Bij
de metingen in de ventrikels bleek dat een meting soms werd verworpen door de
onderzoekers voor een analyse met de conventionel methode, terwijl hetzelfde signaal wel
geanalyseerd kon worden met de nieuwe methode. Wij concludeerden dat de nieuwe methode
de volgende voordelen heeft boven de conventionele methode 1) de nieuwe methode heeft een
betere reproduceerbaarheid indien er in vaten gemeten wordt, 2) er kan volstaan worden met
een kleiner aantal injecties om dezelfde nauwkeurigheid te bereiken, 3) parallelgeleiding kan
tegelijkertijd met bloedstroomsterkte bepaald worden, en 4) de methode kan volledig
geautomatiseerd worden.

Hoofdstuk 6

Het slagvolume van de linker ventrikel, berekend met de conventionele conductantiemethode dient ge-ijkt te worden met een factor α. Men veronderstelt dat deze correctie nodig is omdat in de ventrikel een niet homogeen elektrisch veld wordt geïnduceerd, doordat het ventrikelvolume groot is ten opzichte van de afstand tussen de elektroden op de conductantiekatheter. Bij de conventionele manier om parallelgeleiding te bepalen wordt aangenomen dat parallelgeleiding niet volume afhankelijk is binnen de hartslag. Theoretisch onderzoek wijst er echter op, dat door het niet homogeen zijn van het elektrische veld, de parallelgeleiding volume afhankelijk is. In dit hoofdstuk testen wij de hypothese dat binnen de hartslag parallelgeleiding afhankelijk is van het ventrikelvolume en dat de ijking met α wordt gebruikt om te corrigeren voor het niet constant blijven van parallelgeleiding binnen de hartslag. Wij hebben deze hypothese getest met behulp van een dubbele indicatorverdunningstechniek. Parallelgeleiding werd uitgezet tegen ventrikel volume en een lineaire regressielijn werd getrokken door deze waarden. Parallelgeleiding nam lineair af met toenemend linker ventrikelvolume. De tweemaal bepaalde schattingen van hellingen en intercepten van de lineaire regressielijnen waren gelijk binnen één patiënt maar waren significant verschillend tussen patiënten. De helling bleek wiskundig gekoppeld te zijn aan de factor α. Wij concludeerden dat de parallelgeleiding bepaald moet worden gedurende de gehele hartslag waardoor een correctie met de factor α niet nodig is of dat een correctie met de factor α gebruikt moet worden indien er wordt uitgegaan van een constante parallelgeleiding gedurende de hartslag.

Hoofdstuk 7

In dit hoofdstuk worden de gebruikte methode en de bevindingen geëvalueerd. Het bleek dat de compliantie van de arteria pulmonalis niet constant kan worden verondersteld en afhankelijk is van de pulmonaire arteriële bloeddruk en de hartfrequentie. Tevens bleek de

compliantie sterk te verschillen tussen biggen. Indien men uit een druksignaal, de bloedstroomsterkte wil berekenen zou men daarom voor iedere patiënt of proefdier de compliantie per conditie moeten bepalen. Men zou de compliantie eenvoudig kunnen bepalen bij patiënten die een katheterisatie ondergaan, zich op de "intensive care unit" bevinden, of een thoraxoperatie ondergaan. Bij deze patiënten bevindt zich standaard een arteriële drukkatheter in de arteria pulmonalis of aorta, die uitgebreid zou kunnen worden met vier elektroden. Het segmentale volume van de arterie die verkregen kan worden gedurende de hele hartslag, tijdens het passeren van de verdunningscurve, kan worden gerelateerd aan het continue conductantiesignaal om continu het segmentale volume te verkrijgen. Deze continue meting van het segmentale volume kan samen met de continue drukmeting worden vertaald in een continue compliantiemeting. De compliantie, het segmentale volume en de bloeddruk kunnen vervolgens worden gebruikt om de effecten van farmaca te volgen en om vaatverwijdingen en -vernauwingen te detecteren. Verder kunnen deze gegevens worden ingevoerd in een circulatiemodel om continu bloedstroomsterkte te berekenen uit het arteriële druksignaal. Dit betekent dat zowel de output van de linker als rechterventrikel bepaald kan worden, zodat bijvoorbeeld bloedvolume veranderingen in de longcirculatie tijdens spontane ademhaling of beademing onderzocht kunnen worden. Het voordeel van de bepaling boven de bestaande methoden om bloedstroomsterkte te bepalen uit een bloeddruksignaal, is dat de methode ook toegepast kan worden bij individuen wiens vaten niet gekarakteriseerd zijn op grond van in vitro metingen zoals bijvoorbeeld bij patiënten met aangetaste vaten of bij proefdieren.

References

Aarts PAAM, van den Broek SAT, Prins GW, Kuiken GDC, Sixma JJ and Heethaar RM (1988) Blood platelets area concentrated near the wall and red blood cells, in the center in flowing blood. Artheriosclerosis 8:819-824

Alexander RS (1954) The participation of the venomotor system in pressor reflexes. Circulation Research 2:405-409

Altman DG (1990) Practical Statistics for Medical Research. In: Chapman and Hall, London, United Kingdom, pp 397-399

Applegate RJ, Pign Cheng C and Little WC (1990) Simultaneous conductance catheter and dimension assessment of left ventricle volume in intact animal. Circulation 81:638-648

Apter JT, Rabinowitz M and Cummings DH (1966) Correlation of visco-elastic properties of large arteries with microscopic structure. Circulation Research 29:104-121

Apter JT and Marquez E (1968) Correlation of visco-elastic properties of large arteries with microscopic structure. Circulation Research 22:393-404

Armentano RL, Levenson, Barra JG, Cabrera Fischer EI, Breitbart GJ, Pichel RH and Simon A (1991) Assessment of elastin and collagen contribution to aortic elasticity in conscious dogs. American Journal of Physiology 260:H1870-H1877

Armentano RL, Barra JG, Levenson J, Simon A and Pichel RH (1995) Arterial wall mechanics in conscious dogs. Circulation Research 76:468-478

Arndt JO, Stegall HF and Wicke HJ (1971) Mechanics of the aorta in vivo. A radiographic approach. Circulation Research 28:693-704

Axenborg JE and Olsson SB (1979) An electric impedance method for measurement of aortic cross-sectional areas. In: Abstracts of XII International Conference on Medical and Biological Engineering, Jerusalem, Israel, pp 19-24

Baan J, Iwazumi T, Szidon JP, and Noordergraaf A (1971) Intravascular area transducer measuring dynamic local distensibility of the aorta. Journal of Applied Physiology 31(3): 499-503

Baan J, Jong TTA, Kerkhof PLM, Moene RJ, van Dijk AD, van der Velde ET and Koops J (1981) Continuous stroke volume and cardiac output from intraventricular dimensions obtained with impedance catheter. Cardiovascular Research 15:328-334

Baan J, van der Velde ET, De Bruin HG, Smeenk GJ, Koops J, van Dijk AD, Temmerman D, Senden PJ and Buis B (1984) Continuous measurement of left ventricular volume in animals and humans by conductance catheter. Circulation 70:812-823

Baan J and van der Velde ET (1988) Sensitivity of left ventricular end-systolic pressure-volume relation to type of loading intervention in dogs. Circulation Research 62:1247-58

Baan J, van der Velde ET, Steendijk P and Koops J (1989) Calibration and application of the conductance catheter for ventricular volume measurement. Automedica 11:357-365

Baan J (1994) Continuous measurement of ventricular volume by conductance catheter. In: Thoracic Impedance Measurements in Clinical Cardiology, Eds. Winter UJ, Klocke RK, Kubicek WG and Niederlag W, Thieme Medical Publishers, Inc. New York, pp 139-143

Bader H (1963) Anatomy and physiology of the vascular wall. In: Handbook of Physiology, Circulation, Vol.II (Eds. Hamilton WF and Dow P) Washington DC, American Physiologic Society, pp 865-891

Band W, Goedhard WJ and Knoop AA (1972) Effect of aging on visco-elastic properties of the rat's thoracic aorta. Pflügers Archiv 331(4):357-64

Barra JG, Armentano RL, Levenson J, Cabrera FEI, Pichel RH and Simon A (1993) Assessment of smooth muscle contribution to descending thoracic aorta elastic mechanics in conscious dogs. Circulation Research 73:1040-1050

Bergel DH and Schultz DL (1971) Arterial elasticity and fluid dynamic. Progress in Biophysical Molecular Biology 22:1-36

Bergel DH (1961a) Static elastic properties of arterial wall. Journal of Physiology 156:445-457

Bergel DH (1961b) The dynamic elastic properties of the arterial wall. Journal of Physiology 156:458-468

Bergel DH and Schultz DL (1971) Arterial elasticity and fluid dynamics. Progress in Biophysica and Molecular Biology 22:1-36

Berry CL (1974a) The establishment of the elastic structure of arterial bifurcations and branches. Atherosclerosis 18:117-27

Berry CL (1974b) The growth and development of large arteries. Experimental Embryology and Teratology 1:34-64

Bevan JA, Garcia-Roldan J and Joyce EH (1990) Resistance artery tone is influenced independently by pressure and by flow. Blood vessels 27:202-207

Bialecki RA, Kulik TJ and Colluci WS (1992) Stretching increases calcium influx and efflux in cultured pulmonary arterial smooth muscle cells. American Journal of Physiology 263:L602-L606

Bland JM and Altman DG (1995) Calculating correlation coefficients with repeated observations: Part 1 - correlation within subjects. BMJ 310:633

Boesiger P, Maier SE, Kecheng L, Scheidegger MB and Meier D (1992) Visualization and quantification of the human blood flow by magnetic resonance imaging. Journal of Biomechanics 25(1):55-67

Boltwood CM, Appleyard RF and Glantz SA (1989) Left ventricular volume measurement by conductance catheter in intact dogs. Circulation 80:1360-1377

Bulbring E and Tomita T (1970) Effects of Ca^{2+} removal on the smooth muscle of the guineai-pig taenia coli. Journal of Physiology 210(2):217-32

Bull HB (1957) Protein structure and elasticity. In: Tissue elasticity (Ed. Remington WJ) Waverly Press Inc., Baltimore, pp 33-42

Burkhoff D, van der Velde ET, Kass DA, Baan J, Maughan WL and Sagawa K (1985) Accuracy of volume measurement by conductance catheter in isolated, canine hearts. Circulation 72:440-447

Burkhoff D, Alexander J and Schipke J (1988) Assessment of windkessel as a model of aortic input impedance. American Journal of Physiology 255:H742-H753

Burton AC (1954) Relation of structure to function of tissues of wall of blood vessels. Physiological Reviews 34:619-642

Caro CG, Pedley TJ, Schroter RC and Seed WA (1978) The Mechanics of the Circulation. In: Oxford Medical Publications, Oxford University Press, pp 48

Cassidy SC and Teitel DF (1992) The conductance volume catheter technique for measurement of left ventricular volume in young piglets. Pediatric Research 31:85-90

Clavin OE, Spinelli JC, Alonso H, Solarz P, Valentinuzzi ME and Pichel RH (1986) Left intraventricular pressure-impedance diagrams (DPZ) to asses cardiac function. Part I: morphology and potential sources of artifacts. Med. Prog. Technol. 11(1):17-24

Coburn RF (1987) Stretch-induced membrane depolarization in ferret trachealis smooth muscle cells. Journal of Applied Physiology 62:2320-2335

Corten PMJ, Koops J and Rodrigo FA (1972) Impedance measurements in blood vessels. Proc VI European Congres of Cardiology, Madrid (abstract)

Cox RH (1975a) Anisotropic properties of the canine carotid artery in vitro. Journal of Biomechanics 8:293-300

Cox RH (1975b) Arterial wall mechanics and composition and the effects of smooth muscle activation. American Journal of physiology 229:807-812

Davis G and Reid L (1970) Growth of the alveoli and pulmonary arteries in childhood. Thorax 25:669-681

Dobrin PB and Rovick AA (1969) Influence of vascular smooth muscle on contractile mechanics and elasticity of arteries. American Journal of Physiology 217(6):1644-1651

Edgerton RH (1974) Conductivity of sheared suspensions of ellipsoidal particles with application to blood flow. IEEE Transactions on Biomedical Engineering 21(1):33-44

Ferguson JJ, Miller MJ, Sahagian P, Aroesty JM and McKay RG (1988) Assessment of aortic pressure-volume relationships with an impedance catheter. Catheterization and Cardiovascular diagnosis 15:27-36

Ferguson JJ, Miller MJ, Sahagian P, Aroesty JM and McKay RG (1989) Effects of respiration and vasodilation on venous volume in animals and man, as measured with an impedance catheter. Catheterization and Cardiovascular Diagnosis 16:25-34

Fischell TA, Nellessen, Johnson DE and Ginsburg R (1989) Endothelium-dependent arterial vasoconstriction after balloon angioplasty. Circulation 79:899-910

Frangos JA, Eskin SG, McIntire LV and Ives CL (1985) Flow effects on prostacyclin production by cultured human endothelial cells. Science 227:1477-1479

Fung YC, Zweifach BW and Intaglietta M (1966) Elastic environment of the capillary bed. Circulation Research 19:441-461

Furchgott RF and Zawadzki JV (1980) The obligatory role of endothelial cells in the relaxation of arterial smooth muscle by acetylcholine. Nature 288:373-376

Furchgott RF (1983) Role of endothelium in response of vascular smooth muscle. Circulation Research 53:557-573

Fuster V, Steele PM, Edwards WD, Gersh BJ, Phil D, McGoon MD and Frye RL (1984) Primary pulmonary hypertension: natural history and the importance of thrombosis. Circulation 70(4):580-587

Gawne TJ, Gray KS and Goldstein RE (1987) Estimating left ventricular offset volume using dual-frequency catheters using dual-frequency conductance catheters. Journal of Applied Physiology 63:872-76

Geddes LA, Hoff HE, Mello A and Palmer C (1966) Continuous measurement of ventricular stroke volume by electrical impedance. CardioVascular Research Center Bulletin 4:118-131

Gentile BJ, Chuong CJC and Ordway GA (1988) Regional volume distensibility of canine thoracic aorta during moderate treadmill exercise. Circulation Research 63:1012-19

Goedhard WJ, Knoop AA and Westerhof N (1973) The influence of vascular smooth muscle contraction on elastic properties of pig's thoracic aorta. Acta Cardiologica 28(4):415-30

Gollan F and Namon R (1970) Electrical impedance of pulsatile blood flow in rigid tubes and in isolated organs. Annals New York Academy of Sciences 2:569-576

Gonza ER, Marble AE, Shaw A and Holland JG (1974) Age-related changes in the 'mechanics of the aorta and pulmonary artery of man. Journal of Applied Physiology 36:407-411

Gow BS and Taylor MG (1968) Measurement of visco-elastic properties of arteries in the living dog. Circulation Research 23:111-122

Gow BS (1972) The influence of vascular smooth muscle on the visco-elastic properties of blood vessels. In: Cardiovascular fluid dynamics (Ed. Bergel DH), vol.2 Academic Press, New York, pp 65-110

Grant BJB, Fitzpatrick JM and Lieber BB (1991) Time-varying pulmonary arterial compliance. Journal of Applied Physiology 70(2):575-583

Gratz I, Kraidin J, Jacobi AG, deCastro NG, Spagna P and Larijani GE (1992) Continuous noninvasive cardiac output as estimated from the pulse contour curve. Journal of Clinical Monitoring 8:20-27

Greenfield JC and Patel DJ (1962) Relation between pressure and diameter in the ascending aorta of man. Circulation Research 10:778-781

Greenfield JC and Griggs DM (1963) Relation between pressure and diameter in main pulmonary artery of man. Journal of Applied Physiology 18(3):557-559

Gross DR, Hunter JF, Allert J, Hwang JA and Patel NHC (1981) Pressure-diameter relationship in the coronary of intact, awake calves. Journal of Biomechanics 14:613-620

Hardeman MR, Goedhart P and Breederveld D (1987) Laser diffraction ellipsometry of erythrocytes under controlled shear stress using a rotational viscosimeter. Clinica Chimica Acta 165(2-3):227-234

Hardeman MR, Goedhart PT, Dobbe JGG and Lettinga KP (1994) Laser-assisted optical rotational cell analyser (L.O.R.C.A.); A new instrument for measurement of various structural hemorheological parameters. Clinical Hemorheology :605-618

Harder DR, Gilbert R and Lombard JH (1987) Vascular muscle cell depolarization and activation in renal arteries on elevation of transmural pressure. American Journal of Physiology 253:F778-F781

Harris DE and Warshaw DM (1991) Length versus active force relationship in single isolated smooth muscle cells. American Journal of Physiology 260:C1104-C1112

Harris P, Heath D and Apostopolous A (1965) Extensibility of the human pulmonary trunk. British Heart Journal 27:651-659

Hass GM (1942) Elastic tissue 2. A study of the elasticity of body tissues. In: Medical Physics 2 (Ed. Glasser O) Chicago: Year Book Publishers

Hoeks APG, Brands PJ, Smeets FAM and Reneman RS (1990) Assessment of the distensibility of superficial arteries. Ultrasound in Medicine and Biology 16(2):121-128

Hutcheson IR and Griffith TM (1991) Release of endothelium-derived relaxing factor is modulated by frequency and amplitude of pulsatile flow. American Journal of Physiology 261:H257-262

Ingram RH, Szidon JP, Skalak R and Fishman AP (1968) Effects of sympathetic nerve stimulation of the pulmonary artery tree on the isolated lobe perfused in situ. Circulation Research 22:801-814

Ingram RH, Szidon JP and Fishman AP (1970) Response of the main pulmonary artery of dogs to neurally released versus blood-borne norepinephrine. Circulation Research 26:149-262

Jansen JRC, Schreuder JJ, Boogaard JM, van Rooyen W and Versprille A (1981) Thermodilution technique for measurement of cardiac output during artificial ventilation. Journal of Applied Physiology 50(3):584-591

Jansen JRC, Boogaard JM and Versprille A (1987) Extrapolation of thermodilution curves obtained during a pause in artificial ventilation. Journal of Applied Physiology 63(4):1551-1557

Jansen JRC, Hoorn E, van Goudoever J and Versprille A (1989) A computerized respiratory system including test functions of lung and circulation. Journal of Applied Physiology 67(4):1687-1691

Jansen JRC, Schreuder JJ, Settels JJ, Kloek JJ and Versprille A (1990) An adequate strategy for the thermodilution technique in patients during mechanical ventilation. Intensive Care Medicine 16:422-425

Jansen JRC, Wesseling KH, Settels JJ and Schreuder JJ (1990) Continuous cardiac output monitoring by pulse contour during cardiac surgery. European Heart Journal 11:26-32

Jansen JRC (1995) The thermodilution method for the clinical assessment of cardiac output. Intensive Care Medicine 21(8):691-697

Johnson TA and Henry GW (1985) Two dimensional in vivo pressure/diameter relation-ships in the canine main pulmonary artery. CardioVascular Research 19:442-448

Journo HJ, Chanudet XA, Pannier BM, Laroque PL, London GM and Safar ME (1992) Hysteresis of the venous pressure-volume relationship in the forearm of borderline hypertensive subjects. Clinical Science 82:329-334

Kanemoto N (1987) Natural history of pulmonary hemodynamics in primary pulmonary hypertension. Progress in Cardiology 114(2):407-412

Kannel WB (1991) Hypertension, hypertrophy and the occurrence of cardiovascular disease. American Journal of Medical Science 302:199-204

Kelly RP, Tunin R and Kass DA (1992) Effect of reduced aortic compliance on cardiac efficiency and contractile function of in situ canine left ventricle. Circulation Research 71:490-502

Khalil R, Lodge N, Saida K and van Breemen C (1987) Mechanism of calcium activation in vascular smooth muscle. Journal of Hypertension 5:S5-S15

Kien ND and Kramer GC (1989) Cardiac performance following hypertonic salt. Brazilian Journal of Medical and Biological Research 22:245-248

Kirber MT, Walsh JV Jr and Singer JJ (1988) Stretch-activated ion channels in smooth muscle: a mechanism for the initiation of stretch-induced contraction. Pflügers Archiv 345:412-345

Kirber MT, Ordway RW, Clapp LH, Walsh JV Jr. and Singer JJ (1992) Both membrane stretch and fatty acids directly activate large conductance Ca^{2+}-activated K^+ channels in vascular smooth muscle cells. FEBS 297(1):24-28

Koerner SK (1988) Pulmonary hypertension: etiology and clinical evaluation. Journal of Thoracic Imaging 3(1):25-31

Kornet L, Jansen JRC, Gussenhoven EJ, Hardeman MR and Versprille, A (1996) The conductance method for the measurement of cross-sectional areas of arteries in vivo. Submitted: IEEE Transactions on Biomedical Engineering

Kulik TJ, Evans JN and Gamble WJ (1988) Stretch-induced contraction in pulmonary arteries. American Journal of Physiology 255:H1391-H1398

Kulik TJ, Bialecki RA, Colucci WS, Rothman A, Glennon ET and Underwood RH (1991) Stretch increases inositol triphosphate and inositol tetrakiphosphate in cultured pulmonary vascular smooth muscle cells. Biochemical and Biophysical Research Communications 180(2):982-987

Kun S and Peura RA (1994) Analysis of conductance volumetric measurement error sources. Medical and Biological Engineering and Computing 32:94-100

Landgren S (1952) The baroreceptor activity in the carotid sinus nerve and the distensibility of the sinus wall. Acta Physiologica Scandinavica 26:35-56

Langewouters GJ (1984) The static elastic properties of 45 human thoracic and 20 abdominal aortas in vitro and the parameters of a new model. Journal of Biomechanics 17(6):425-436

Langewouters GJ, Wesseling KH and Goedhard WJ (1985) The pressure dependent dynamic elasticity of 35 thoracic and 16 abdominal human aortas in vitro described by a five component model. Journal of Biomechanics 18(8):613-620

Lankford EB, Kass DA, Maughan WL and Shouskas AA (1990) Does volume catheter parallel conductance vary during a cardiac cycle? American Journal of Physiology 258(27):1933-1942

Latson TW, Hunter WC, Kotoh N and Sagawa K (1988) Effect of nitroglycerin on aortic impedance, diameter and pulse-wave velocity. Circulation Research 62:884-890

Learoyd BM and Taylor MG (1966) Alterations with age in the visco-elastic properties of human arterial walls. Circulation Research 18:287-292

Lehmann ED, Gosling RG and Sönsken PH (1992a) Arterial compliance in diabetis. Diabetic Medicine 9:114-9

Lehmann ED, Watts GF, Fatemi-Landgroudi B and Gosling RG (1992b) Aortic compliance in young patients with familial hypercholesterolaemia. Clinical Science 83:717-721

Lehmann ED, Watts GF and Gosling RG (1992c) Aortic distensibility and hyper-cholesterolaemia. Lancet 340:1171-1172

Lehmann ED, Hopkins KD, Weisberger AJ, Gosling RG and Sönsken PH (1993) Aortic distensibility in growth hormone deficient adults. Lancet 341:309

Leitz KH and Arndt JO (1968) Die Durchmesser-Druck-Beziehung des intakten Gefassgebietes der Arterie Carotis Communis der Katzen. Pflügers Archiv für die Gesamte Physiologist des Menschen und der Tier 301:50-69

Lieber BB, LI Z and Grant BJB (1994) Beat-by-beat changes of viscoelastic and inertial properties of the pulmonary arteries. Journal of Applied Physiology 76(6):2348-2355

Liebman FM (1974) Electrical impedance pulse tracings from pulsatile blood flow in rigid tubes and volume restricted vascular beds: theoretical explanations. In: Annals New York Academy of Sciences, pp. 437-551

Lo CS, Relf IR, Myers KA and Walqvist ML (1986) Doppler ultrasound recognition of preclinical changes in arterial wall in diabetic subjects: compliance and pulse wave damping. Diabetis Care 9:27-31

Long CJ and Stone TW (1985) The release of endothelium-derived relaxant factor is calcium dependent. Blood Vessels 7:399-411

van Loon P, Klip W and Bradley EL (1977) Length-force and volume-pressure relationships of arteries. Biorheology 14:181-201

Lundholm L and Mohme-Lundholm E (1966) Length at inactivated contractile elements, length-tension diagram, active state and tone of vascular smooth muscle. Acta Physiologica Scandinavica 68:347-359

Mallos AJ (1962) An electrical caliper for continuous measurement of relative displacement. Journal of Applied Physiology 17:131-134

Maloney JE, Rooholamini SA and Wexler L (1970) Pressure-diameter relations of small blood vessels in isolated dog lung. MicroVascular Research 2:1-12

Marcus RH, Korcarz C, McGray G, Neumann A, Murphy M, Borow K, Weinert L, Bednarz J, Gretler DD and Spencer KT (1994) Noninvasive method for determination of arterial compliance using doppler echocardiography and subclavian pulse tracings Circulation 89:2688-2699

McDonald DA (1960) Blood flow in arteries. Williams and Wilkins, Baltimore.

McKay RG, Spears JR, Arousty JM, Baim DS, Royal HD, Heller GV, Lincoln W, Salo RW, Braunwald E and Grossman W (1984) Instantaneous measurement of left and right ventricular stroke volume and pressure-volume relations-ships with an impedance catheter. Circulation 69:703-710

Melkumyants AM, Balashov SA and Khayutin VM (1989) Endothelium dependent control of arterial diameter by blood viscosity. CardioVascular Research 23:741-747

Melkumyants AM, Balashov SA and Kartamyshev SP (1994) Anticonstrictor effect of endothelium sensitivity to shear stress. Pflügers Archiv 427:264-269

Mergerman J, Hasson JE, Warnock DF, I'Italien GJ and Abbott WM (1986) Noninvasive measurement of nonlinear arterial elasticity. American Journal of Physiology 250:H181-H188

Merillon JP, Motte G, Fruhaud J, Masquet C and Gourgon RC (1978) Evaluation of the elasticity and characteristic impedance of the ascending aorta in man. CardioVascular Research 12:401-6

van Merode T, Hick PJJ, Hoeks APG, Rahn KH and Reneman RS (1988) Carotid artery wall properties in normotensive and borderline hypertensive subjects of various ages. Ultrasound in Medicine and Biology 14(7):563-569

van Merode T, Brands PJ, Hoeks PGH and Reneman RS (1993) Faster ageing of the carotid artery bifurcation in borderline hypertensive subjects. Journal of Hypertension 11:171-176.

van Merode T, Brands PJ, Hoeks APG and Reneman RS (1996) Different effects of ageing on elastic and muscular bifurcations in men. Journal of Vascular Research 22:47-52

Milnor WR (1975) Arterial impedance as ventricular afterload. Circulation Research 36:565-570

Milnor WR (1982) Hemodynamics. Williams and Wilkens, Baltimore.

Minns RJ, Soden PD and Jackson DS (1973) The role of fibrous components and ground substance in the mechanical properties of biological tissues: A preliminary investigation. Journal of Biomechanics 6:153-165

Mohandas N, Clark MR, Jacobs MS and Shohet SB (1980) Analysis of factors regulating erythrocyte deformability. Clinical Investigations 54:563-572

Monos E, Contney S, Cowley AW Jr. and Stekiel WJ (1986) Effects of hemodynamic stress on membrane potential of vascular smooth muscle cells in vivo and in vitro. Physiologist 29:155

Nakajima T, Kon K, Maeda N, Tsunekawa K and Shiga T (1990) Deformation response of red blood cells in oscillatory shear flow. American Journal of Physiology 259:H1071-H1078

Naruse K and Sokabe M (1993) Involvement of stretch-activated ion channels in Ca^{2+} mobilization to mechanical stretch in endothelial cells. American Journal of Physiology 264:C1037-C1044

Newman DL and Lallemand RC (1978) The effect of age on the distensibility of the abdominal aorta of man. Surgery in Gynaecology and Obstetrics 147:211-214

Ninomiya M, Fujii M, Niwa M, Sakamoto K and Kanai H (1988) Physical properties of flowing blood. Biorheology 25(1-2):319-328

Nobel MIM (1979) Left ventricular load, arterial impedance and their relationship. CardioVascular Research 13:183-198

O'Rourke MF (1982) Vascular impedance in studies of arterial and cardiac function. Physiological Reviews 62:570-623

Odake M, Takeuchi M, Takaoka M, Hata H, Hayashi Y and Yokoyama M (1992) Determination of left ventricular volume using a conductance catheter in the diseased human heart. European Heart Journal 13E:22-27

Olivari M (1991) Southwestern internal medicine conference: primary pulmonary hypertension. American Journal of Medical Science 302(3):185-198

Pagani M, Schwartz PJ, Bishop VS and Malliani A (1975) Reflux sympathetic changes in aortic diastolic pressure-diameter relationship. American Journal of Physiology 229:286-90

Pagani M, Gaig H, Sherman A, Quinn WT, Patrick P and Vatner D (1978) Measurement of multiple simultaneous small dimensions and study of arterial pressure-diameter relation in conscious animals. American Journal of Physiology 234:610-17

Patel JD, Schilder DP and Mallos AJ (1960) Mechanical properties and dimensions of the major pulmonary arteries. Journal of Applied Physiology 15(1):92-96

Patel JD, De Freitas FM, Greenfield JC Jr. and Fry DL (1963) Relationship of radius to pressure along the aorta in living dogs. Journal of Applied Physiology 18:1111-1117

Patel JD and Fry DL (1964) In situ pressure-radius-length measurement in ascending aorta of anaesthetized dogs. Journal of Applied Physiology 19:413-416

Patel JD, Janicki JS and Carew TE (1969) Static anisotropic elastic properties of the aorta in living dogs. Circulation Research 25:765-779

Peterson LH, Jensen RE and Parnell J (1960) Mechanical properties of arteries in vivo. Circulation Research 8:622-639

Peura RA, Penney BC, Arcuri J, Anderson FA and Wheeler HB (1978) Influence of erythrocyte velocity on impedance plethysmographic measurements. Medical and Biological Engineering and Computing 16(2):147-154

Piene H (1976) Some physical properties of the pulmonary arterial bed deduced from pulsatile arterial flow and pressure. Acta Physiologica Scandinavica 98:295-306

Piene H and Hauge A (1976) Reduction of pulsatile hydraulic power in the pulmonary circulation caused by moderate vasoconstriction. Circulation Research 10:503-513

Pohl U, Busse R, Kuon E and Bassence E (1986) Pulsatile perfusion stimulates the release of endothelial autocoids. Journal of Applied Physiology 1:215-235

Remington (1955) Hysteresis loop behaviour of the aorta and other extensible tissues. American Journal of Physiology 180:83-95

Reneman RS, van Merode T, Brands PJ and Hoeks APG (1992) Inhomogeneites in arterial wall properties under normal and pathologic conditions. Journal of Hypertension 10: S35-S39

Reuterwall OP (1921)   Über die Elastizität der Gefässwände und die Methoden ihrer näheren Prüfung. Acta Medica Scandinavica Suppl 2:1-175

Rhodin JAG (1980) Architecture of the vessel wall. In: Bohr DF, Somlyo AP, Sparks Jr HV: Handbook of Physiology, American Physiological Society, Bethesda, pp 1-29

Roach M and Burton AC (1957) Reason for the shape of the distensibility curves of arteries. Canadian Journal of Biochemistry and Physiology 35:681-688

Rubanyi GM, Romero JC and Vanhoutte PM (1986) Flow induced release of endothelium-derived relaxing factor. American Journal of Physiology 250:H1145-H1149

Rushmer RF, Crystal DK, Wagner C and Ellis RM (1953) Intracardiac impedance plethysmography. American Journal of Physiology 174:171-174

Sϕmod L, Hasenkam JM, Yong Kim W, Nygaard H and Paulsen PK (1993) Three dimensional visualisation of velocity profiles in the normal porcine pulmonary trunk. Cardiovascular Reseach 27:291-295

Sakamoto K and Kanai H (1979) Electrical characteristics of flowing blood. IEEE Transactions on Biomedical Engineering 26(12):686-695

Schabert A, Bauer RD and Busse R (1980) Photo-electric device for the recording of diameter changes of opaque and transparent blood vessels in vitro. Pflügers Archiv 385:239-242

Schmid-Schönbein H, Gaeghtgens P and Hirsch H (1968) On the shear rate dependence of red cell aggregation in vitro. The Journal of Clinical Investigation 47:1447-1454

Schmid-Schönbein H and Wells R (1969) Fluid drop-like transition of erythrocytes under shear. Science 165:288-291

Schwan HP (1963) Determination of biological impedance. In: Physical techniques in biological research, Ed. W. Nastuck, New York, Academic press

Schwan HP (1983) Electrical properties of blood and its constituents: alternating current spectroscopy. Blut 46:185-197

Shelton DK and Olson RM (1972) A nondestructive technique to measure pulmonary artery diameter and its pulsatile variations. Journal of Applied Physiology 33(4):542-544

Skalak R and Zhu C (1990) Rheological aspects of red blood cell aggregation. Biorheology 27(3-4):309-325

Smith (1976) A comparison of the orientation of elastin fibres in the elastic lamellae of the pulmonary trunk and aorta of rabbits using the scanning electron microscope. Laboratory Investigations 35:525-529

Smith JE, Mohandas N and Shohet SB (1979) Variability in erythrocyte deformability among various animals. American Journal of Physiology 236(5):H725-H730

Snabre P, Bitbol M and Mills P (1987) Cell disaggregation behavior in shear flow. Biophysical Journal 51:795-807

Somlyo AV and Somlyo AP (1964) Vasomotor function of smooth muscle in the main pulmonary artery. American Journal of Physiology 206:1196-1200

Sparks, HV (1964) Effect of quick stretch on isolated vascular smooth muscle. Circulation Research 1:1254-1260

Spinelli JC and Valentinuzzi (1986) Conductivity and geometrical factors affecting volume measurements with an impedancimetric catheter. Medical and Biological Engineering and Computing 24:460-464

Steendijk P (1992) Single and dual excitation of the conductance-volume catheter analyzed in a spheroidal mathematical model of the canine left ventricle. European Heart Journal 13:28-34

Steendijk P, van der Velde ET and Baan J (1993) Left ventricular volume by dual excitation of the conductance catheter. American Journal of Physiology 246:2198-207

Stefanadis C, Wooley CF, Bush CA, Kolibash AJ and Boudoulas H (1987) Aortic distensibility abnormalities in coronary artery disease. American Journal of Cardiology 59:1300-4

Stewart GN (1921) The output of the heart in dogs. American Journal of Physiology 57:27-50

Sumpio BE and Widmann MD (1990) Enhanced production of an endothelium-derived contracting factor by endothelial cells subjected to pulsatile stretch. Surgery 108:277-282

Szwarc RS, Mickleborough LL, Mizuno S, Wilson J, Liu P and Mohamed S (1994) Conductance catheter measurements of left ventricular volume in the intact dog: parallel conductance is independent of left ventricular size. Cardiovascular research 28:252-258

Szwarc RS, Laurent D, Allegrini PR and Ball HA (1995) Conductance catheter measurement of left ventricular volume: evidence for non-linearity within cardiac cycle. American Journal of Physiology 37:H1490-H1498

Tajimi T, Sunagawa K, Yamada A, Nose Y, Takeshita A, Kikuchi Y and Nakamura M (1983) Evaluation of pulse contour methods in calculating stroke volume from pulmonary artery pressure curve (comparison with aortic pressure curve). European Heart Journal 4:502-511

Tannenbaum GA, Mathews D and Weissman C (1993) Pulse contour cardiac output in surgical intensive care unit patients. Journal of Clinical Anaesthesia 5:471-478

Teitel DF, Klautz R, Steendijk P, van der Velde ET, van Bel F and Baan J (1991) The end-systolic pressure-volume relationship in the newborn lamb: effects of loading and inotropic interventions. Pediatric Research 29(5):473-482

Teitel DF, Klautz RJM, Cassidy SC, Steendijk P, van der Velde ET, van Bel F and Baan J (1992) The end-systolic pressure volume relationship in young animals using the conductance technique. European Heart Journal 13(E):40-46

Tomoike H, Ootsubo H, Sakai K, Kichuchi Y and Nakamura M (1981) Continuous measurement of coronary artery diameter in situ. American Journal of Physiology 240:73-9

van der Velde ET, van Dijk AD, Steendijk P, Glantz SA, Diethelm L, Chagas T, Lipton MJ and Baan J (1992) LV segmental by conductance catheter and cine CT. European Heart Journal 13(Suppl E):15-21

Vatner SF, Pagani M, Manders WT and Pasipoularides AD (1980) Alpha-adrenergic vasoconstriction and nitroglycerin vasodilation of large coronary arteries in the conscious dog. Journal of Clinical Investigations 65:5-14

Vatner SF and Hintze HT (1982) Effects of calcium channel antagonist on large and small coronary arteries in conscious dogs. Circulation 66:579-88

Velasco IT, Pontieri V, Silva MRE and Lopes OU (1980) Hyperosmotic NaCl and severe haemorrhagic shock. American Journal of Physiology 239:664-673

Versprille A and Jansen JRC (1985) Mean systemic filling pressure as a characteristic pressure for venous return. Pflügers Archiv 405:226-233

Versprille A and Jansen JRC (1993) Tidal variation of pulmonary blood flow and blood volume in piglets during mechanical ventilation during hyper-, normo- and hypovolemia. Pflügers Archiv 424:255-265

Visser KR, Lamberts R, Korsten HHM, Zijlstra WG (1976) Observations on blood flow related electrical impedance changes in rigid tubes. Pflügers Archiv 366(2-3):289-291

Visser KR (1989) Electrical properties of flowing blood and impedance cardiography. Annals of Biomedical Engineering 17(5):463-473

Vorp DA, Rajagopal KR, Smolinski PJ and Borovetz HS (1995) Identification of elastic properties of homogenous, orthotropic vascular segments in distension. Journal of Biomechanics 28:501-512

Walsh JV and Singer JJ (1980) Calcium action potentials in single freshly isolated smooth muscle cells. American Journal of Physiology 239:C162-C174

Weissman C, Ornstein EJ and Young WL (1993) Arterial pulse contour analysis trending of cardiac output: hemodynamic manipulations during cerebral arteriovenous malformation resection. Journal of Clinical Monitoring 9:347-353

Wenguang L, Gussenhoven WJ, Bosch JG, Mastik F, Reiber JHC and Bom N (1990) A computer-aided analysis system for the quantitative assessment of intra-vascular ultrasound images. Computer in Cardiology :333-336

Wenguang L, Gussenhoven WJ, Zhong Y, The SHK, Di Mario C, Madretsma S, van Egmond F, De Feyter P, Pieterman H, van Urk H, Rijsterborgh H and Bom N (1991) Validation of quantitative analysis of intra-vascular ultrasound images. International Journal of Cardiac images 6:247-253

Wesseling KH, Purschke R, Smith NT and Nichols WW (1976) Continuous monitoring of cardiac output. Medicamundi 21(2):78-90

Wesseling KH, Wit de B, Weber JAP and Smith NT (1983) A simple device for the continuous measurement of cardiac output. Its model basis and experimental verification. Advances in Cardiovascular Physiology 5(2):16-52

Wesseling KH, Jansen JRC, Settels JJ and Schreuder JJ (1993) Computation of aortic flow from pressure in humans using a non-linear, three-element model. Journal of Applied Physiology 74(5):2566-2573

Wiederhielm CA (1965) Distensibility characteristics of small arteries. Federation of Proceedings 24:1075-1084

Winston FK, Thibault LE and Macarak EJ (1993) An analysis of the time dependent changes in intracellular calcium concentration in endothelial cells in culture induced by mechanical stimulation. Journal of Biomechanical Engineering 115:160-168

Wolinsky H and Glagov S (1964) Structural basis for the static mechanical properties of the aortic media. Circulation Research 14:400-413

Yanagisawa M, Kurihara H, Kimura S, Tomobe Y, Kobayashi M, Mitsui Y, Yazaki Y, Goto K and Masaki T (1988) A novel potent vasoconstrictor peptide produced by vascular endothelial cells. Nature 332(6163):411-415

Zatzman M, Stacy RW, Randall J and Eberstein A (1954) Time courses of stress relaxation in isolated arterial segments. American Journal of Physiology 177:299-3021

Zheng E, Shao S and Webster JG (1984) Impedance of skeletal muscle from 1 Hz to 1 MHz. IEEE Transactions on Biomedical Engineering 31:477-483

Zierler KL (1962) Theoretical basis of indicator dilution methods for measuring flow and volume. Circulation Research 10:393-407

Dankwoord

Dankwoord

Op deze plaats wil ik graag iedereen bedanken die direct of indirect heeft bijgedragen aan de totstandkoming van dit proefschrift.

In het bijzonder wil ik mijn promotor Prof.Dr. A. Versprille bedanken. Met name in het schrijfstadium heeft u veel bijgedragen, o.a. door formuleringen steeds weer aan te scherpen. Ook in de toekomst zal ik tijdens het schrijven het gevoel hebben dat u over mijn schouder meekijkt.

Tevens wil ik mijn co-promotor Dr. JRC Jansen bedanken. Beste Jos, je hebt je de afgelopen jaren flink met de inhoud van dit proefschrift bemoeid. De vele gesprekken tussendoor waren erg motiverend. Als we er niet uitkwamen was het altijd van "nou dan eerst maar een bak koffie" (verder nog bedankt voor de kledingadviezen).

Dhr. A. Drop droeg de proefdierexperimenten beschreven in dit proefschrift. Beste Arnold, zonder jouw kundige, precieze en stressbestendige handelen waren er geen resultaten geweest en dus ook geen proefschrift. Van jou heb ik leren experimenteren.

Prof.Dr. J. Baan, Prof.Dr.Ir. N. Bom and Prof.Dr. P.D. Verdouw wil ik bedanken voor het beoordelen van dit proefschrift en hun nuttige kritiek hierop.

Ing. E. Hoorn ik heb het zeer gewaardeerd dat ik je altijd weer lastig kon vallen met de vraag of je een computerprogramma wilde aanpassen en dat je ook die keer na zes vragen binnen één uur nog geduldig bleef.

Dhr. PT. Goedhart, dhr J. Honkoop en Michael van Oosterhout wil ik bedanken voor hun technische ondersteuning.

Ik wil de medeauteurs Dr. EJ Gussenhoven, Dr. MR Hardeman, Dr. GJ Langewouters, Dr. J Schreuder en Dr. ET van der Velde bedanken voor het leveren van materiaal, data en kritiek.

Francis en emiel, bedankt voor de "isosferisch" getinte lunchgesprekken. Ik vond het heel gezellig met jullie en hoop dat ik jullie ook privé blijf tegen komen. Verder fijn dat ik altijd bij francis terecht kon met vragen over o.a. anatomie en statistiek en bij emiel

met vragen over o.a. matlab. Hiernaast bedank ik ook leon voor zijn therapeutische bijdrage aan de lunchpauzes van de laatste maanden.

Cristina, vlak voordat de stukken de deur uitgingen zeefde jij de allerlaatste dingen er nog uit.

En natuurlijk heb ik altijd de steun van mijn ouders, die het mij mogelijk gemaakt heeft mijn kindertoekomstbeeld te verwezenlijken, gewaardeerd.

Last but not least is daar steven, die mij laat realiseren dat er nog leven is na een proefschrift.

Curriculum Vitae

Curriculum Vitae

Lilian Kornet werd op 7 juli 1968 te Hellevoetsluis geboren. Na het behalen van het eindexamen VWO aan de Rijksscholengemeenschap in Hellevoetsluis, begon zij in 1986 aan de Propaedeuse van de studie BioMedische Wetenschappen aan de Rijksuniversiteit Leiden. Van 1987-1991 volgde zij de bovenbouwstudie BioFarmaceutische Wetenschappen, eveneens aan de Rijksuniversiteit Leiden. Zij deed in 1990 haar afstudeerstage bij de vakgroep "Farmaceutische Technologie". Hier bestudeerde ze het iontoforetische transport van kwikionen door de humane huid met behulp van elektronenmicroscopie. Vervolgens liep ze in 1991 stage bij de afdeling "Drug Delivery Systems" van de firma Sandoz te Basel, Zwitserland, waar de pulmonale toediening van liposomen bestudeerd werd. Vanaf april 1992 tot april 1996 was zij als Assistent in Opleiding (AIO) verbonden aan het Pathofysiologisch Laboratorium van het Instituut Longziekten, Erasmus Universiteit Rotterdam, onder leiding van Prof.Dr. A. Versprille. Het onderzoek beschreven in dit proefschrift werd in deze periode uitgevoerd en werd begeleid door Dr. J.R.C. Jansen. Sinds mei 1996 is Lilian Kornet, voor de periode van twee jaar, werkzaam als post-doc onderzoeker aan de Universiteit van Limburg, waar zij voor 0,5 fte ondergebracht is bij de vakgroep Fysiologie en voor 0,5 fte bij de onderzoeksschool CARIM. Zij bestudeert hier de relatie tussen vaatwandeigenschappen en afschuifspanning op de vaatwand van bloedvaten met behulp van ultrageluidstechnieken.